

Improved Space Vector PWM Technique Operating in Over-modulation Region for Induction Machine Drive

Thesis submitted
in partial fulfillment of the
requirements for the degree

Master of Technology
ⁱⁿ
Power Electronics and Drives Engineering

by

Sahu Mithun
19PD06004

Under the supervision of
Dr. Dipankar De



SCHOOL OF ELECTRICAL SCIENCES INDIAN INSTITUTE OF
TECHNOLOGY BHUBANESWAR

May 2021

©2021 Sahu Mithun. All rights reserved.

APPROVAL OF THE BOARD

May 15, 2021

Certified that the report entitled "**Improved Space Vector PWM Technique Operating in Over-modulation Region for Induction Machine Drive**" submitted by **Sahu Mithun** (19PD06004) to the Indian Institute of Technology Bhubaneswar in partial fulfilment of the requirements for the degree Master of Technology has been accepted by the examiners during the viva-voce examination held today.

(Supervisor)

(External Examiner)

(Internal Examiner 1)

(Internal Examiner 2)

CERTIFICATE

This is to certify that the report entitled "**Improved Space Vector PWM Technique Operating in Over-modulation Region for Induction Machine Drive**" submitted by **Sahu Mithun** (16PD06004) to Indian Institute of Technology Bhubaneswar is a record of bonafide research work under my supervision and I accept the Thesis submitted as the worthy of consideration for the final evaluation of the M. Tech thesis work.

(Supervisor)

DECLARATION

I certify that

1. The work contained in the thesis is original and has been done by myself under the general supervision of my supervisor.
2. The work has not been submitted to any other Institute for any degree or diploma.
3. I have followed the guidelines provided by the Institute in writing the report.
4. I have conformed to the norms and guidelines given in the Ethical Code of Conduct of the Institute.
5. Wherever I have used materials (data, theoretical analysis, and text) from other sources, I have given due credit to them by citing them in the text of the thesis and giving their details in the references.
6. Whenever I have quoted written materials from other sources, I have put them under quotation marks and given due credit to the sources by citing them and giving required details in the references.

**Sahu Mithun
19PD06004**

Abstract

Till now, there are many sine PWM techniques and Space Vector PWM techniques existed. They perform well for Under-Modulation Indexes. When they enter into Over-Modulation region, their performance degraded. In this paper, we are going to discuss about a new Space Vector PWM technique, which gives better performance in Over-Modulation zone also. Here, we are going to check Electromagnetic Torque ripple, stator flux ripple, stator current ripple and inverter switching losses of proposed technique by using MATLAB/Simulink and compared with existed techniques.

Contents

Abstract	iv
Contents	v
List of symbols	vi
List of figures	ix
List of tables	x
Abbreviations	xi
1 Introduction	1
1.1 Sine PWM Technique	1
1.2 Space Vector PWM Technique	2
2 Literature Survey	4
2.1 Stator Flux Ripple Over a Sub-cycle	4
2.2 Stator Current Ripple Over a Sub-cycle	8
2.3 Switching Loss	8
3 Implementation of SVPWM Technique	10
4 Over-Modulation	13
4.0.1 Over-modulation Zone-1	14
4.0.2 Over-modulation Zone-2	15
4.1 Stator Flux Ripple Over a Sub-cycle	16
4.1.1 When Modified Reference Vector is on Hexagon	16
5 Simulation Results	19
6 Experimental Results	42
7 Conclusion and Future Work	67
Conclusions	67
Appendix-A	68
Appendix-B	69

List of symbols

p	: Number of stator poles
V_{Err}	: Error Voltage Vector
V_{Ref}	: Reference Voltage Vector
F_{Seq}	: RMS value of Flux error vector for particular sequence
i	: Current in each phase of machine
Φ_1	: Fundamental RMS flux
F_{Dist}	: Total RMS flux harmonic distortion factor
E_{Sub}	: Normalized switching loss per sub-cycle
$E_{Sub(avg)}$: Average value of normalized switching loss over a fundamental cycle

List of Figures

1.1	Circuit Diagram of Three Phase VSI	1
1.2	Switching Signals of Sine PWM Technique	2
1.3	Space Vector Modulation Operation in Linear Region	3
2.1	Stator Flux Ripple Vectors Over a Sub-cycle and Their d-axis and q-axis Components for Different Sequences	6
3.1	Flow Chart for Implementing Space Vector PWM	11
4.1	Phase and Fundamental Voltages for Six-step Operation	13
4.2	Operation in Over-modulation Zone-1	14
4.3	Voltage Vector Trajectory in Over-modulation Zone-2	15
4.4	Fundamental Voltage in Over-modulation Zone-2	16
4.5	Stator Flux Ripple Vector and d-q components	17
5.1	Stator Flux for All Sequences in d and q axes	20
5.2	Stator Flux Ripple for All Sequences in d and q axes	21
5.3	RMS Stator flux ripple and THD Vs Frequency Curve for Different Sequences	22
5.4	Stator Current Ripple and Torque for All Sequences	23
5.5	Voltage Between Inverter Phase to DC Bus Neutral for Different Sequences for 30Hz	24
5.6	Voltage Between Inverter Phase to DC Bus Neutral for Different Sequences for 50Hz	25
5.7	Voltage Between Inverter Phase to Phase for Different Sequences for 50Hz	26
5.8	Inverter Line Current and Its THD Values for Different Sequences	27
5.9	Switch Current and Losses at 5Nm load for Different Sequences	28
5.10	Switch Current and Losses at 10Nm load for Different Sequences	29
5.11	Switch Current and Losses at 15Nm load for Different Sequences	30
5.12	The voltage between inverter phase to dc bus neutral, phase current and operating sector for 012 sequences at different frequencies	32
5.13	The voltage between inverter phase to dc bus neutral, phase current and operating sector for 12 sequences in Over-modulation region at different voltage references	33
5.14	FFT analysis of the voltage between inverter phase to dc bus neutral for 012 sequences at different frequencies	34
5.15	FFT analysis of the voltage between inverter phase to dc bus neutral for 12 sequences in Over-modulation region at different reference voltages	35
5.16	The voltage between inverter phase to dc bus neutral, phase current and operating sector for 0121 sequences at different frequencies	36

5.17	The voltage between inverter phase to dc bus neutral, phase current and operating sector for 0121 sequences in Over-modulation region at different voltage references	37
5.18	FFT analysis of the voltage between inverter phase to dc bus neutral for 0121 sequences at different frequencies	38
5.19	FFT analysis of the voltage between inverter phase to dc bus neutral for 0121 sequences in Over-modulation region at different reference voltages . .	39
5.20	RMS Stator Flux Ripple for Modulation index of 1.02	40
5.21	Total RMS Harmonic Distortion Factor Vs Frequency Curve	40
5.22	Total RMS Harmonic Distortion Factor Vs Frequency Curve	41
6.1	Project Setup	43
6.2	The voltage between inverter phase to dc bus neutral, phase current and operating sector for 0127 sequences at different frequencies	44
6.3	FFT analysis of the voltage between inverter phase to dc bus neutral for 0127 sequences at different frequencies	45
6.4	FFT analysis of the inverter phase current for 0127 sequences at different frequencies	46
6.5	The voltage between inverter phase to dc bus neutral, phase current and operating sector for 012 sequences at different frequencies	47
6.6	The voltage between inverter phase to dc bus neutral, phase current and operating sector for 012 sequences in Over-modulation region at different voltage references	48
6.7	FFT analysis of the voltage between inverter phase to dc bus neutral for 012 sequences at different frequencies	49
6.8	FFT analysis of the voltage between inverter phase to dc bus neutral for 012 sequences in Over-modulation region at different reference voltages . .	50
6.9	FFT analysis of the inverter phase current for 012 sequences at different frequencies	51
6.10	FFT analysis of the inverter phase current for 012 sequences in Over-modulation region at different reference voltages	52
6.11	The voltage between inverter phase to dc bus neutral, phase current and operating sector for 721 sequences at different frequencies	53
6.12	FFT analysis of the voltage between inverter phase to dc bus neutral for 721 sequences at different frequencies	54
6.13	FFT analysis of the inverter phase current for 721 sequences at different frequencies	55
6.14	The voltage between inverter phase to dc bus neutral, phase current and operating sector for 0121 sequences at different frequencies	56
6.15	The voltage between inverter phase to dc bus neutral, phase current and operating sector for 0121 sequences in Over-modulation region at different voltage references	57
6.16	FFT analysis of the voltage between inverter phase to dc bus neutral for 0121 sequences at different frequencies	58
6.17	FFT analysis of the voltage between inverter phase to dc bus neutral for 0121 sequences in Over-modulation region at different reference voltages . .	59
6.18	FFT analysis of the inverter phase current for 0121 sequences at different frequencies	60

6.19 FFT analysis of the inverter phase current for 0121 sequences in Over-modulation region at different reference voltages	61
6.20 The voltage between inverter phase to dc bus neutral, phase current and operating sector for 7212 sequences at different frequencies	62
6.21 FFT analysis of the voltage between inverter phase to dc bus neutral for 7212 sequences at different frequencies	63
6.22 FFT analysis of the inverter phase current for 7212 sequences at different frequencies	64

List of Tables

5.1	Fundamental voltage values for different sequences at different frequencies	31
6.1	Fundamental voltage and its THD values for different sequences at different frequencies	43
6.2	Fundamental current and its THD values for different sequences at different frequencies	65
6.3	Fundamental voltage, current and Their THD values for 12 sequence in over-modulation at different reference voltages	65
6.4	Fundamental voltage, current and Their THD values for 121 sequence in over-modulation at different reference voltages	66
7.1	Simulation parameters	68

Abbreviations

VSI	:	Voltage Source Inverter
CSVPWM	:	Conventional Space Vector PWM
BCPWM	:	Bus Clamping PWM
THIPWM	:	Triple Harmonic Injection PWM

Chapter 1

Introduction

From past decades, the usage of Induction machine with Voltage Source inverter is gradually increasing. The Figure 1.1 shows the circuit diagram of three phase VSI. To control the ON/OFF of the switches of the VSI, there should be gating pulses given. There are mainly two methods, to generate gating pulses. They are 1. Sine PWM technique and 2. Space Vector PWM technique.

1.1 Sine PWM Technique

Sine PWM technique is very commonly used method and simple method to implement. In this method, a sinusoidal modulating signal is compared with a triangular carrier. The sine wave is called as reference signal and its frequency is equal to the required output fundamental voltage frequency. The triangular waveform is called as carrier signal and it's frequency is decided by switching frequency of inverter switching devices. When reference signal is greater than carrier signal, then gating signal is generated. Otherwise, no gating signal is generated for inverter switches. The pulses of sine PWM technique is shown in Figure 1.2.

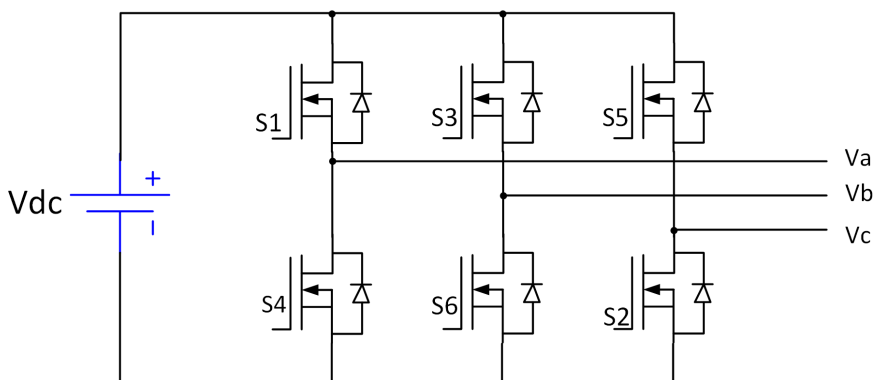


Figure 1.1: Circuit Diagram of Three Phase VSI

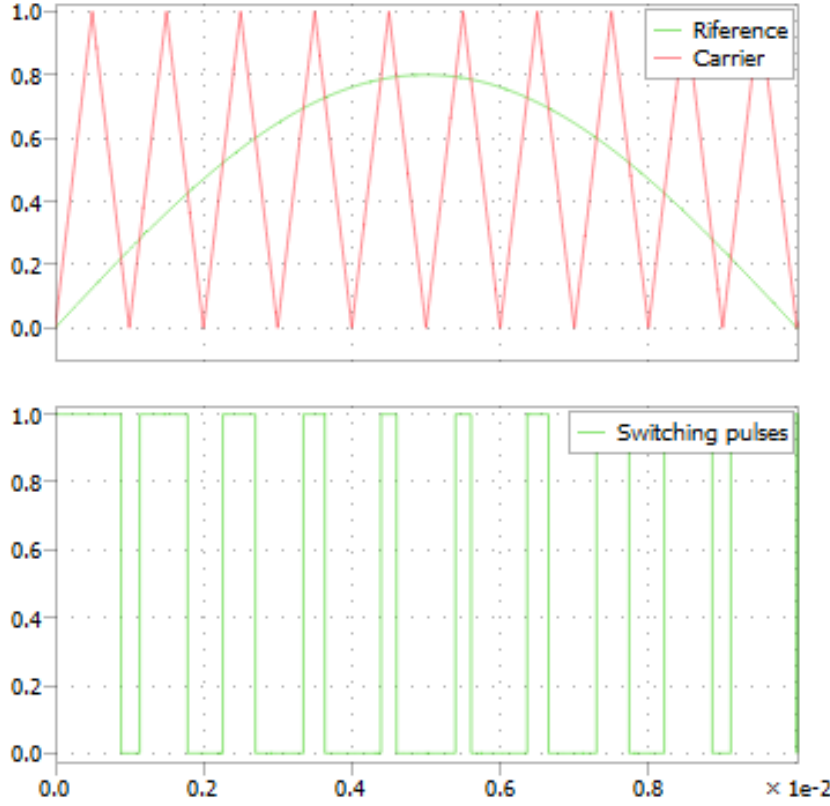


Figure 1.2: Switching Signals of Sine PWM Technique

1.2 Space Vector PWM Technique

This is also another control technique to control VSI gating signals. The switches of VSI can be turn ON/OFF in eight different combinations. Due to each combination one vector is generated. When all the upper switches are ON or all the lower switches are ON then, the output of VSI is zero and that vector called as zero vector. Remaining all combinations the output has some particular value and they are called as active vectors.

The active vectors are normalized by dc bus voltage V_{DC} and displaced by 60° in space vector plane. The required output voltage is given as reference vector, V_{Ref} in space vector plane and it can be generated by applying active vectors and zero vectors for time T_1 , T_2 and T_0 respectively, over a sampling time period, T . The sector and reference vector information can be given by diagrammatically and shown in Figure 1.3. When the reference vector lies in sector I, the active vectors and the zero vector operating times are given by

$$T_1 = V_{Ref} \frac{\sin(60^\circ - \alpha)}{\sin(60^\circ)} T \quad (1.1)$$

$$T_2 = V_{Ref} \frac{\sin(\alpha)}{\sin(60^\circ)} T \quad (1.2)$$

$$T_0 = T - T_1 - T_2 \quad (1.3)$$

In conventional Space vector PWM, the zero vector is divided in equal halves and operated in a sampling time. In Bus-Clamping Space Vector PWM technique, the time period of zero vector is continuously applied. In Advanced Bus-Clamping Space Vector

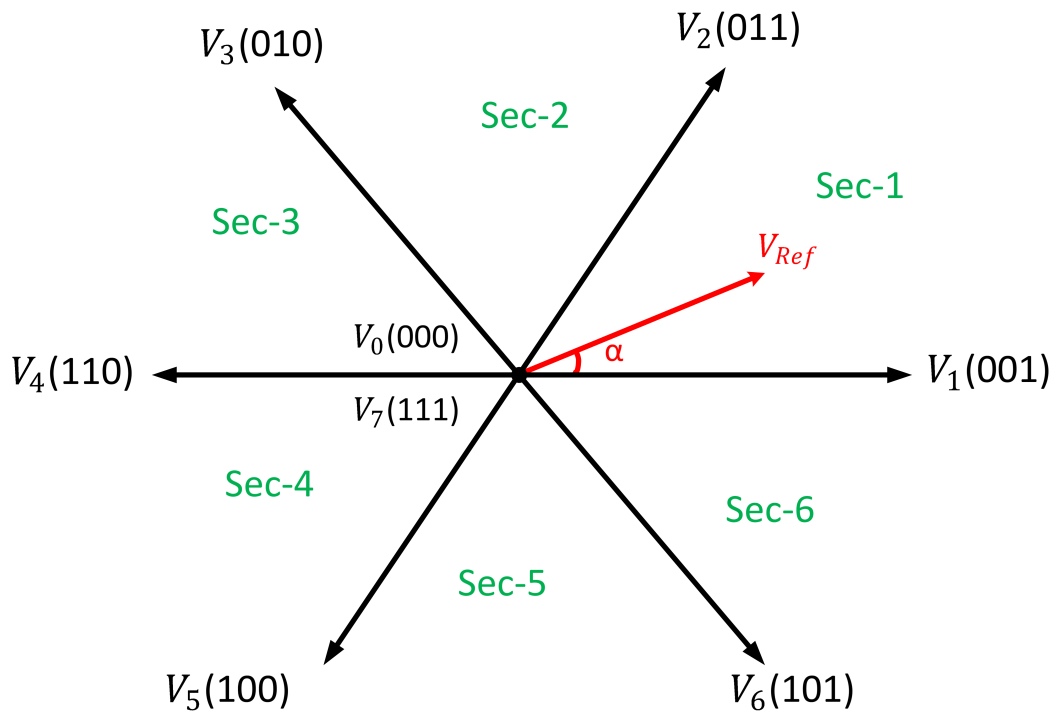


Figure 1.3: Space Vector Modulation Operation in Linear Region

PWM technique, the active vectors are divided in two equal halves and operated at different timings in a sampling period. The Over-Modulation technique is used to extend the range of operation and increase the DC bus utilization.

Chapter 2

Literature Survey

From past decades, the usage of Induction machine with Voltage Source inverter is gradually increasing. Before the invention of microprocessor, carrier base PWM methods are used. After the invention of microprocessor, the space vector PWM technique becomes one of the best method for inverter switching. For three phase 2-level inverter has eight valid switching states. To reduce RMS current ripple, use hybrid space vector PWM over the conventional method. In this, at one sector 2 or 3 switching sequences are applied together. In bus clamping method, two phases switching once and third phase should be clamped. While, in advanced clamping method one phase is switching twice, other phase switching once and remaining phase is at clamping situation. By using this advanced clamping sequence, the torque ripple of induction machine reduced.

While the reference vector lies inside of the hexagon then it is referred as under-modulation region. When the reference vector crosses the hexagon boundary it gives time for zero vector in negative values, it means that inverter is enter into over-modulation region. In over modulation region there are two zones. in zone-1, when the reference lies on hexagon side, then only active vectors are applied and zero vector is stopped for particular time and inside of hexagon it operated in normal one. During zone zone 2, only one active vector is applied at the extreme corners of vector. In previous days 12 switching sequence is preferred but now 121 switching have good performance characteristics in over modulation region.

There exist different types of Space Vector PWM techniques based on division of zero vector or active vectors. According to this division, in conventional sequences like 0127 and 7210, have the two zero vectors in a sub-cycle and time for each Zero vector is half of T_0 . It is also done by sine PWM technique by injecting third harmonic components to reference sine waveform. In bus-clamping sequences 012,120,721 and 217 only one zero vector is applied over a sub-cycle. The division of active vectors is only possible in Space Vector PWM technique and not possible in sine PWM technique. Due to that, the advanced bus-clamping sequence 0121, 1210, 7212, and 2127, have the equal division in active vectors.

2.1 Stator Flux Ripple Over a Sub-cycle

The stator flux ripple vector is calculated by integrating the error voltage vector with respect to time. At any time instant, there is a difference between applied voltage vector and reference voltage vector and that difference vector is known as error voltage

vector. These error vectors are also revolving with synchronous speed in d-q frame and given as

$$V_{\text{Err}} = V_{\text{applied}} - V_{\text{Ref}} \quad (2.1)$$

So, error voltage vectors for different voltage vectors are applied are given as

$$V_{\text{Err}1} = \sin(\alpha) + j[\cos(\alpha) - V_{\text{Ref}}] \quad (2.2)$$

$$V_{\text{Err}2} = -\sin(60^\circ - \alpha) + j[\cos(60^\circ - \alpha) - V_{\text{Ref}}] \quad (2.3)$$

$$V_{\text{Err}0} = -jV_{\text{Ref}} \quad (2.4)$$

The time period of sub-cycle for 0127, 0121 and 7212 sequences is T, where as it is $2T/3$ for 012 and 721 sequences. By using this, all the sequences are compared for a average switching frequency, F_{sw} . The flux ripple vector components along the d-axis and q-axis are given as

$$Q_1 = [\cos(\alpha) - V_{\text{Ref}}]T_1 \quad (2.5)$$

$$Q_2 = [\cos(60^\circ - \alpha) - V_{\text{Ref}}]T_2 \quad (2.6)$$

$$Q_z = -V_{\text{Ref}}T_0 \quad (2.7)$$

$$D = \sin(\alpha)T_1 \quad (2.8)$$

The error voltage vectors and their flux error vectors and corresponding d-axis and q-axis components for different switching sequences are shown in Figure 2.1. The RMS value of stator flux ripple over a sub-cycle for different sequences is given below

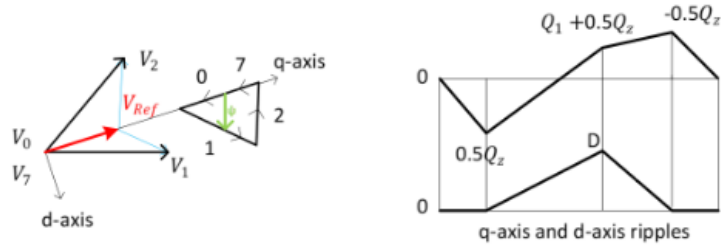
$$\begin{aligned} F_{0127}^2 &= \frac{1}{3}(0.5Q_z)^2 \frac{T_0}{2T} + \frac{1}{3}[(0.5Q_z)^2 + 0.5Q_z(0.5Q_z + Q_1) + (0.5Q_z + Q_1)^2] \frac{T_1}{T} \\ &\quad + \frac{1}{3}[(-0.5Q_z)^2 - 0.5Q_z(0.5Q_z + Q_1) + (0.5Q_z + Q_1)^2] \frac{T_2}{T} + \frac{1}{3}(-0.5Q_z)^2 \frac{T_0}{2T} \\ &\quad + \frac{1}{3}D^2 \frac{(T_1 + T_2)}{T} \end{aligned} \quad (2.9)$$

$$\begin{aligned} F_{012}^2 &= \frac{4}{27}Q_z^2 \frac{T_0}{T} + \frac{4}{27}[Q_z^2 + Q_z(Q_z + Q_1) + (Q_z + Q_1)^2] \frac{T_1}{T} \\ &\quad + \frac{4}{27}[(Q_z + Q_1)^2] \frac{T_2}{T} + \frac{4}{27}D^2 \frac{(T_1 + T_2)}{T} \end{aligned} \quad (2.10)$$

$$\begin{aligned} F_{721}^2 &= \frac{4}{27}Q_z^2 \frac{T_0}{T} + \frac{4}{27}[Q_z^2 + Q_z(Q_z + Q_2) + (Q_z + Q_2)^2] \frac{T_2}{T} \\ &\quad + \frac{4}{27}[(Q_z + Q_2)^2] \frac{T_1}{T} + \frac{4}{27}D^2 \frac{(T_1 + T_2)}{T} \end{aligned} \quad (2.11)$$

$$\begin{aligned} F_{0121}^2 &= \frac{1}{3}(Q_z)^2 \frac{T_0}{T} + \frac{1}{3}[Q_z^2 + Q_z(Q_z + 0.5Q_1) + (Q_z + 0.5Q_1)^2] \frac{T_1}{2T} \\ &\quad + \frac{1}{3}[(-0.5Q_1)^2 - 0.5Q_1(0.5Q_1 + Q_z) + (0.5Q_1 + Q_z)^2] \frac{T_2}{T} + \frac{1}{3}(-0.5Q_1)^2 \frac{T_1}{2T} \\ &\quad + \frac{1}{3}(0.5D)^2 \frac{(T_1 + T_2)}{T} \end{aligned} \quad (2.12)$$

$$\begin{aligned} F_{7221}^2 &= \frac{1}{3}(Q_z)^2 \frac{T_0}{T} + \frac{1}{3}[Q_z^2 + Q_z(Q_z + 0.5Q_2) + (Q_z + 0.5Q_2)^2] \frac{T_2}{2T} \\ &\quad + \frac{1}{3}[(-0.5Q_2)^2 - 0.5Q_2(0.5Q_2 + Q_z) + (0.5Q_2 + Q_z)^2] \frac{T_1}{T} + \frac{1}{3}(-0.5Q_2)^2 \frac{T_2}{2T} \\ &\quad + \frac{1}{3}(0.5D)^2 \frac{(T_1 + T_2)}{T} \end{aligned} \quad (2.13)$$



The RMS value of stator flux ripple over a sector is normalised with respect to fundamental flux, Φ_1 and it is given as

$$\Phi_1 = \frac{V_{\text{Ref}}}{2\pi F_1} \quad (2.14)$$

The total RMS stator flux ripple harmonic distortion factor is denoted by F_{Dist} and given as

$$F_{\text{Dist}} = \frac{1}{\Phi_1} \sqrt{\frac{3}{\pi} \int_0^{\pi/3} F_{\text{Seq}}^2 d\alpha} \quad (2.15)$$

where F_1 is the Fundamental output voltage frequency. For a given sequence, the F_{Dist} is expressed as a function of F_1 or V_{Ref} . Because, in V/f controlled drive the ratio between fundamental voltage and fundamental frequency remains constant. The harmonic distortion factor of continual clamping type and split clamping type are given below

$$F_{\text{Dist}(\text{conti})} = \frac{1}{\Phi_1} \sqrt{\frac{3}{\pi} \left(\int_0^\gamma F_{7212}^2 d\alpha + \int_\gamma^{\pi/3} F_{0121}^2 d\alpha \right)} \quad (2.16)$$

$$F_{\text{Dist}(\text{split})} = \frac{1}{\Phi_1} \sqrt{\frac{3}{\pi} \left(\int_0^\gamma F_{0121}^2 d\alpha + \int_\gamma^{\pi/3} F_{7212}^2 d\alpha \right)} \quad (2.17)$$

From above equations, the harmonic distortion factor is directly proportional to RMS value of flux ripple over a sector and RMS flux ripple depends on switching sequence and reference vector, V_{Ref} . The mean square of flux ripple is less upto 30° in sector I for 0121 sequence and after 30° 7212 has less value of mean square flux ripple. So, in equation form

$$F_{0121}^2(\alpha) < F_{7212}^2(\alpha), \quad \text{for } 0^\circ < \alpha < 30^\circ \quad (2.18)$$

$$F_{7212}^2(\alpha) < F_{0121}^2(\alpha), \quad \text{for } 30^\circ < \alpha < 60^\circ \quad (2.19)$$

$$F_{0121}^2(\alpha) < F_{7212}^2(60^\circ - \alpha) \quad (2.20)$$

The continual clamping with $\gamma = 30^\circ$, gives the high value of flux ripple. Where as, split clamping with $\gamma = 30^\circ$, gives the less value of flux ripple throughout the sector. All the proposed sequences give better results in one half of sector and the same sequence gives poor performance in other half of the sector. In general, split clamping, the worse sequence is used for $\gamma - 30^\circ$ in every sector. So, harmonic distortion is reduced with reduce in $\gamma - 30^\circ$. In continual clamping , the better sequence is used from $\alpha = 30$ to $\alpha = \gamma$ in every sector. So, harmonic distortion decrease with increase in $\gamma - 30^\circ$

The sequence 012 also have less staror flux ripple in first half of a sub-cycle then the 721 sequence and in second half 721 sequence has the less ripple then the 012 sequence. Mathematically,

$$F_{012}^2(\alpha) < F_{721}^2(\alpha), \quad \text{for } 0^\circ < \alpha < 30^\circ \quad (2.21)$$

$$F_{721}^2(\alpha) < F_{012}^2(\alpha), \quad \text{for } 30^\circ < \alpha < 60^\circ \quad (2.22)$$

$$F_{012}^2(\alpha) < F_{721}^2(60^\circ - \alpha) \quad (2.23)$$

2.2 Stator Current Ripple Over a Sub-cycle

The RMS value of current ripple not only depend on magnitude and angle of reference vector, V_{Ref} but also depend upon switching sequence used in that sub-cycle. According to switching only, the zero vector selected and active vector is divided.

Except the 0127 sequence, all other sequences are uses only one zero state. The RMS d-axis flux ripple over a sub-cycle is same for 012 sequence and 721 sequence and also same for 0121 sequence and 7212 sequence. So, here the RMS value of d-axis ripple over a sub-cycle is independent of zero state selected. In case of conventional sequence, the d-axis RMS ripple does not depend on the ratio of division of T_0 between two zero states. When zero vector is applied to the inverter, the q-axis slope of stator flux is always negative, $-V_{\text{Ref}}$. When, active vector V_1 is applied, then the slope is non-negative in the first half of sectorI and its value is $[\cos(\alpha) - V_{\text{Ref}}]$. If active vector, V_2 applied, the q-axis flux ripple has the slope of $[\cos(60^\circ - \alpha) - V_{\text{Ref}}]$, which is either positive or negative in the first half of sectorI depending on relative values of terms in slope. The applied zero vector is effects the q-axis flux ripple to increase it in negative direction. To reduce the q-axis RMS ripple, the vector which is applied next should have the q-axis RMS ripple in positive direction increase.

The 0121 sequence and 7212 sequence have the active vector division. Due to this, double switching is happening in particular phase. These sequences reduce the d-axis zero peak ripple by 50%. So, the d-axis RMS ripple also reduced by 50%. The q-axis is aligned to the error vector direction and d-axis is located at 90° to it. So, the zero error vector is reduce the d-axis flux ripple. The 012 sequence and 0121 sequence has less current ripple in the sector middle and conventional sequence has less ripple at close to $\alpha = 0^\circ$. Finally, the 0121 sequence gives good results at higher values of V_{Ref} with α close to 30° . This is also applicable for 7212 sequence. The torque ripple is calculated from q-axis current current ripple because torque is directly proportional to q-axis current. The instantaneous torque equation is given as

$$\tau = \frac{p}{2} \frac{V_{s1}}{\omega} (1 - \sigma) i_q \quad (2.24)$$

Where p is no of stator poles, V_{s1} is peak value of fundamental phase voltage, σ is ratio to total leakage inductance to magnetising inductance and ω is fundamental angular frequency.

2.3 Switching Loss

The inverter efficiency is depends on power loss by inverter switches. This losses are classified as switching loss and conduction loss. The conduction losses are decided by magnitude of dc bus voltage, load current value, switching frequency and switch dynamic parameters. The normalized switching loss per sub-cycle, E_{Sub} and average value of normalized switching loss over a fundamental cycle, $E_{\text{Sub(avg)}}$ is given by

$$E_{\text{Sub}} = \frac{n i_1}{I_m} = n |\sin(\omega t - \phi)| \quad (2.25)$$

$$E_{\text{Sub(avg)}} = \frac{1}{\pi} \int_0^{\pi} E_{\text{Sub}} d\omega t \quad (2.26)$$

Where n is number of switchings of phase in a given cycle, i_1 is fundamental value of phase current, I_m is peak value of fundamental phase current and ϕ is power factor angle. The dc bus voltage and device switching time are assumed as constant and ripple current is neglected, while calculating switching loss. In order to obtain the inverter switching losses, the average energy loss per sub-cycle is multiplied with the sampling frequency. The sampling frequency is $2F_{sw}$ for conventional sequence, 0121 sequence and 7212 sequence. Where as, it is $3F_{sw}$ for 012 sequence and 721 sequence. The normalised switching loss for 0121 sequence, 012 and 721 sequences and 0121 and 7212 sequences are given respectively,

$$P_{sw} = \frac{E_{Sub(avg)}}{(2/\pi)} \frac{F_s}{F_{sw}} \quad (2.27)$$

$$P_{sw1} = \frac{3\pi}{4} E_{Sub(avg)} \quad (2.28)$$

$$P_{sw2} = \frac{\pi}{2} E_{Sub(avg)} \quad (2.29)$$

Chapter 3

Implementation of SVPWM Technique

The flow chart for implementation of space vector PWM is shown in Figure 3.1. For implementation of space vector PWM technique, the following steps should be followed

Step-1: The reference voltage and frequency values are selected based on required output voltage and frequency for the desired operation.

Step-2: Convert those three phase voltages into two phase voltages by using abc to $\alpha\beta$ conversion. In this conversion, if V_a , V_b and V_c are three phase voltages, then the two phase voltages V_α and V_β are given as

$$V_\alpha = \frac{2}{3}[V_a - \frac{V_b}{2} - \frac{V_c}{2}] = V_a \quad (3.1)$$

$$V_\beta = \frac{2}{3}[\frac{\sqrt{3}}{2}V_b - \frac{\sqrt{3}}{2}V_c] = \frac{1}{\sqrt{3}}[V_b - V_c] \quad (3.2)$$

Step-3: The V_α and V_β components are real and imaginary components of the reference voltage vector. To get the magnitude and phase angle of reference voltage vector, the rectangle form of reference vector is converted into polar form. From the magnitude calculate the modulation index, M_a .

Step-4: As the region of space vector is divided into six sectors, it needs to be found in which sector, the reference vector is going to lie. Each sector takes angle of 60 degrees. From the reference voltage phase angle, the operating sector is easily identified. After identification of sector, the space vectors of that sector should be applied for specific time periods and those timings are calculated.

Step-5: From the value of modulation index find out the operating one. If M_a is less than 1, it operates in under-modulation zone. If M_a is greater than 1, it operates in over-modulation region. The over-modulation region is divided into two zones according to values of M_a . They are zone-1, which operates for M_a values of greater than 1 and less than 1.05. Another one is zone-2, which operates for M_a values of greater than 1.05 and less than 1.1. If M_a value is more than 1.1 then, it enters into six-step mode. The Timing calculation for vectors in each region is explained below

In under-modulation region, For example, the reference vector lies in sector-1, then the space vector-1 is operated for T_1 seconds, the space vector-2 is operated for T_2 seconds

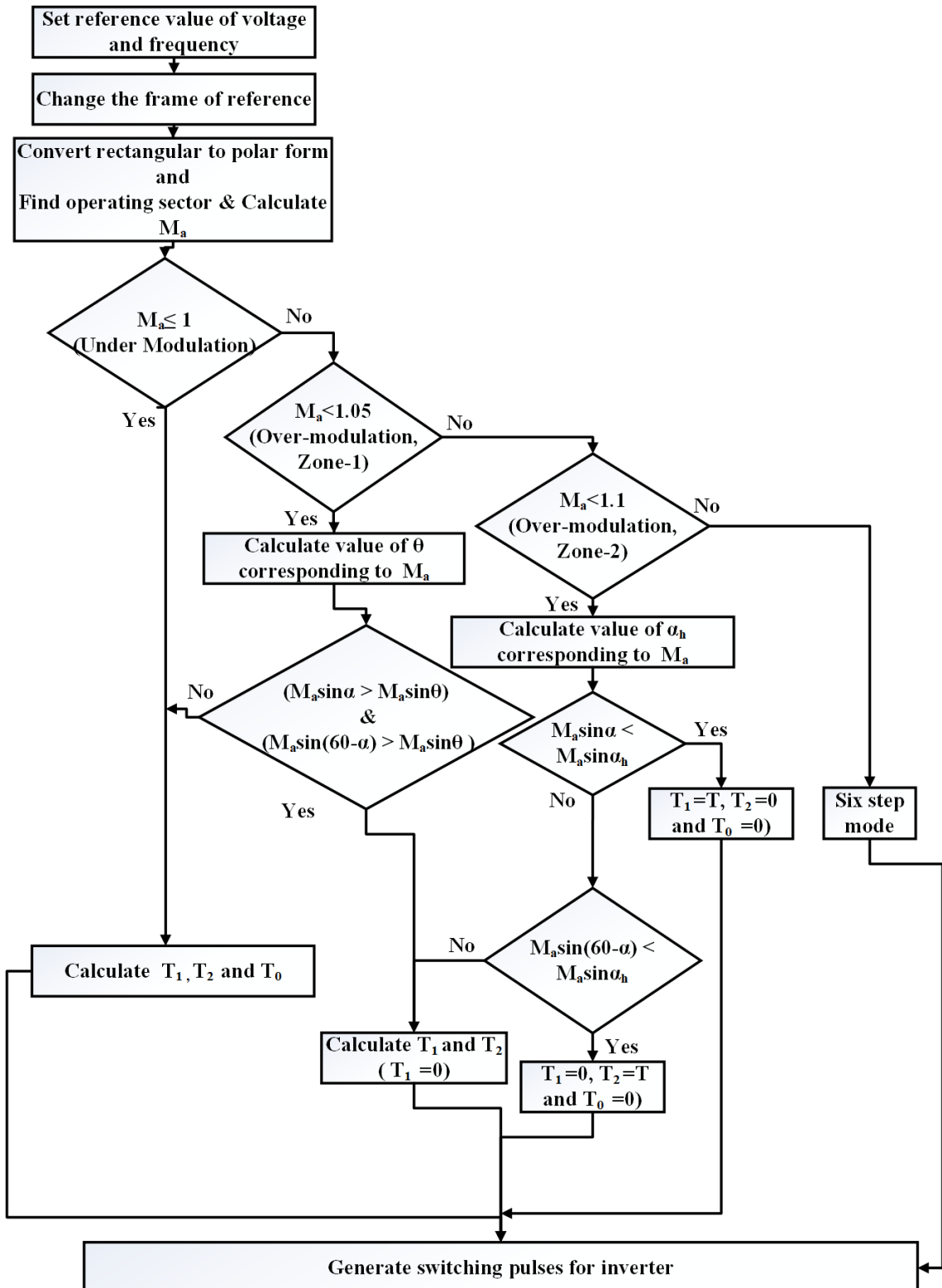


Figure 3.1: Flow Chart for Implementing Space Vector PWM

and zero vector is applied for T_0 seconds and they are given as

$$T_1 = V_{\text{Ref}} \frac{\sin(60^\circ - \alpha)}{\sin(60^\circ)} T \quad (3.3)$$

$$T_2 = V_{\text{Ref}} \frac{\sin(\alpha)}{\sin(60^\circ)} T \quad (3.4)$$

$$T_0 = T - T_1 - T_2 \quad (3.5)$$

In over-modulation region zone-1, first the value of θ is calculated according to M_a . When the reference vector lies inside the hexagon it generates the timings as the under-modulation region. If the reference vector lies on the hexagonal side then only active vectors are operated. So that, the time for zero vector becomes zero. For example, the reference vector belongs to sector-1, then the space vector-1 is operated for T_1 seconds, the space vector-2 is operated for T_2 seconds and they are given as

$$T_1 = \frac{\sin(60^\circ - \alpha)}{\sin\alpha + \sin(60^\circ - \alpha)} T \quad (3.6)$$

$$T_2 = T - T_1 \quad (3.7)$$

In over modulation zone-2, first the value of α_h is calculated according to M_a . When the reference vector lies in this region it holds the nearest active vector for the duration of α_h . In remaining time it switches like zone-1. For example, in sector-1, if holds the active vector-1, then the time for zero vector and active vector-2 becomes zero. It means the time for active vector becomes T . Similarly, if reference vector near to active vector-2, then only T_2 becomes T and other are equal to zero.

Step-6: By using this timings, reference signal is generated and compared with carrier signal to generate the switching pulses for inverter.

Chapter 4

Over-Modulation

For low voltage motor drive applications, in order to increase the dc bus voltage utilisation rate and extend the operating boundary of induction motors, the modulation index is often extended from the linear modulation region to the over-modulation region. By going to over-modulation region, the dynamic performance of the PWM controlled ac drive also improved and steady state operating region also increased.

Before going to over-modulation region, let us discuss about how the modulation index is calculated. From Figure 4.1, the maximum value of fundamental voltage in six-step mode is given by

$$V_{\max6} = \frac{4}{\pi} \frac{V_{dc}}{2} = \frac{2V_{dc}}{\pi} \quad (4.1)$$

We know that the modulation index is the ratio between the peak of reference fundamental to the peak fundamental output voltage in six-step operation. By using this statement, m is given as

$$m = \frac{|V_{Ref}|}{V_{\max6}} = \frac{V_{Ref}}{\frac{2V_{dc}}{\pi}} = \frac{\pi}{2} \frac{V_{Ref}}{V_{dc}} \quad (4.2)$$

The maximum amount of reference voltage, that can be applied in the linear modulation region is given as

$$|V_{Ref}|_{\max} = \frac{2}{3} V_{dc} * \frac{\sqrt{3}}{2} = \frac{V_{dc}}{\sqrt{3}} \quad (4.3)$$

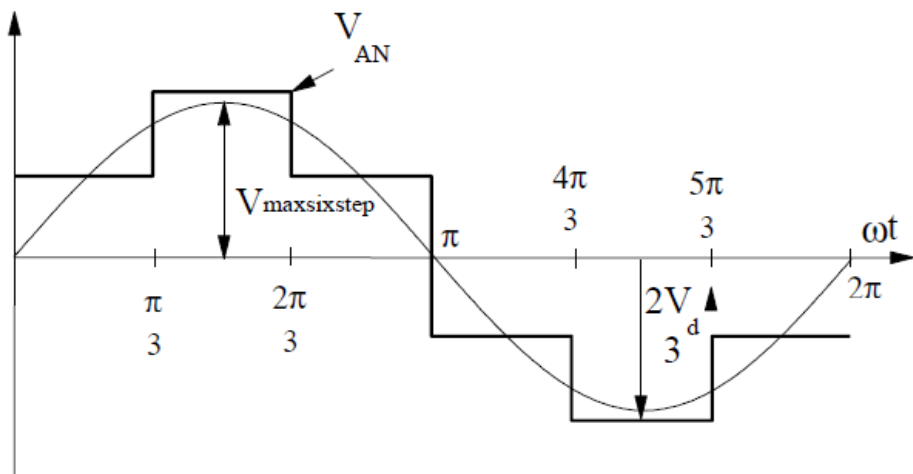


Figure 4.1: Phase and Fundamental Voltages for Six-step Operation

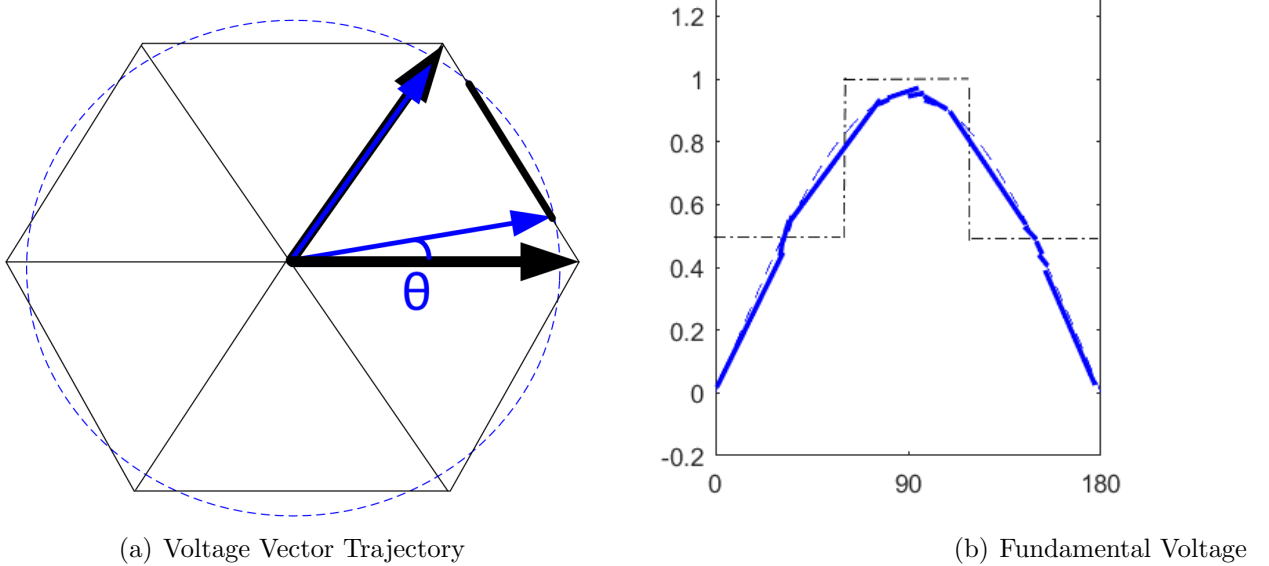


Figure 4.2: Operation in Over-modulation Zone-1

From the equations 4.2 and 4.3, the maximum amount of modulation in the linear zone is given as

$$m_{L\text{-max}} = \frac{\frac{V_{dc}}{\sqrt{3}}}{\frac{2V_{dc}}{\pi}} = \frac{\pi}{2\sqrt{3}} = 0.907 \quad (4.4)$$

If the modulation index value exceeds than the 0.907, then it is called as over-modulation region of operation. Here the reference voltage V_{Ref} crosses the hexagonal area. The over-modulation region is again classified into two zones based on modulation index value. They are explained below in detailed manner.

4.0.1 Over-modulation Zone-1

In this zone, the modulation index value varies from 0.907 to 0.952. In this region, the modified reference vector is lies on hexagon side when the actual reference crosses the hexagonal region and stay on the circle when it lies inside of hexagon. The Figure 4.2 shows the modified reference voltage trajectory and its corresponding fundamental phase voltage. When the reference vector lies inside of the hexagon, the switching timings are calculated as normally. At angle θ , the reference voltage vector is crosses the hexagonal region. When the reference voltage crosses the hexagonal region, then the operating time for zero vector becomes negative, which is a meaningless. Due to that, the reference vector need to be modify. This modified reference vector lies on hexagon side, then the operating time of zero vector becomes zero and only active vectors are applied to generate that modified reference vector. The operating timings of this active vectors are given as

$$T_1 = \frac{T}{2} \left(\frac{\sqrt{3}\cos\alpha - \sin\alpha}{\sqrt{3}\cos\alpha + \sin\alpha} \right) \quad (4.5)$$

$$T_2 = \frac{T}{2} - T_1 \quad (4.6)$$

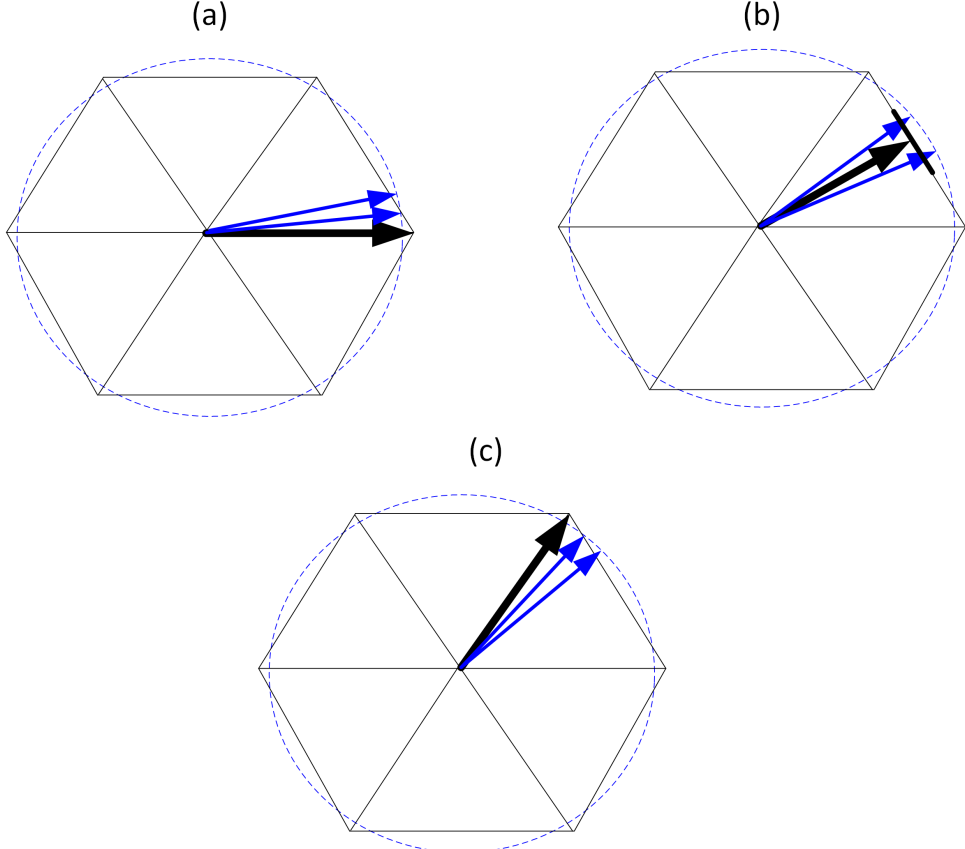


Figure 4.3: Voltage Vector Trajectory in Over-modulation Zone-2

When the modified reference vector moves on the hexagonal side, then the fundamental voltage rises linearly. When the reference vector lies inside of hexagon, then fundamental voltage follows its original sinusoidal path. The modified reference voltage magnitude V with respect to α is given as

$$|V| = \begin{cases} V_{ref}, & 0 \leq \alpha \leq \theta \\ \frac{\sqrt{3}}{\cos(\frac{\pi}{6} - \alpha_{ref})}, & \theta \leq \alpha \leq (\frac{\pi}{3} - \theta) \\ V_{ref}, & (\frac{\pi}{3} - \theta) \leq \alpha \leq (\frac{\pi}{3}) \end{cases}$$

4.0.2 Over-modulation Zone-2

In this zone, the modulation index varies from 0.952 to 1. The modulation index is equal to 1 means it operated at six-step mode. Here the modified voltage reference vector is always applied on the hexagonal side only as discussed above. The Figure 4.3 shows the modified reference vector trajectory with its fundamental phase voltage for this zone. If modulation index value is greater than 0.952, the reference voltage vectors are moved very closer to active vectors which are nearer to them. In this zone, the reference voltage is Hold for certain time, α_h at corner points of hexagon. During this time the fundamental voltage is constant and follows the output of six-step mode. But, when modified reference voltage is on the hexagon side, the fundamental voltage is increased linearly. In this zone, the angle of reference vector is varied and given as

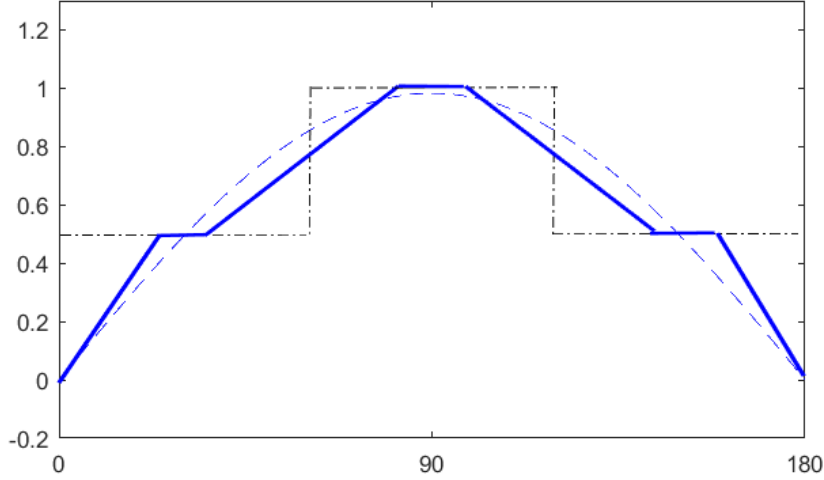


Figure 4.4: Fundamental Voltage in Over-modulation Zone-2

$$\alpha = \begin{cases} 0, & 0 \leq \alpha \leq \alpha_h \\ \frac{\pi}{6} \left(\frac{\alpha - \alpha_h}{\frac{\pi}{6} - \alpha_h} \right), & \alpha_h \leq \alpha_{ref} \leq \left(\frac{\pi}{3} - \alpha_h \right) \\ \frac{\pi}{3}, & \left(\frac{\pi}{3} - \alpha_h \right) \leq \alpha \leq \left(\frac{\pi}{3} \right) \end{cases}$$

4.1 Stator Flux Ripple Over a Sub-cycle

4.1.1 When Modified Reference Vector is on Hexagon

When the synthesized applied vector is on the edge of the hexagon, it is only required to apply the active vectors. Hence, the flux error vector has only d-axis component and q-axis component becomes zero. The stator flux ripple vector and its d-axis and q-axis components are shown in Fig. 4.5. Fig. 4.5(a) shows one of the possible combination of the applied vectors in the over-modulation zone (except during six-step mode or during the reference tracing mode). In this case the flux error vector tip will move from point 1 to 2 (when voltage vector V_1 is applied), the d-axis ripple increases with positive slope and reaches its maximum value at the end and consequently from point 2 to 1 (when voltage vector V_2 is applied), the d-axis ripple start decreasing to zero as its slope becomes negative.

Fig. 4.5(b) shows the second possible combination of the applied vectors in the over-modulation zone (except during six-step mode or during the reference tracing mode). In this case the flux error vector tip will move from point 1 to 2 (when voltage vector V_2 is applied), the d-axis flux ripple start increase in negative direction due to negative slope and reaches its peak at the point 2. Consequently from point 2 to 1 (when voltage vector V_1 is applied), the d-axis flux ripple start increase towards zero due to positive slope. The q-axis component is zero. So that,

$$\Psi_q^2 = 0 \quad (4.7)$$

$$\Psi_d^2 = \frac{1}{3} D^2 \frac{(T_1 + T_2)}{T} \quad (4.8)$$

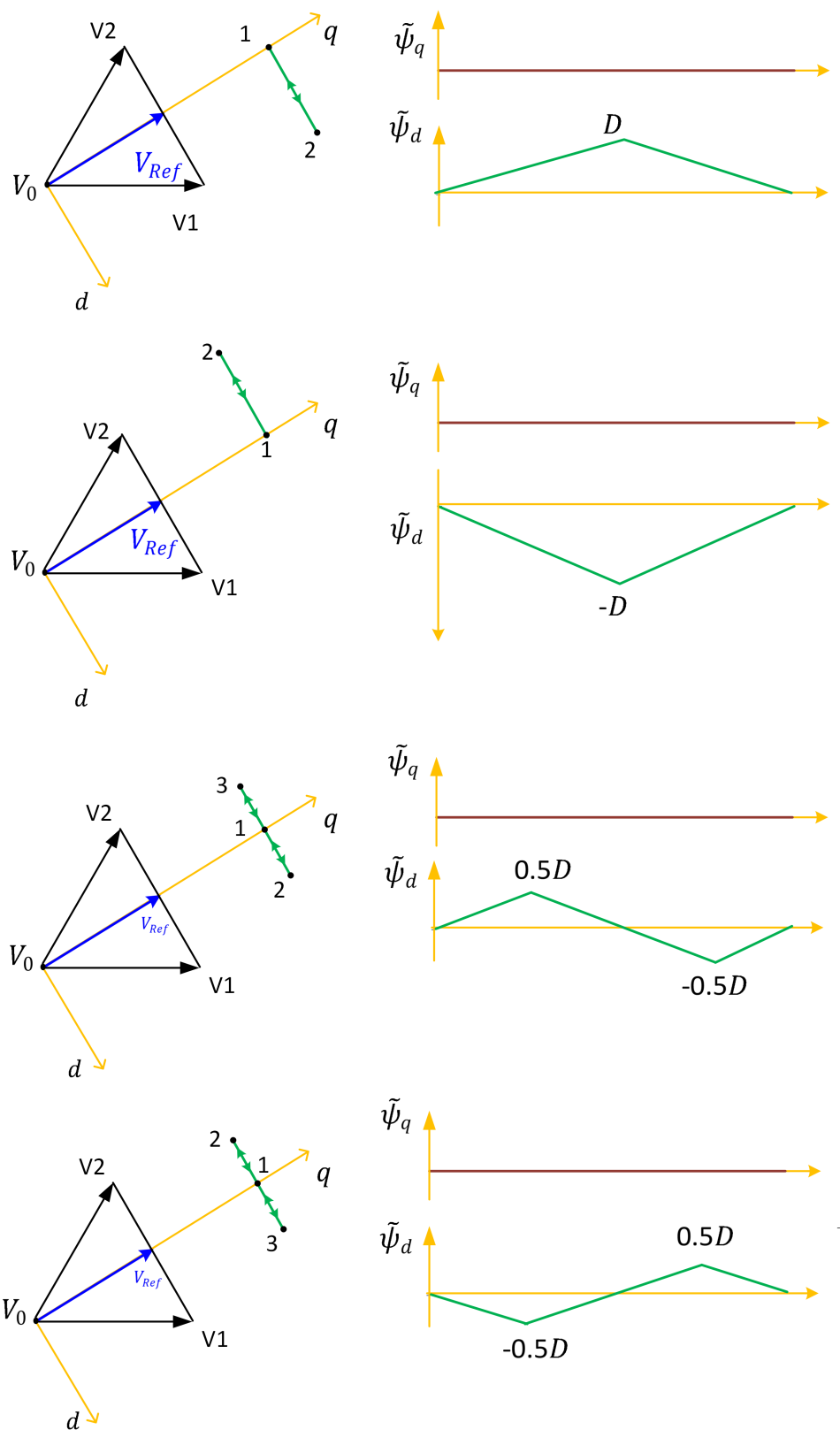


Figure 4.5: Stator Flux Ripple Vector and d-q components

In over-modulation region, only active vectors are applied. So

$$T_1 + T_2 = T \quad (4.9)$$

Now equation 4.8 changes as,

$$\Psi_d^2 = \frac{1}{3}D^2 \quad (4.10)$$

The RMS value of stator flux ripple over a sub-cycle for reference vector on hexagon is given as

$$F_{\text{hex}}^2 = \Psi_q^2 + \Psi_d^2 = \frac{1}{3}D^2 \quad (4.11)$$

Fig. 4.5(c) shows the third possible combination of the applied vectors in the over-modulation zone (except during six-step mode or during the reference tracing mode). In this case the flux error vector tip will move from point 1 to 2 (when voltage vector V_1 is applied), point 2 to 3 (when voltage vector V_2 is applied) and consequently from point 3 to 1 (when voltage vector V_1 is applied again). In this case, it is important to note that the peak of the d-axis error flux ripple is equal to $0.5D$, Whereas in other two cases it is D . Hence, in this method flux ripple can be reduced significantly. Similarly if the vectors are applied in the opposite sequence it will lead to swapping of point 2 and 3 in Fig. 4.5(c). Here also q-axis component is zero. So d-axis component is given by

$$\Psi_d^2 = \frac{1}{3}0.5D^2 \frac{(T_1 + T_2)}{T} = \frac{1}{3}0.5D^2 \quad (4.12)$$

The RMS value of stator flux ripple over a sub-cycle for reference vector on hexagon is given as

$$F_{\text{hex}}^2 = \Psi_q^2 + \Psi_d^2 = \frac{1}{3}(0.5D)^2 \quad (4.13)$$

Chapter 5

Simulation Results

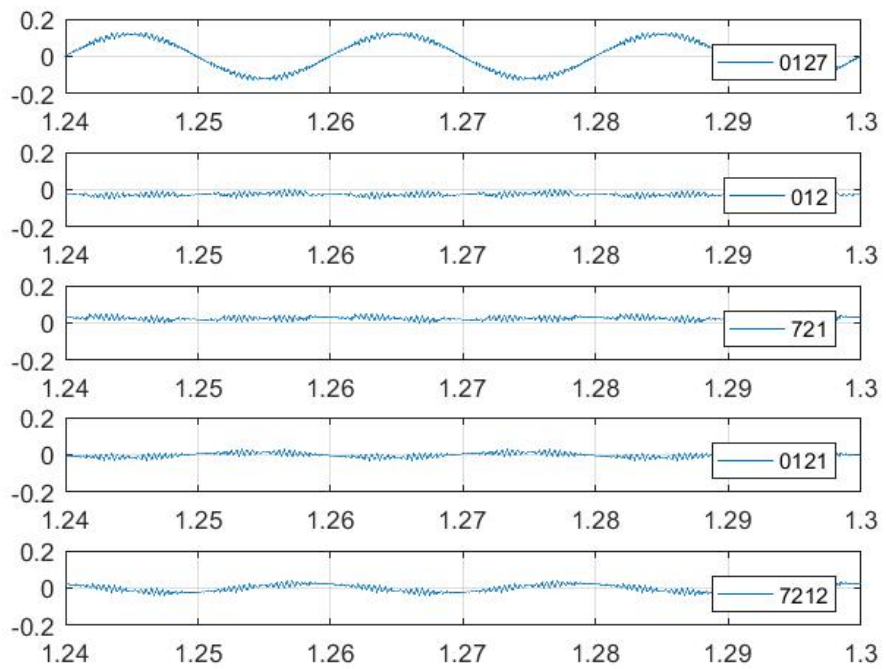
This chapter tell about the results obtained so far from simulation as well as from the DSP programming part. All the simulations are carried out with the same machine parameter for different applied sequences. The Stator d-axis flux, q-axis flux for different sequences are observed and it is shown in Figure 5.1. It can seen from the figure that 0127 gives the highest d-axis flux ripple among the all other sequences.

The ripple quantities of these sequences are shown in Figure 5.2. From Figure 5.2, we can say that except traditional sequence reaming all sequences are giving less flux ripple.

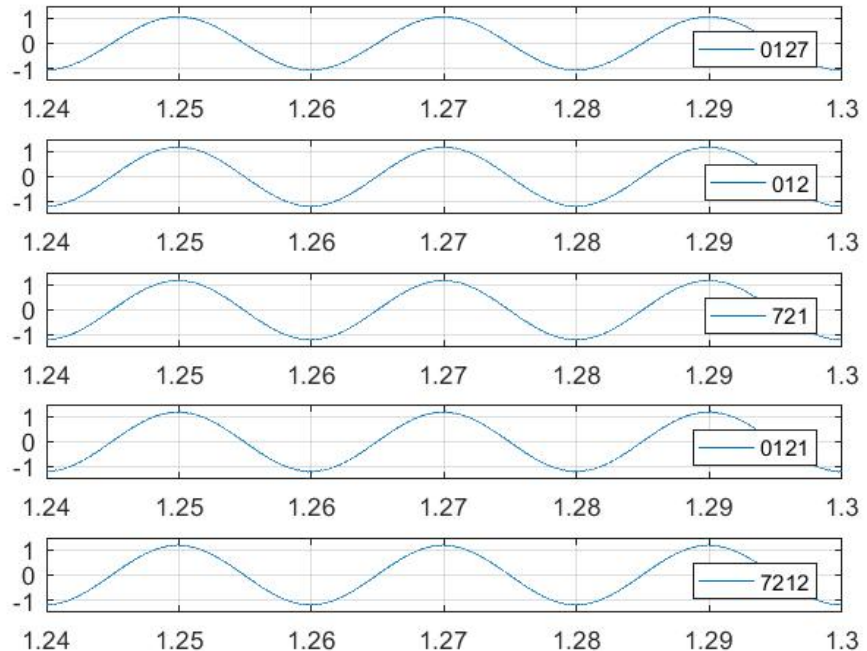
The RMS value of stator flux ripple vs reference voltage angle α , is shown in Figure 5.3(a). From this figure we can observe that the RMS flux ripple is very high and it is nearly double at $\alpha=30$. From 012 and 721 sequences, 721 has less ripple upto 30 degrees. After 30 degrees 012 has the less ripple than the 721 sequence. Overall the 7212 sequence has the less RMS flux ripple upto 30 degrees and after that the 0121 sequence has the less amount of RMS flux ripple. The total RMS harmonic distortion factor of stator flux vs frequency graph is shown in Figure 5.3(b). Here the 0121 and 7212 sequences and 012 and 721 sequences are as single curves because their operating vectors are similar type for same duration. The stator current ripple and machine torque ripple for different sequences are shown in Figure 5.4. These two graphs looks similar, because the torque ripple is mainly depend on the current ripple.

The voltage between inverter phase to dc bus neutral and inverter phase to phase voltages for different sequences are shown in Figure 5.5 and Figure 5.7, respectively. From the phase voltage waveform, we can clearly observe double pulses in 0121 sequence which are not present in remaining sequences. In 0121 sequence we get double pulse due to the active vector division is happening in each sub-cycle. The stator current waveform with THD analysis for different sequences are plotted and shown in Figure 5.8. From that we can say, the traditional sequence has the less current ripple than all sequences. The 0121 sequence also has the less current ripple while compared with 012 and 721 sequences. By keeping load on the machine as constant, the switch current and switching loss of 0127, 012, 721 and 0121 sequences at 5Nm, 10Nm and 15Nm are shown in Figure 5.9, Figure 5.10, and Figure 5.11, respectively. The switching loss in 012, 721 and 0121 sequences are going zero during the bus clamping period. The 0121 has the double amount of switching loss during the double switching happening. All of these results are collected by using MATLAB Simulink and PLECS softwares.

The 012 sequence and 0121 sequences are extended to over-modulation region. Ac-

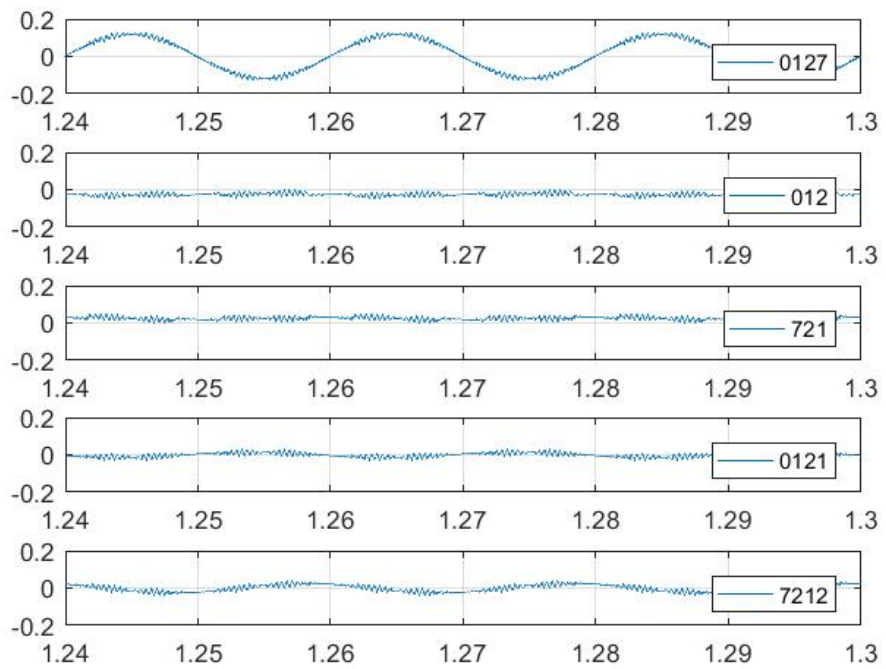


(a) d-axis

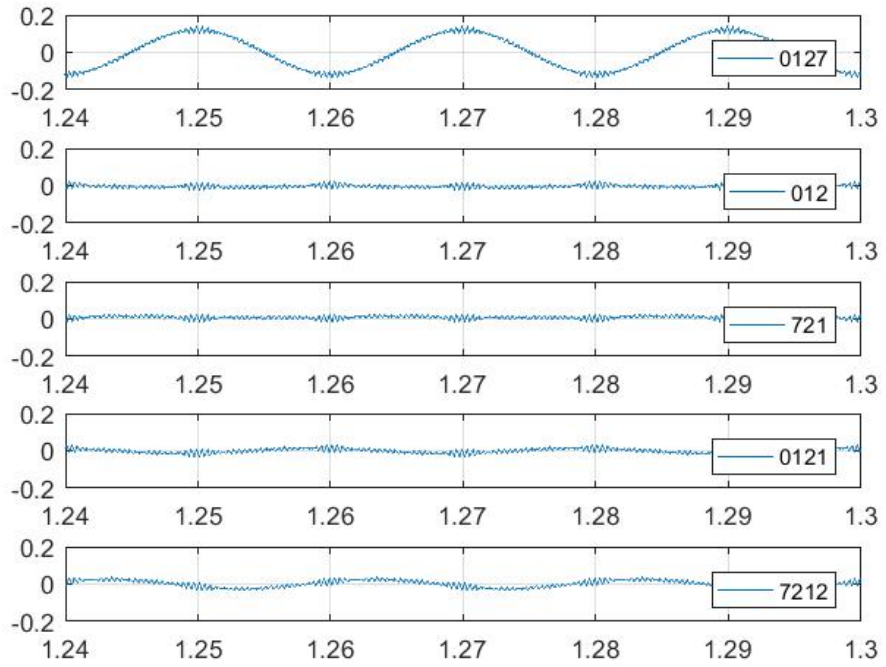


(b) q-axis

Figure 5.1: Stator Flux for All Sequences in d and q axes

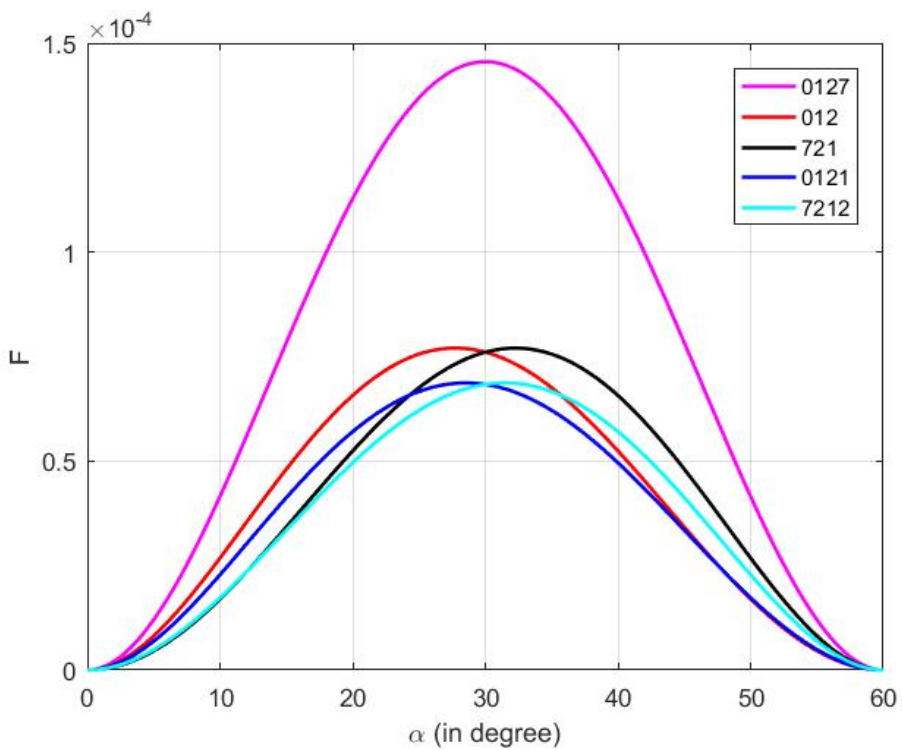


(a) d-axis

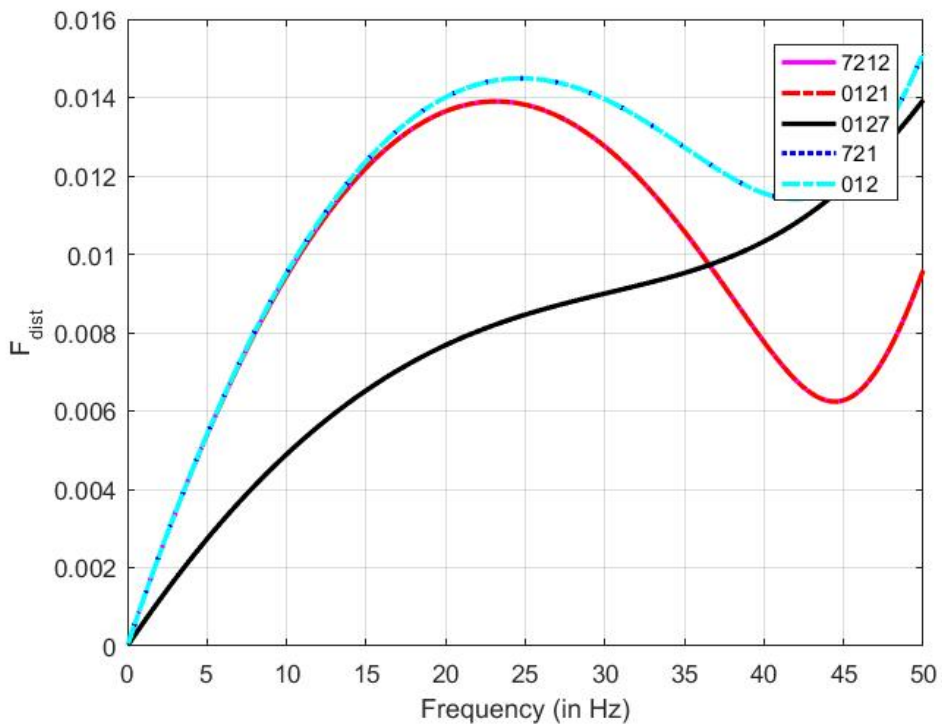


(b) q-axis

Figure 5.2: Stator Flux Ripple for All Sequences in d and q axes

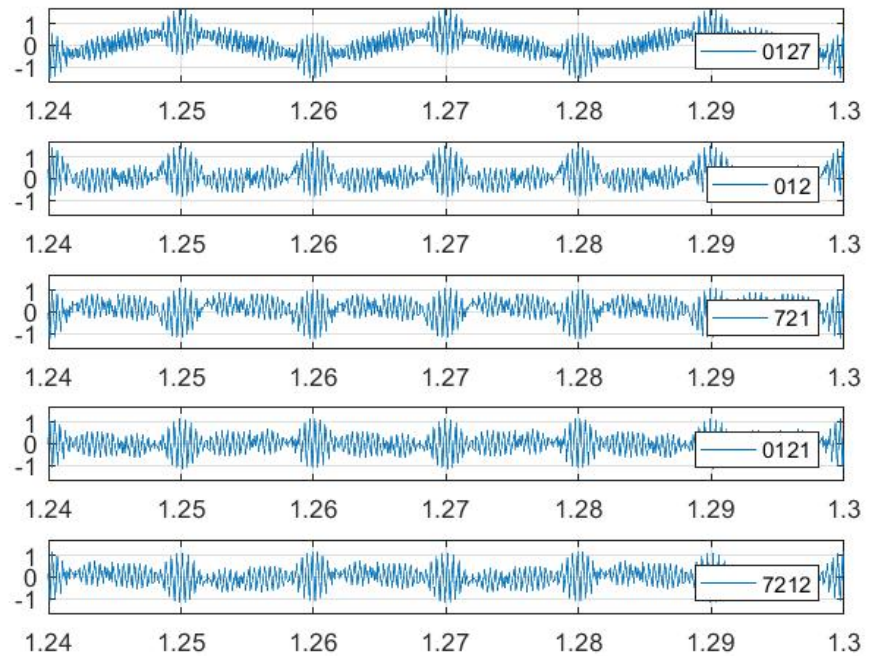


(a) RMS Stator Flux Ripple

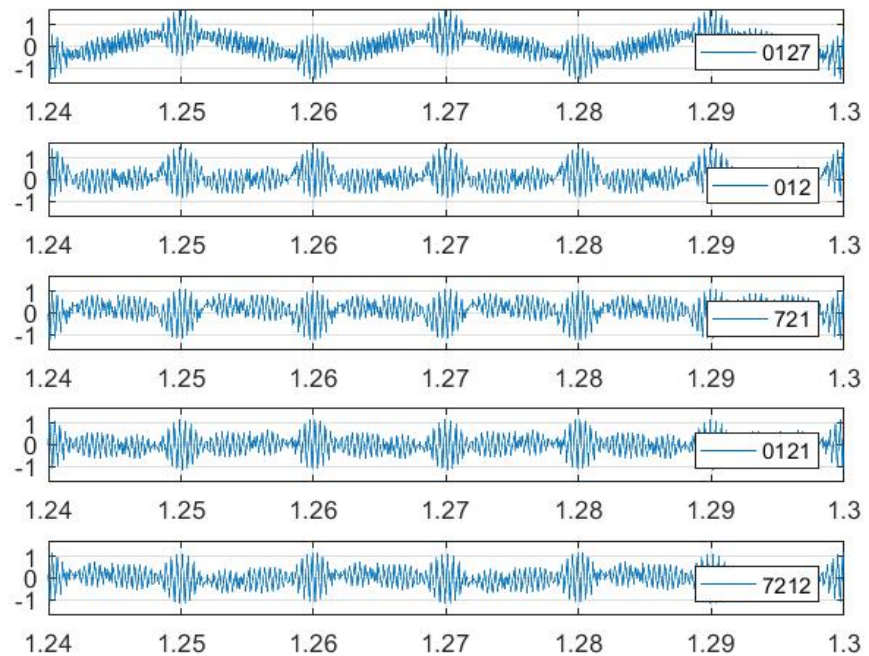


(b) Total RMS Harmonic Distortion Factor Vs Frequency Curve

Figure 5.3: RMS Stator flux ripple and THD Vs Frequency Curve for Different Sequences

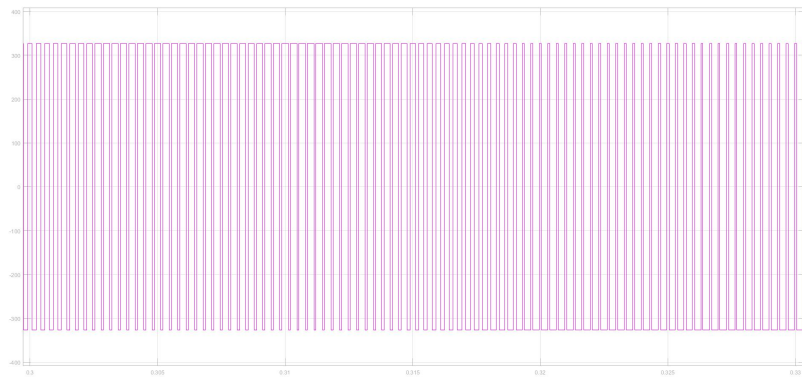


(a) Stator Current Ripple



(b) Machine Torque Ripple

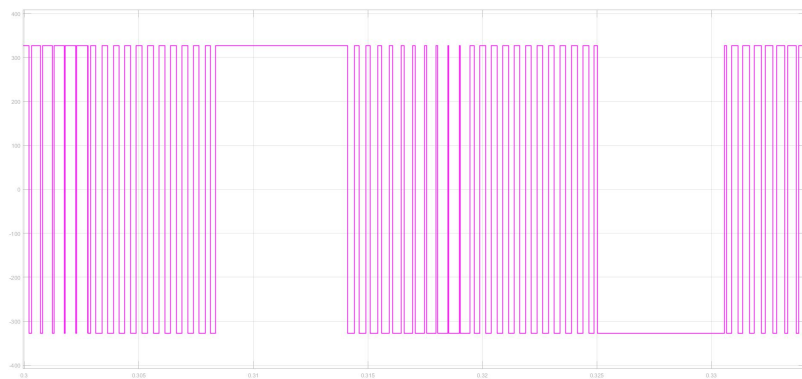
Figure 5.4: Stator Current Ripple and Torque for All Sequences



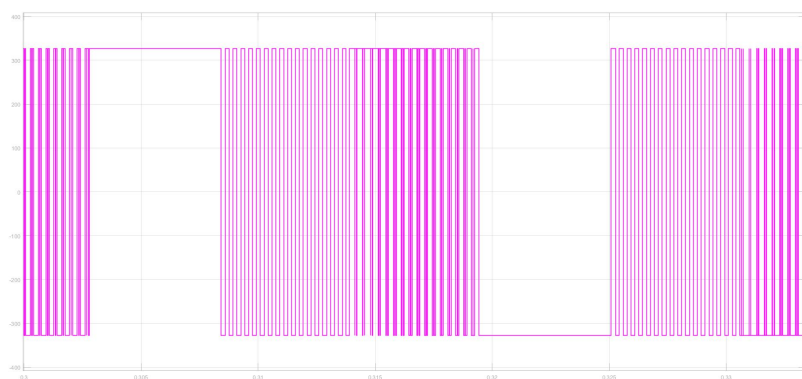
(a) 0127 Sequence



(b) 012 Sequence

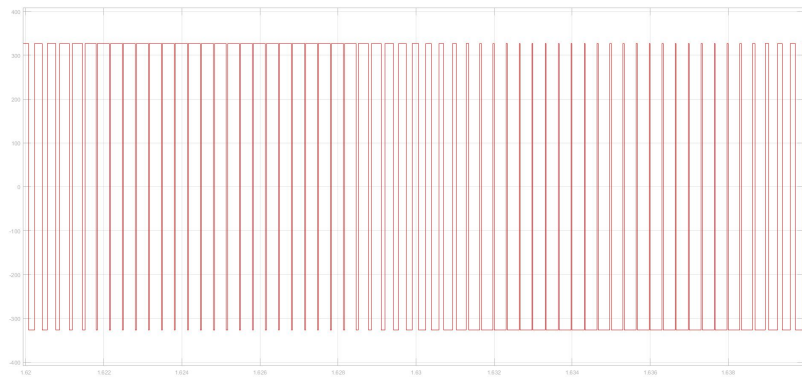


(c) 721 Sequence

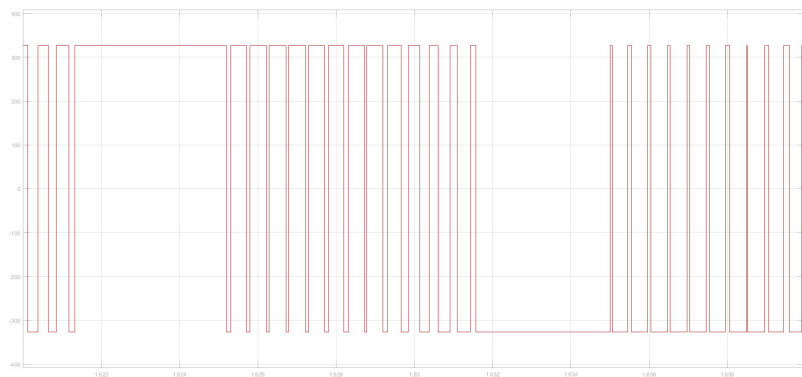


(d) 0121 Sequence

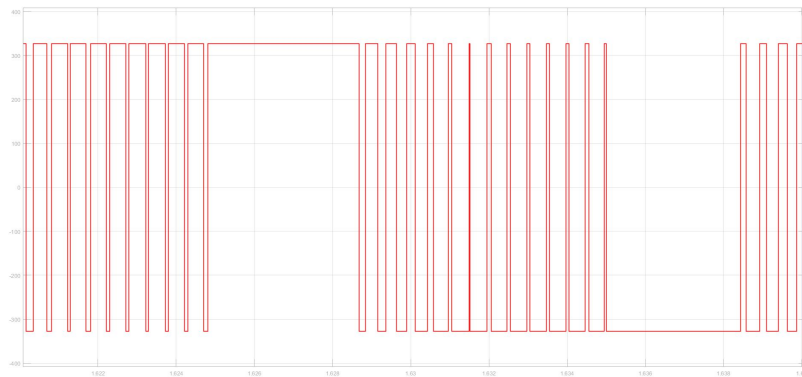
Figure 5.5: Voltage Between Inverter Phase to DC Bus Neutral for Different Sequences for 30Hz



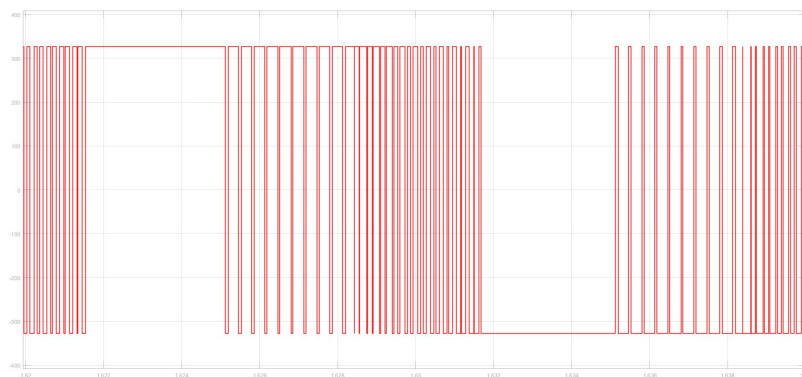
(a) 0127 Sequence



(b) 012 Sequence

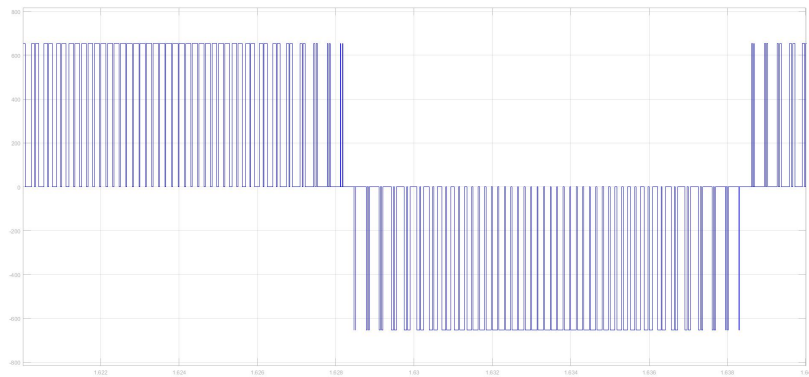


(c) 721 Sequence

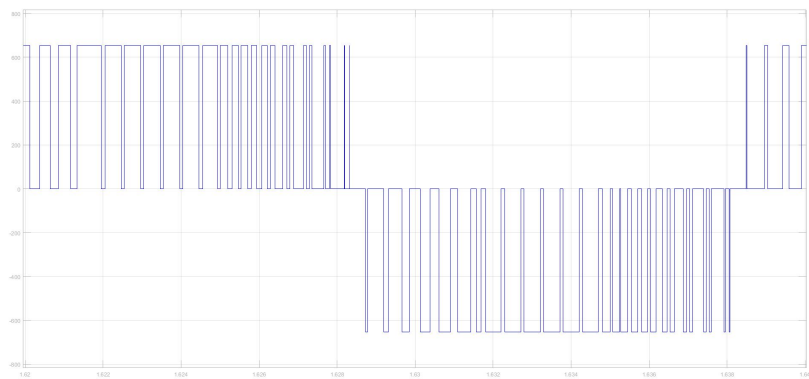


(d) 0121 Sequence

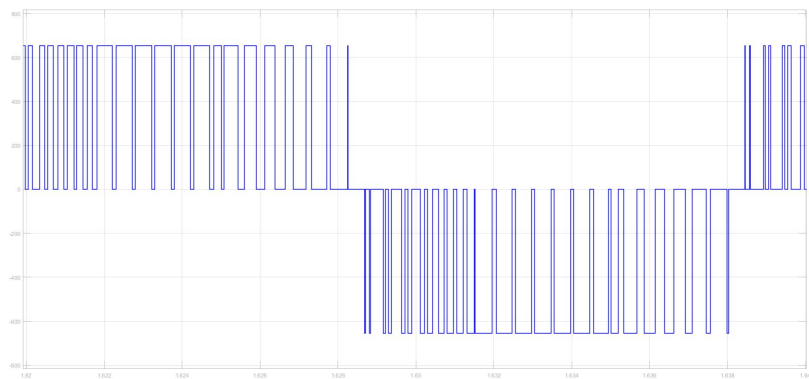
Figure 5.6: Voltage Between Inverter Phase to DC Bus Neutral for Different Sequences for 50Hz



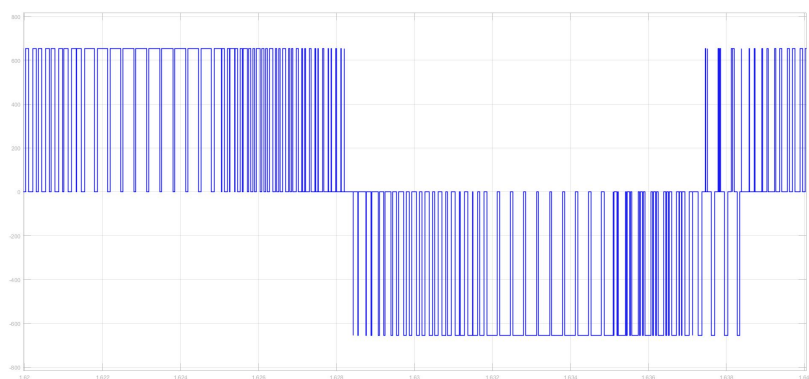
(a) 0127 Sequence



(b) 012 Sequence



(c) 721 Sequence



(d) 0121 Sequence

Figure 5.7: Voltage Between Inverter Phase to Phase for Different Sequences for 50Hz

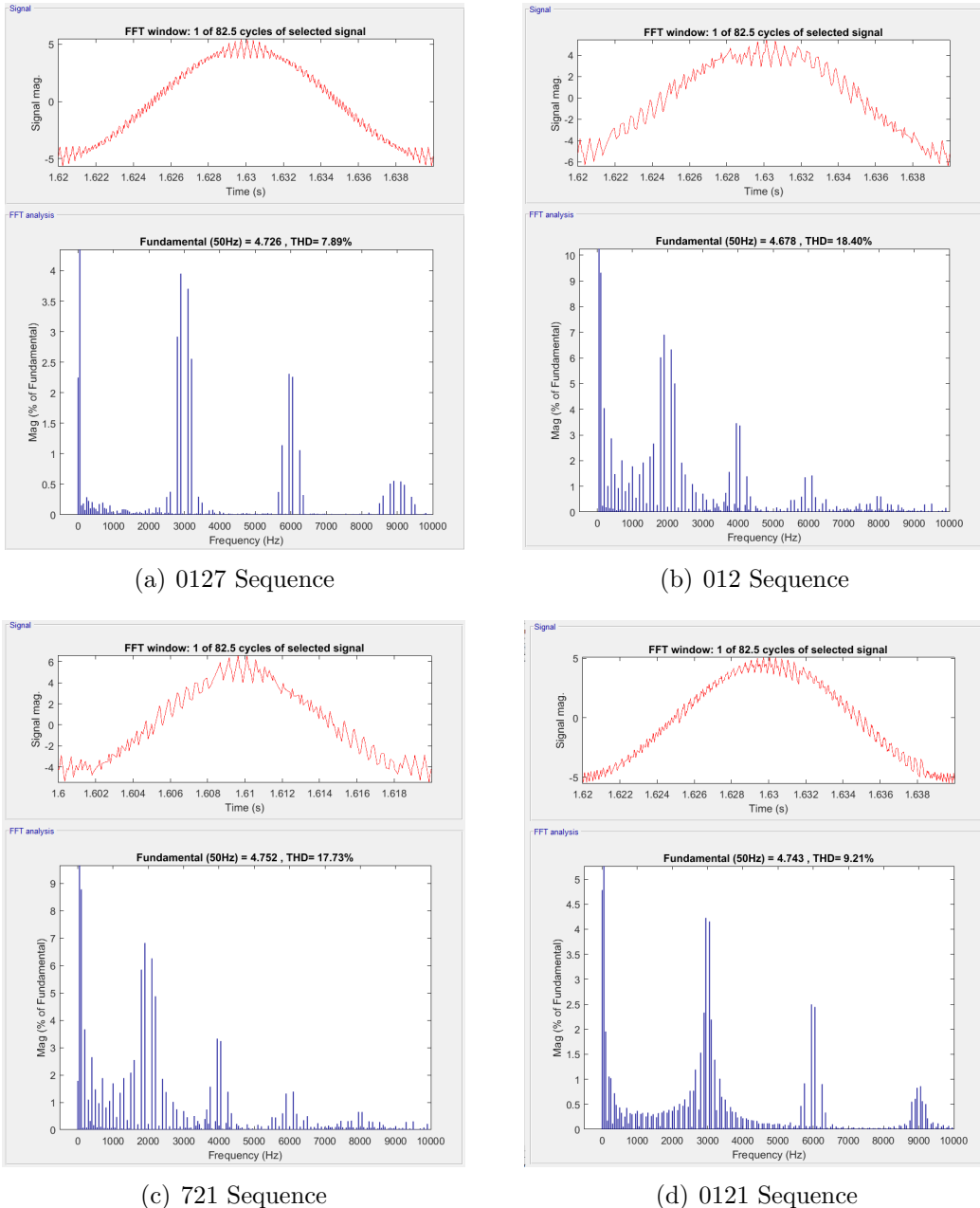
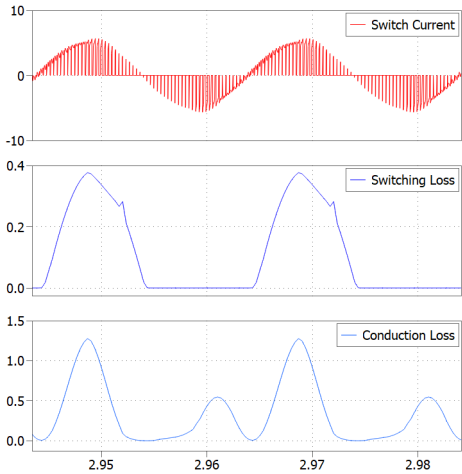
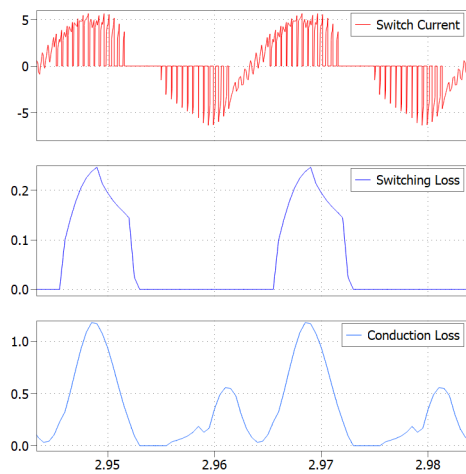


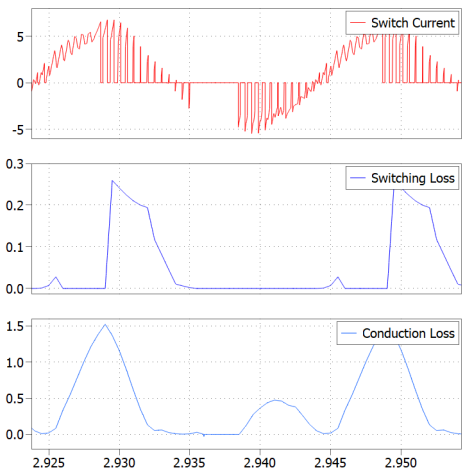
Figure 5.8: Inverter Line Current and Its THD Values for Different Sequences



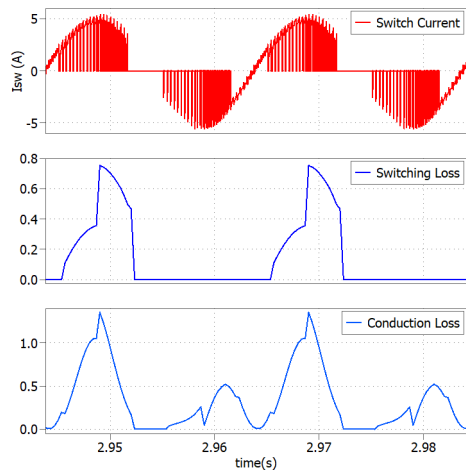
(a) 0127 Sequence



(b) 012 Sequence

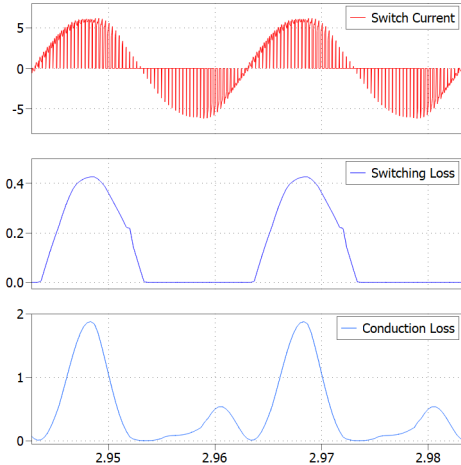


(c) 721 Sequence

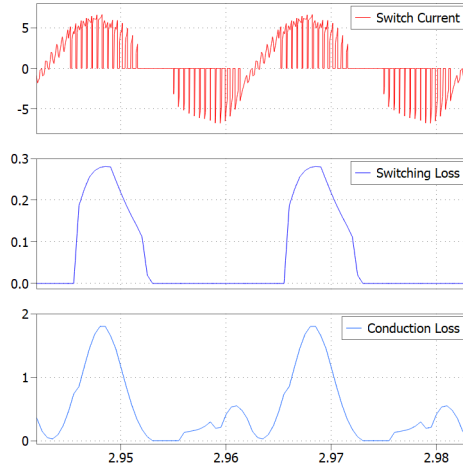


(d) 0121 Sequence

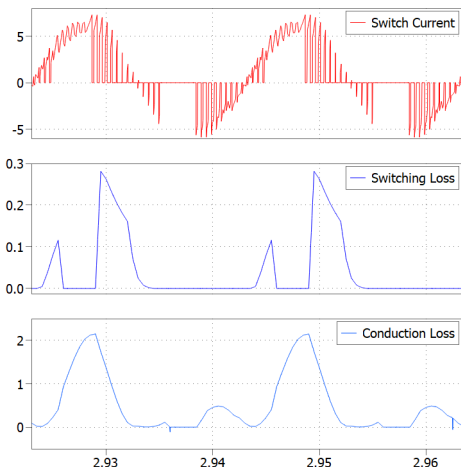
Figure 5.9: Switch Current and Losses at 5Nm load for Different Sequences



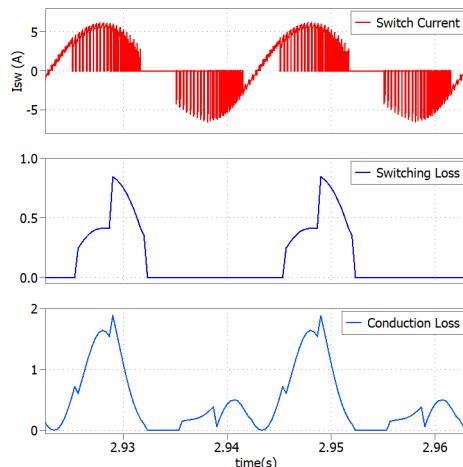
(a) 0127 Sequence



(b) 012 Sequence

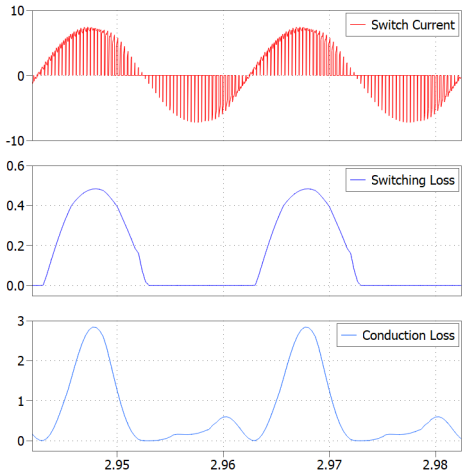


(c) 721 Sequence

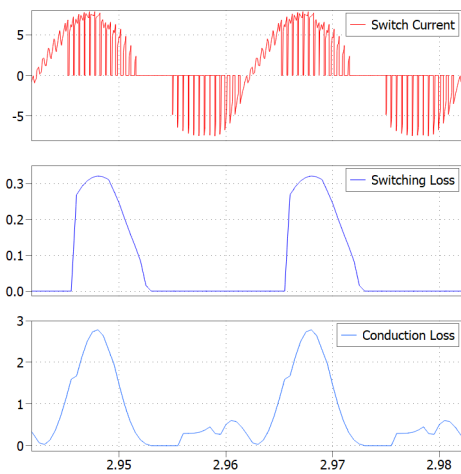


(d) 0121 Sequence

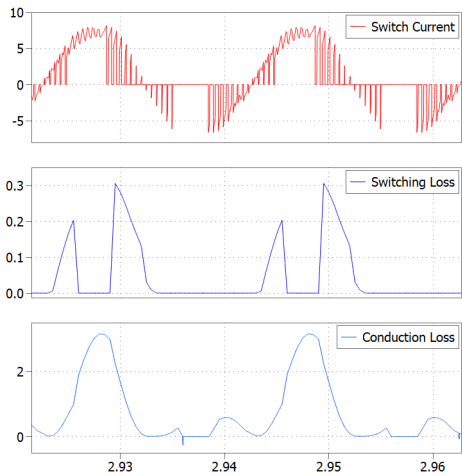
Figure 5.10: Switch Current and Losses at 10Nm load for Different Sequences



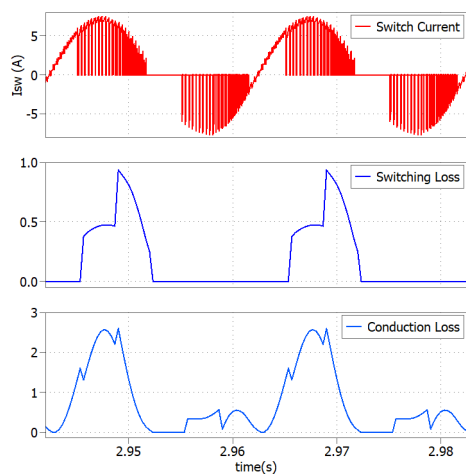
(a) 0127 Sequence



(b) 012 Sequence



(c) 721 Sequence



(d) 0121 Sequence

Figure 5.11: Switch Current and Losses at 15Nm load for Different Sequences

tually, the 012 sequence is operated in under modulation region and it switches as 12 sequence in over-modulation region. Similarly, the 0121 sequence is operated in under modulation region and it switches as 121 in over-modulation region. This is due to, in over modulation region the zero vector is absent or in other words, only active vectors are operated in over-modulation zone. Some of their results, which contains the phase voltages, currents and operating sectors and the FFT analysis of phase voltages are shown in below figures. The figure 5.12 shows the inverter phase voltage, phase current and operating sector for 012 sequence in under-modulation region at different phase voltages. Here the length of switching pulses are increase with the operating frequency gradually. This is due to, here v/f control is implemented. Because of that, the fundamental value of voltage is also increased.

The figure 5.13 shows the voltage between inverter phase to dc bus neutral, phase current and operating sector for 012 sequences in Over-modulation region at different voltage references. In this region, it switches as 12 sequence. Here also, as the reference voltage increases, then the clamping time period also increases gradually and frequency of fundamental component is also increase. The current changes its shape little bit, due to increased length of clamping period. The figure 5.14 and figure 5.15 shows the FFT analysis of phase voltage. from those figures, it is also observed that as the reference voltage increases then the operating frequency also increases. Because here v/f control is implemented. These results are obtained with the 500 volts of dc bus.

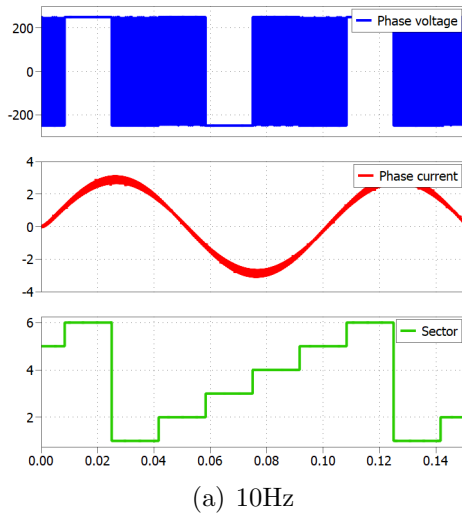
The figure 5.16 shows the inverter phase voltage, phase current and operating sector for 0121 sequence in under-modulation region. Here, at low frequencies the current ripple is more than the high frequencies. During high frequencies the double switching pulses can be seen clearly. The figure 5.17 shows the voltage between inverter phase to dc bus neutral, phase current and operating sector for 0121 sequences in Over-modulation region at different voltage reference voltages. in over-modulation region, it switches as 121 sequence. Here we can observe that the distortions in current waveform is more than the 012 sequence. The figure 5.18 and figure 5.19 shows the FFT analysis of phase voltage at different reference voltages and frequencies. This simulation results are taken with dc bus voltage of 320 volts.

The table 5.1 shows the fundamental voltage values for different sequences at different frequencies. Here the ratio between fundamental voltage to the corresponding operating frequency is nearly constant. Here the fundamental voltage values are different, because of DC bus voltage variation.

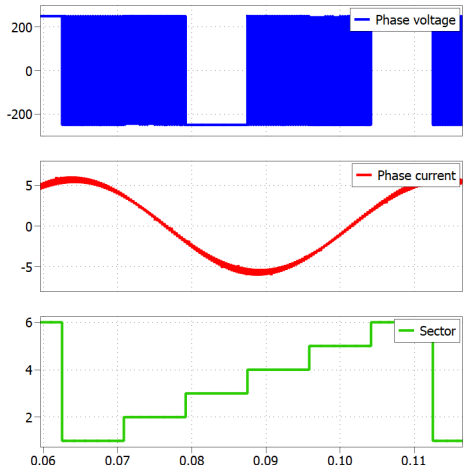
Sequence	10Hz	20Hz	30Hz	40Hz	50Hz
012	57.7414	115.48	173.243	230.953	288.919
0121	36.9545	73.9069	110.873	147.812	184.882

Table 5.1: Fundamental voltage values for different sequences at different frequencies

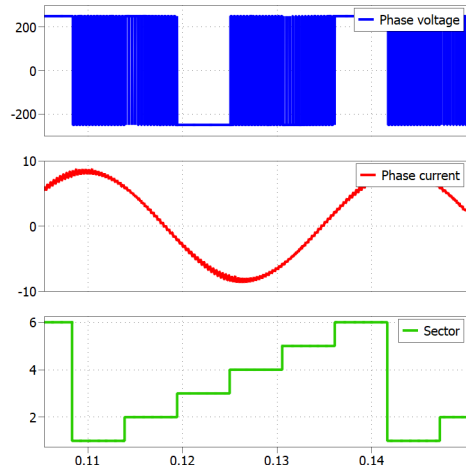
The figure 5.20 shows the RMS Stator Flux Ripple for Modulation index of 1.02 for 012 and 0121 sequences at sector-1. Here, the reference vector is rotating from 0 degree to 60 degree. When the reference vector lies inside the hexagon then it switches 012 or 0121 sequence. If reference vector lies on the side of hexagon then, it switches as 12 or 121 sequence respectively. From that figure we can say that the value of stator flux ripple for 121 sequence is less than the 12 sequence.



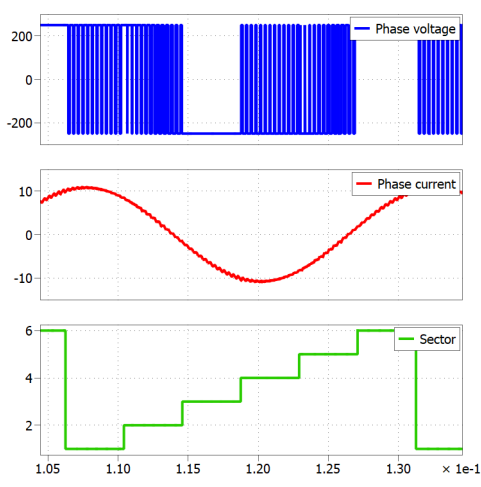
(a) 10Hz



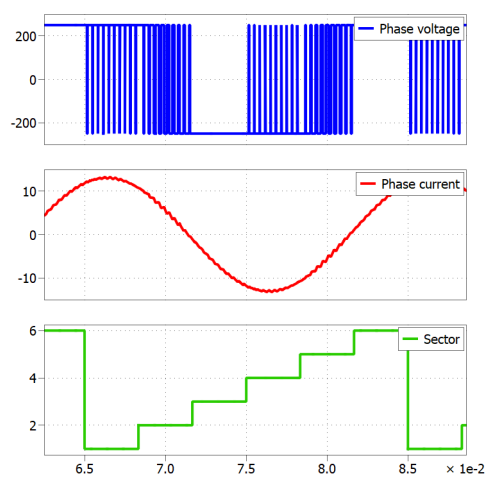
(b) 20Hz



(c) 30Hz



(d) 40Hz



(e) 50Hz

Figure 5.12: The voltage between inverter phase to dc bus neutral, phase current and operating sector for 012 sequences at different frequencies

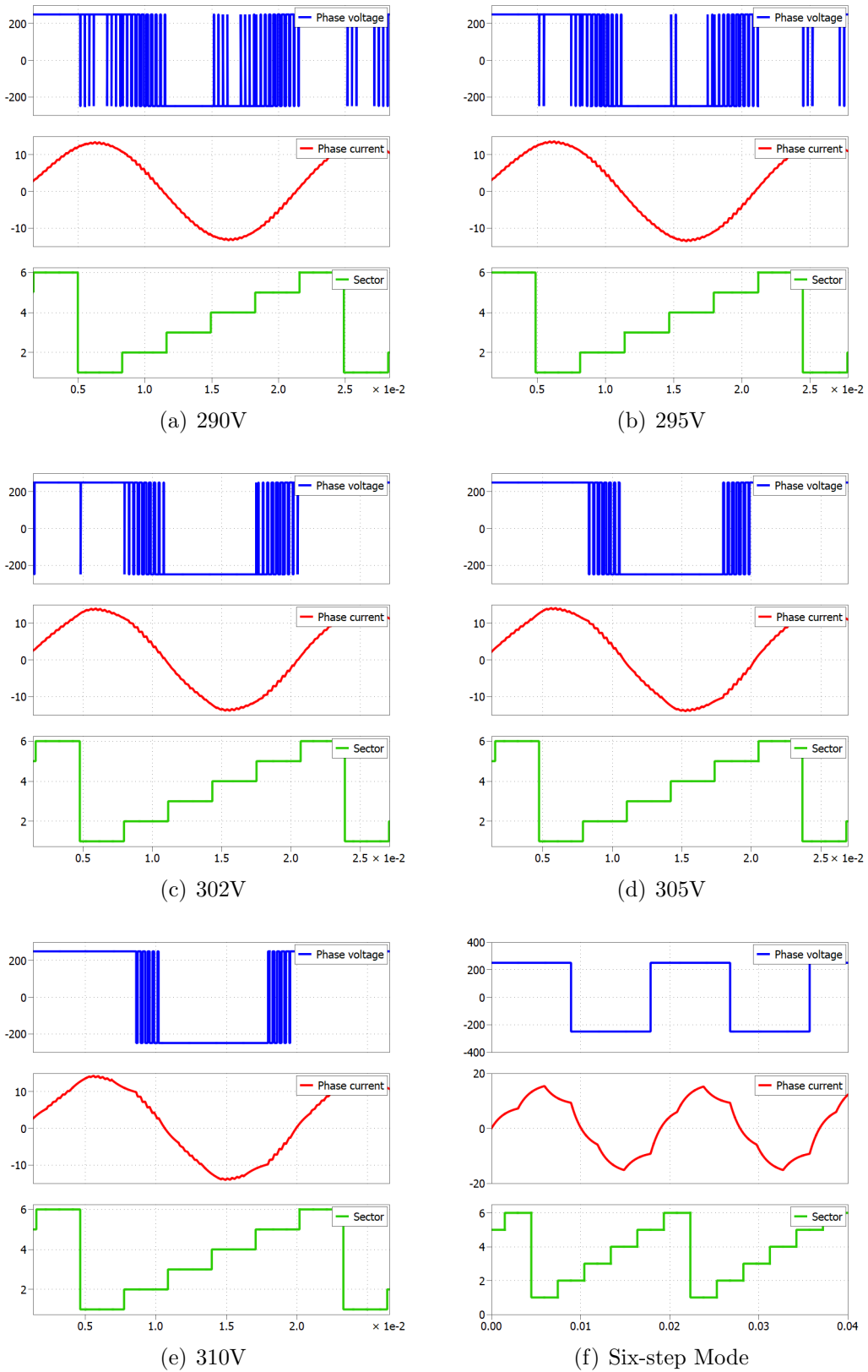
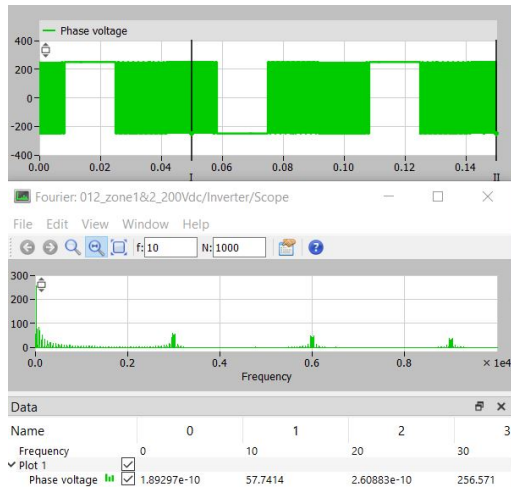
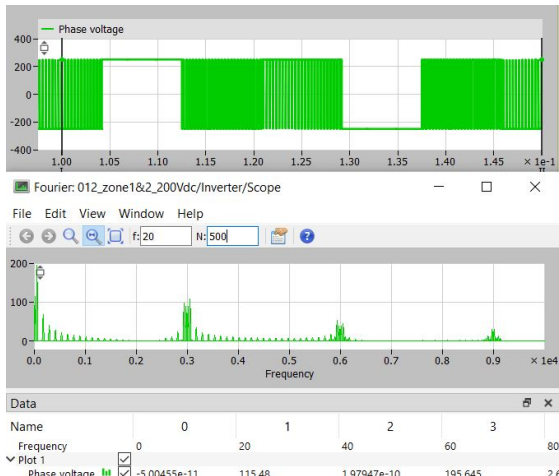


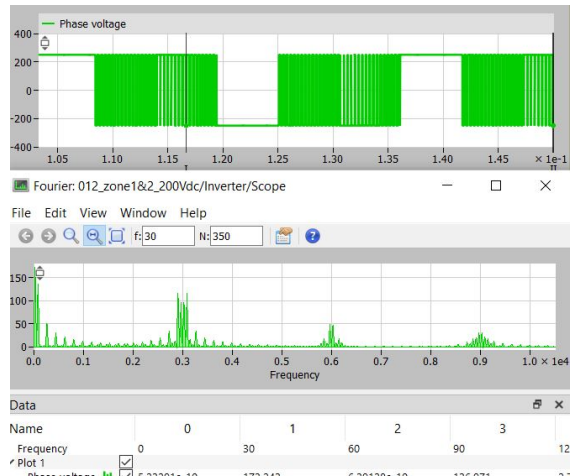
Figure 5.13: The voltage between inverter phase to dc bus neutral, phase current and operating sector for 12 sequences in Over-modulation region at different voltage references



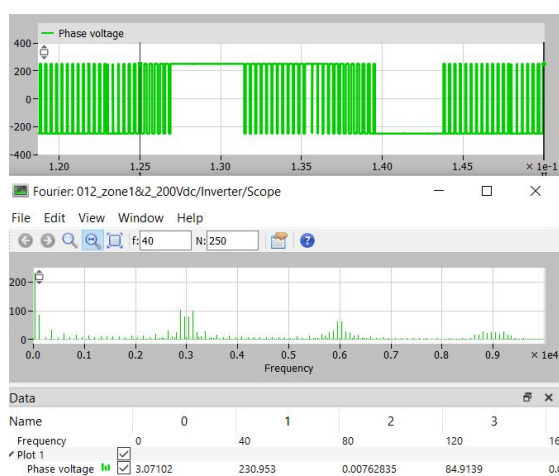
(a) 10Hz



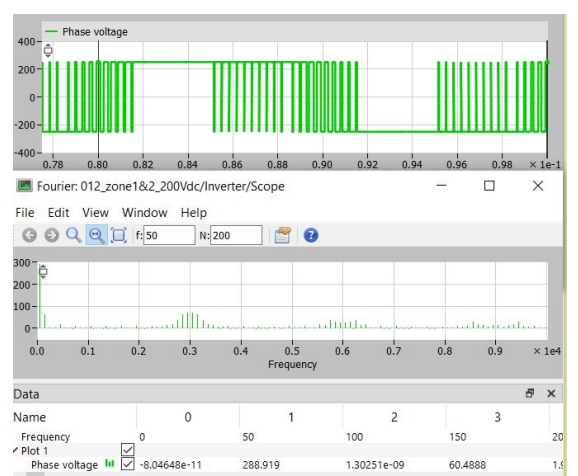
(b) 20Hz



(c) 30Hz

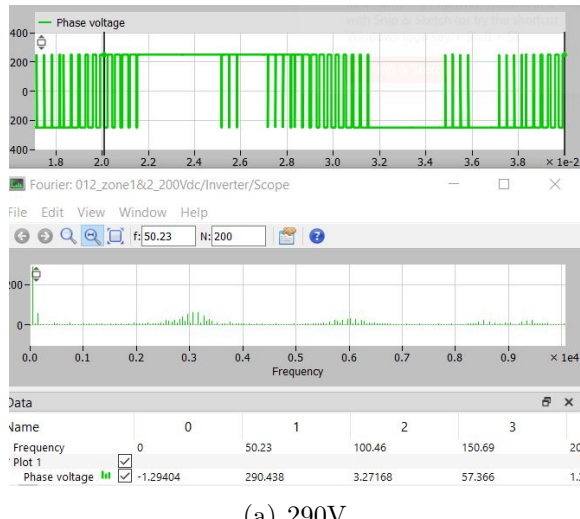


(d) 40Hz

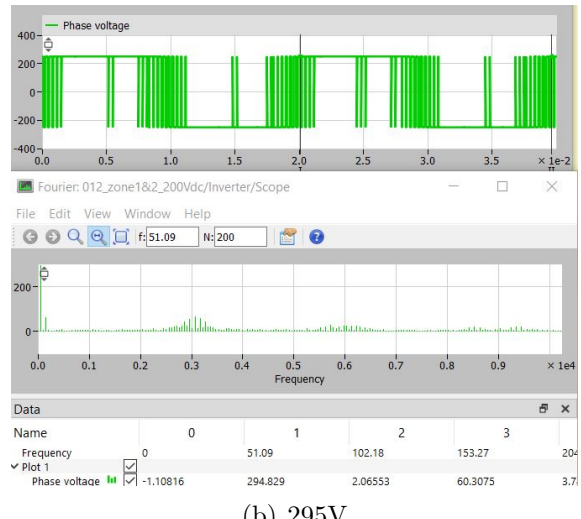


(e) 50Hz

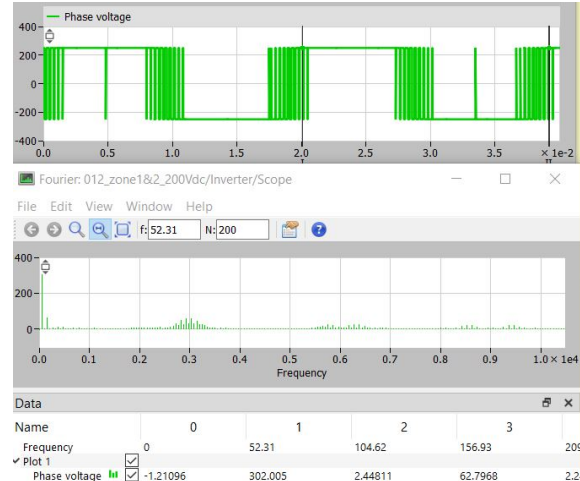
Figure 5.14: FFT analysis of the voltage between inverter phase to dc bus neutral for 012 sequences at different frequencies



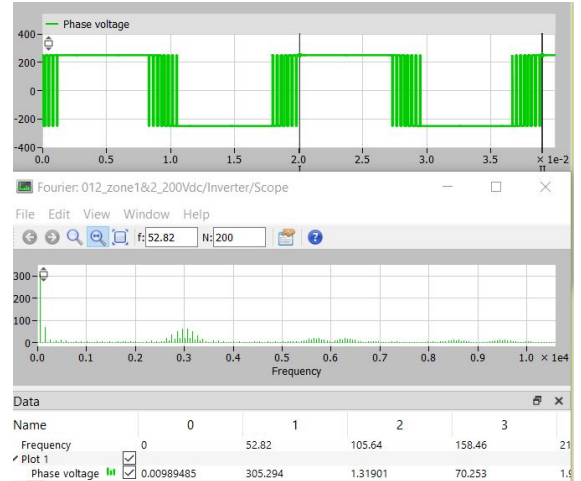
(a) 290V



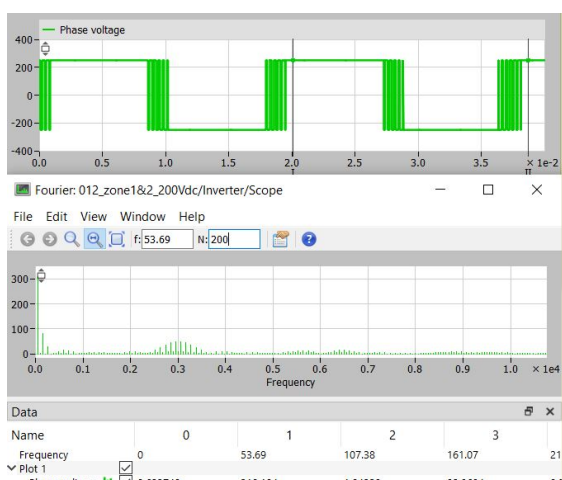
(b) 295V



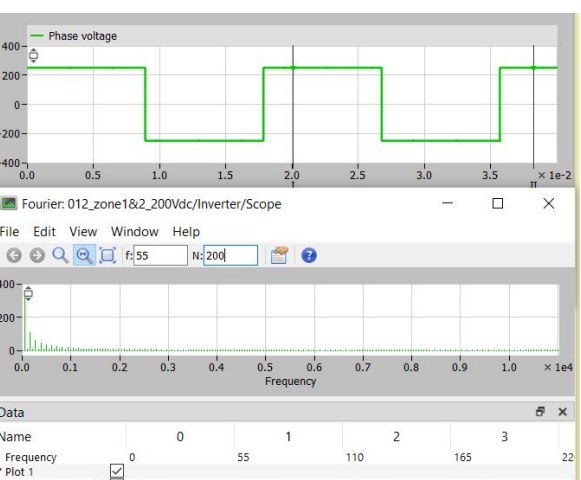
(c) 302V



(d) 305V

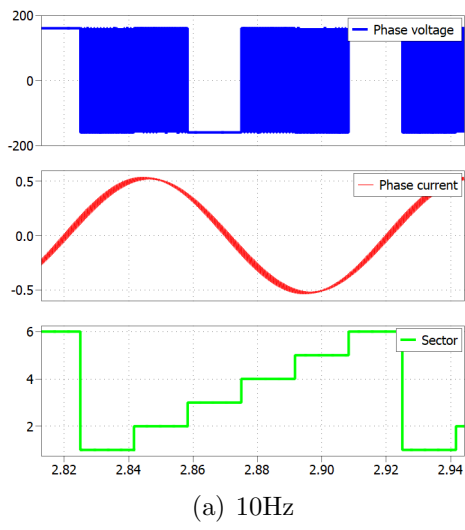


(e) 310V

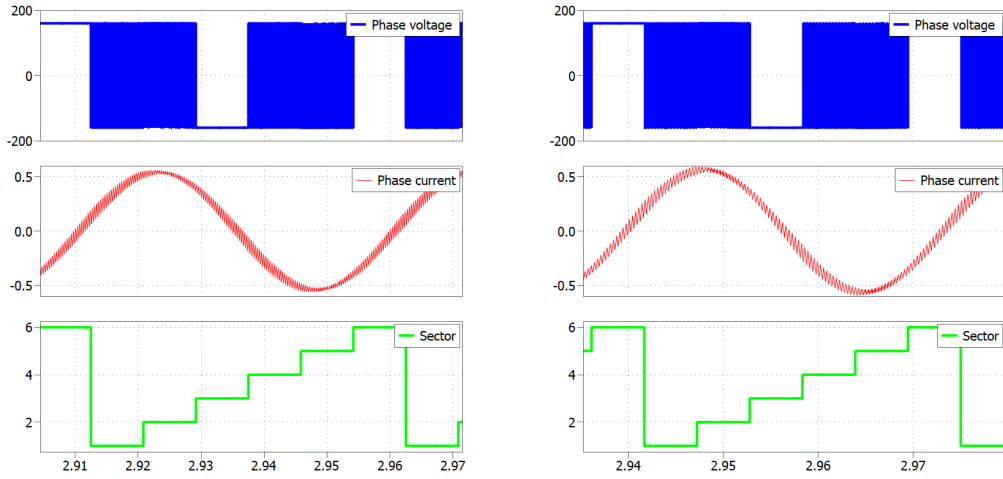


(f) Six-step Mode

Figure 5.15: FFT analysis of the voltage between inverter phase to dc bus neutral for 12 sequences in Over-modulation region at different reference voltages

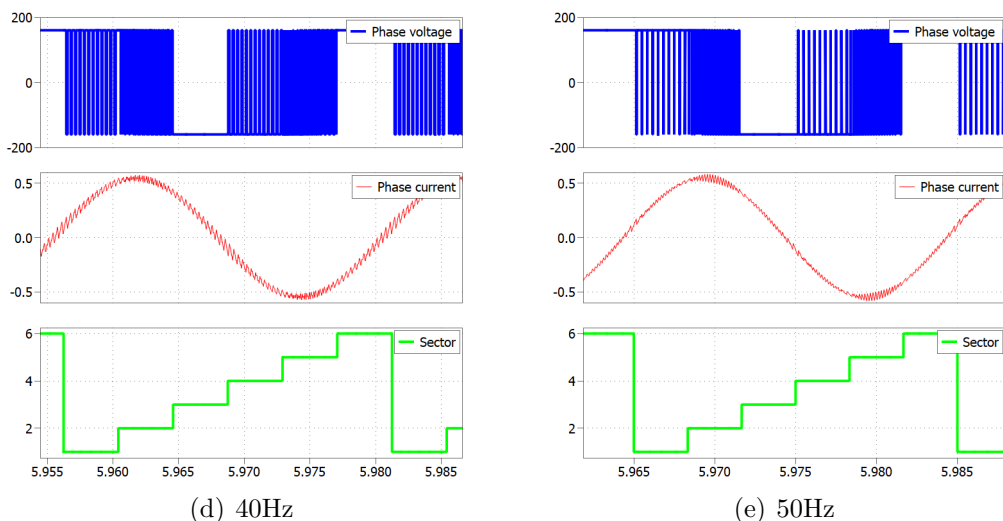


(a) 10Hz



(b) 20Hz

(c) 30Hz



(d) 40Hz

(e) 50Hz

Figure 5.16: The voltage between inverter phase to dc bus neutral, phase current and operating sector for 0121 sequences at different frequencies

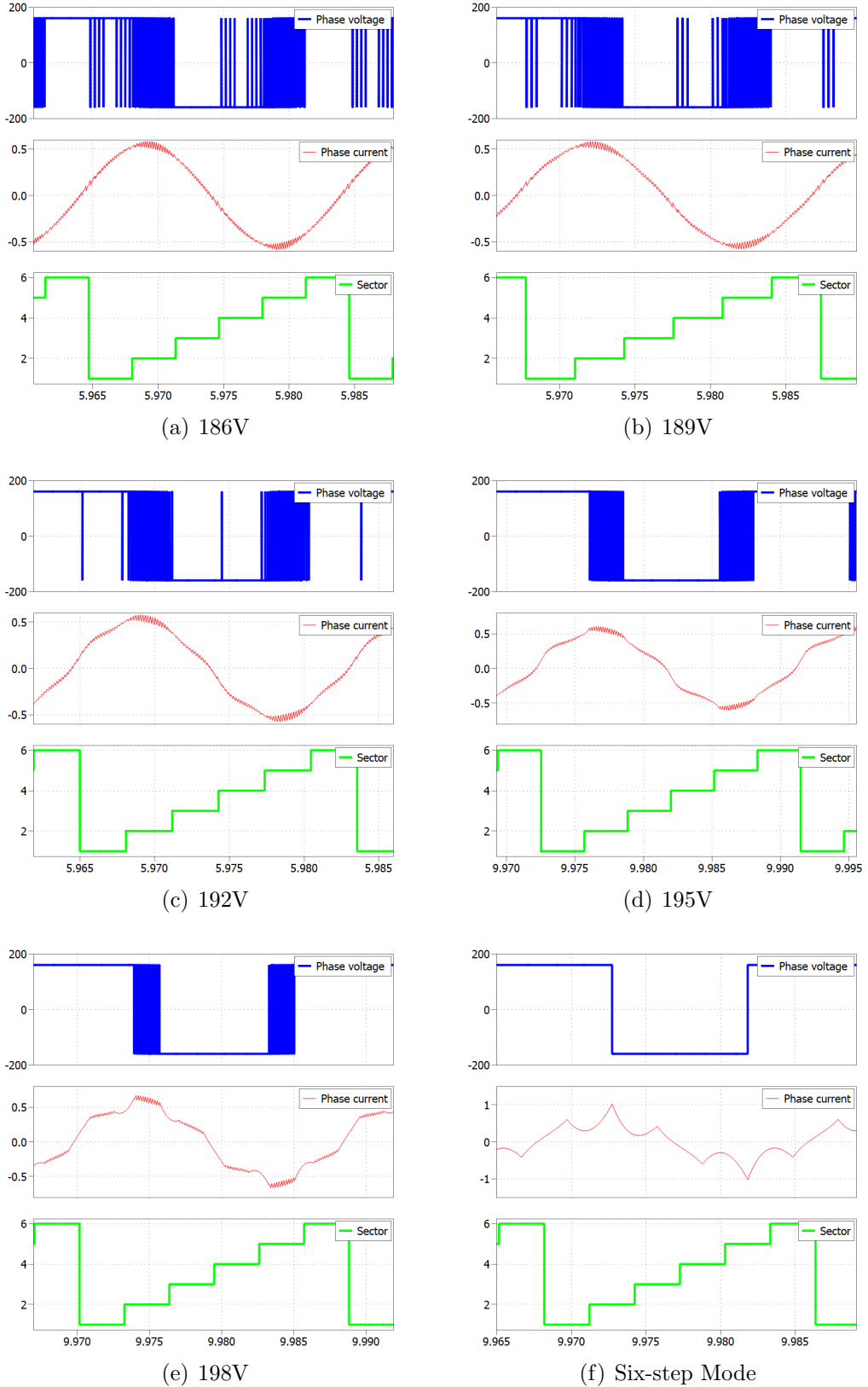
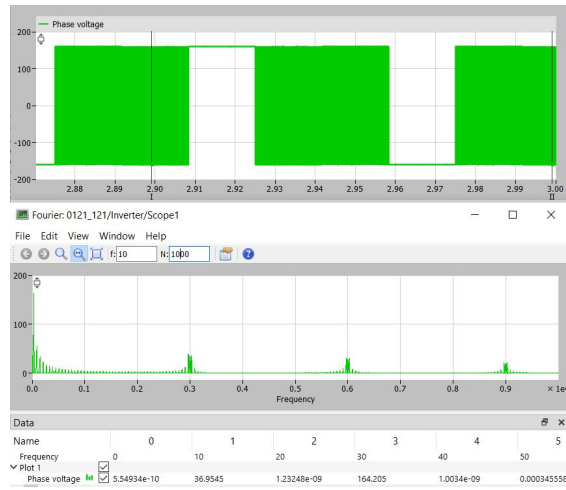
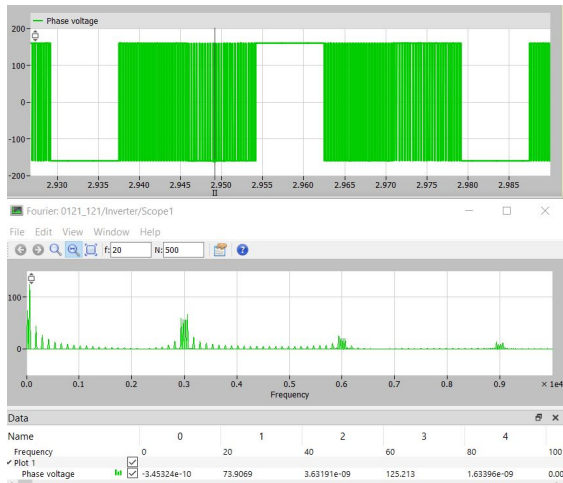


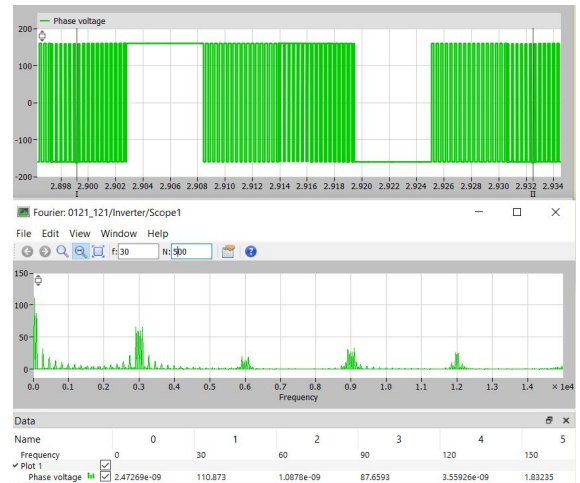
Figure 5.17: The voltage between inverter phase to dc bus neutral, phase current and operating sector for 0121 sequences in Over-modulation region at different voltage references



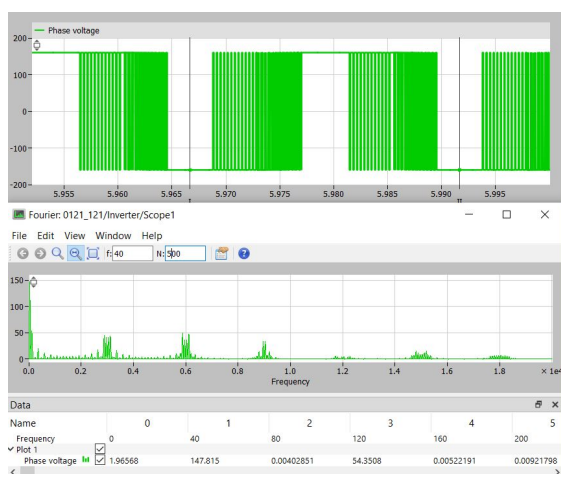
(a) 10Hz



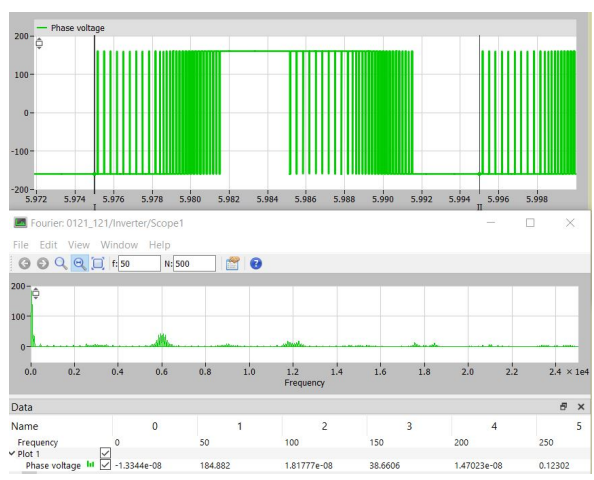
(b) 20Hz



(c) 30Hz



(d) 40Hz



(e) 50Hz

Figure 5.18: FFT analysis of the voltage between inverter phase to dc bus neutral for 0121 sequences at different frequencies

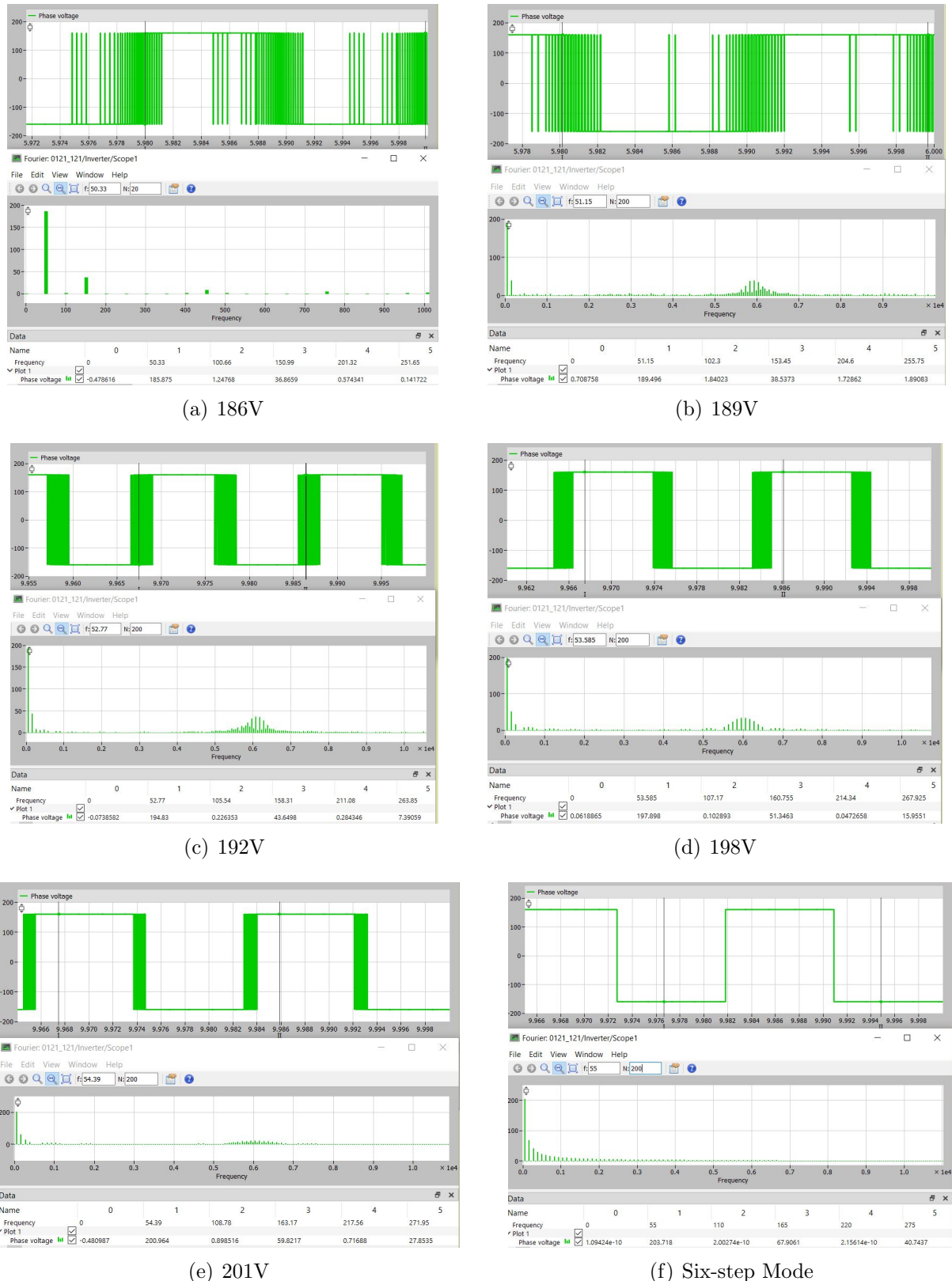


Figure 5.19: FFT analysis of the voltage between inverter phase to dc bus neutral for 0121 sequences in Over-modulation region at different reference voltages

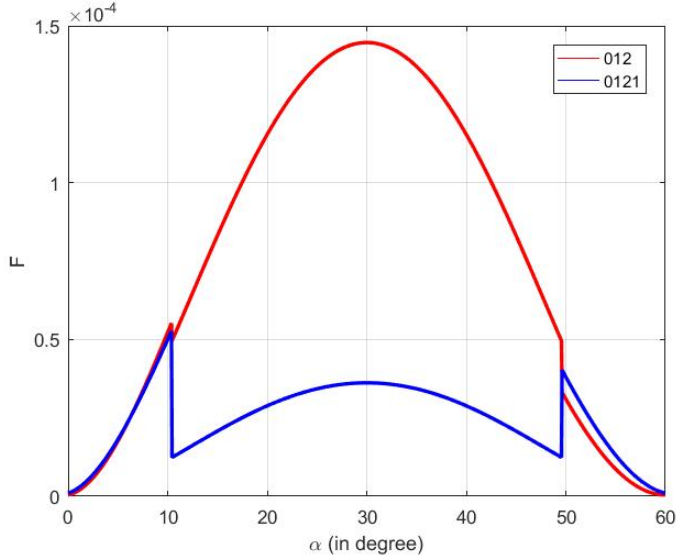


Figure 5.20: RMS Stator Flux Ripple for Modulation index of 1.02

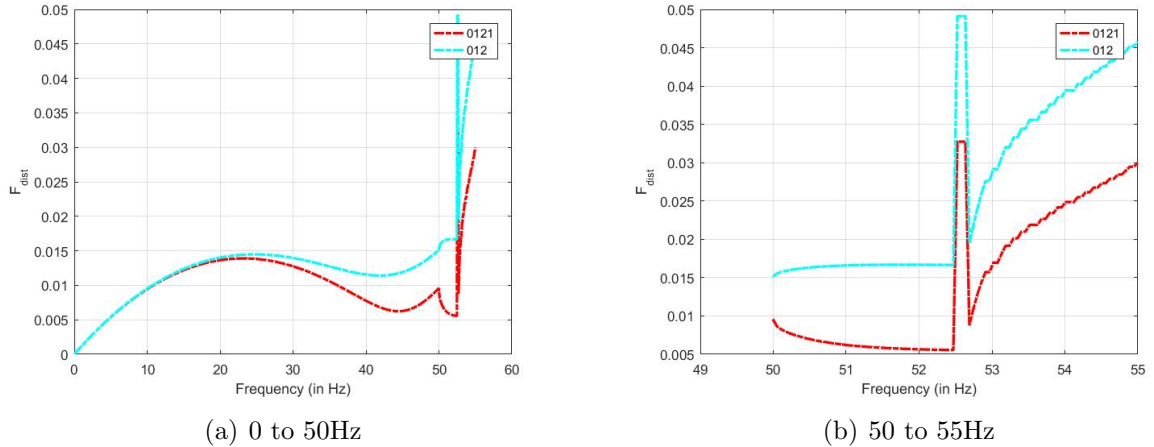


Figure 5.21: Total RMS Harmonic Distortion Factor Vs Frequency Curve

The figure 5.21(a) shows the Total RMS Harmonic Distortion Factor Vs Frequency Curve for different sequences. Here the curve is extended to over-modulation region. In over-modulation region, the 012 sequence changes to 12 sequence and 0121 changes to 121 sequence. From this figure also we can observe the RMS distortion factor for 0121 is very less than the 012 sequence. The figure 5.21(b) shows the zoomed version for that figure. Here the frequency range is 50Hz to 55Hz.

The sequences in over-modulation region can be exchanged. It means, in under modulation it operates in 012 sequence and during over-modulation region it switches in 121 sequence. Similarly, in under modulation the 0121 sequence is operated and in over-modulation it switches in 12 sequence. The Total RMS harmonic distortion factor vs frequency curve corresponding this situation shows in the figure 5.22

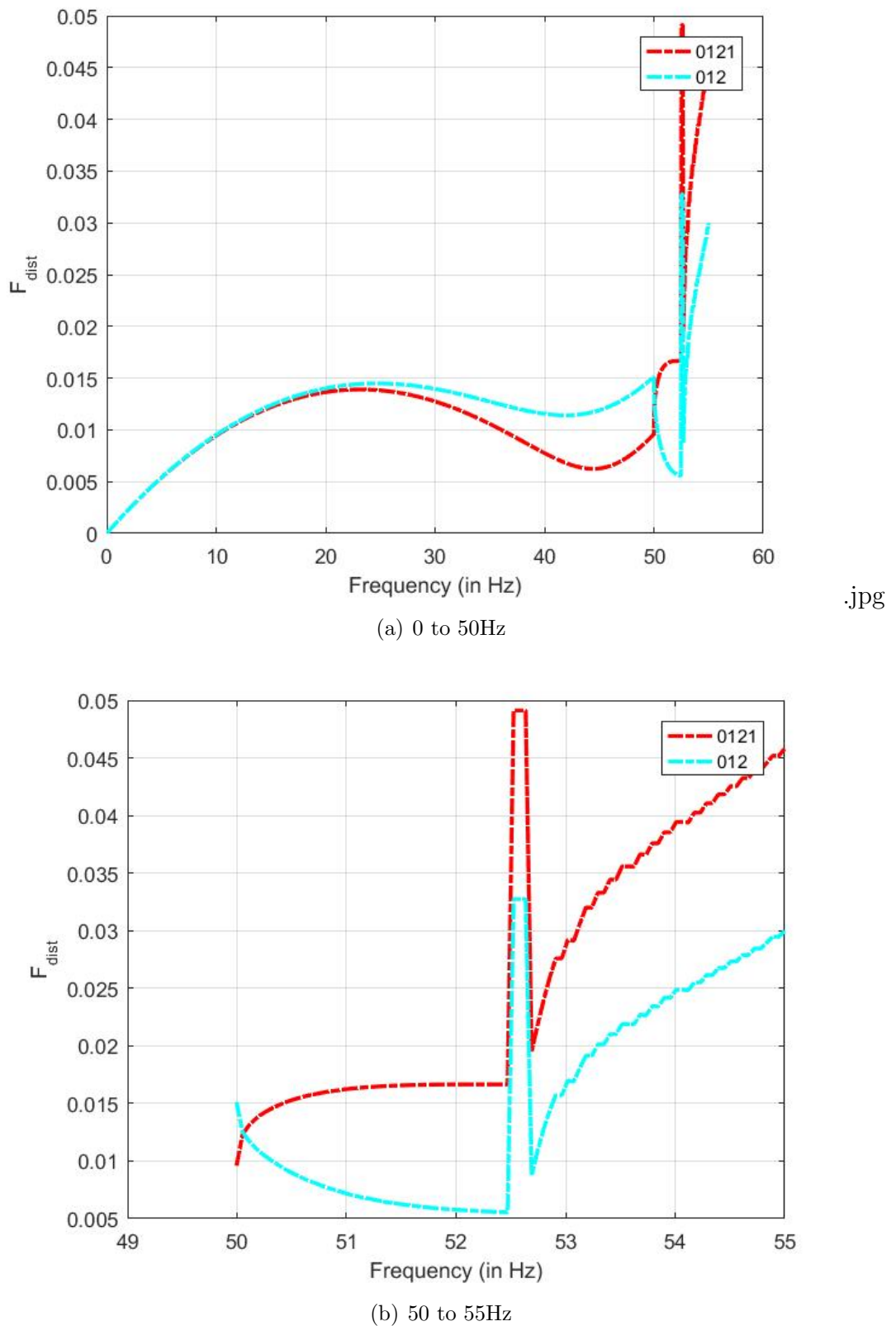


Figure 5.22: Total RMS Harmonic Distortion Factor Vs Frequency Curve

Chapter 6

Experimental Results

What ever the results we got from the simulation, most of those things are achieved by using hardware also with the help of DSP board. The figure 6.1 shows the hardware set up of improved space vector PWM technique operating in over-modulation region for induction machine drive. Here for providing the dc bus voltage, three phase rectifier is used. The rectifier is energised through the three phase auto transformer. An inductor is utilized as filter for rectifier output. For the inverter switches, switching pulses are required. For generating switching pulses, the code should be written in code composer studio. That code is injected to the DSP board. According to code, the DSP board generate 6 PWM signals. These signals given to a X-OR gate to generate required switching pulses. From the output of X-OR gate, these signals given to PID card to split this 3 switching signals to 6 signals for six switches. The output terminals of inverter is connected to the induction machine.

The figure 6.2 shows the voltage between inverter phase to dc bus neutral, phase current and operating sector for 0127 sequences at different frequencies. The figures 6.3 and 6.4 shows the FFT analysis of phase voltage and phase current of 0127 sequence. The figure 6.5 shows the voltage between inverter phase to dc bus neutral, phase current and operating sector for 012 sequences at different frequencies in under modulation region. The figure 6.6 shows the voltage between inverter phase to dc bus neutral, phase current and operating sector for 012 sequences in Over-modulation region at different voltage references. These results are similar to the simulation results. The figure 6.7 and figure 6.9 shows the FFT analysis of the phase voltage and inverter phase current for 012 sequences at different frequencies in under modulation region. While, figure 6.7 and figure 6.10 shows the FFT analysis of the inverter phase voltage and current for 012 sequences in Over-modulation region at different reference voltages. The figure 6.11 shows the voltage between inverter phase to dc bus neutral, phase current and operating sector for 721 sequences at different frequencies in under modulation region. The figure 6.12 and 6.13 shows the FFT analysis of the inverter phase voltage and current for 721 sequences at different frequencies.

For 0121 sequence, the figure 6.14 shows the voltage between inverter phase to dc bus neutral, phase current and operating sector at different frequencies in under modulation region. The figure 6.16 and figure 6.18 shows the FFT analysis of the inverter phase voltage and current for 0121 sequences at different frequencies in under modulation region. The figure 6.15 shows the voltage between inverter phase to dc bus neutral, phase current

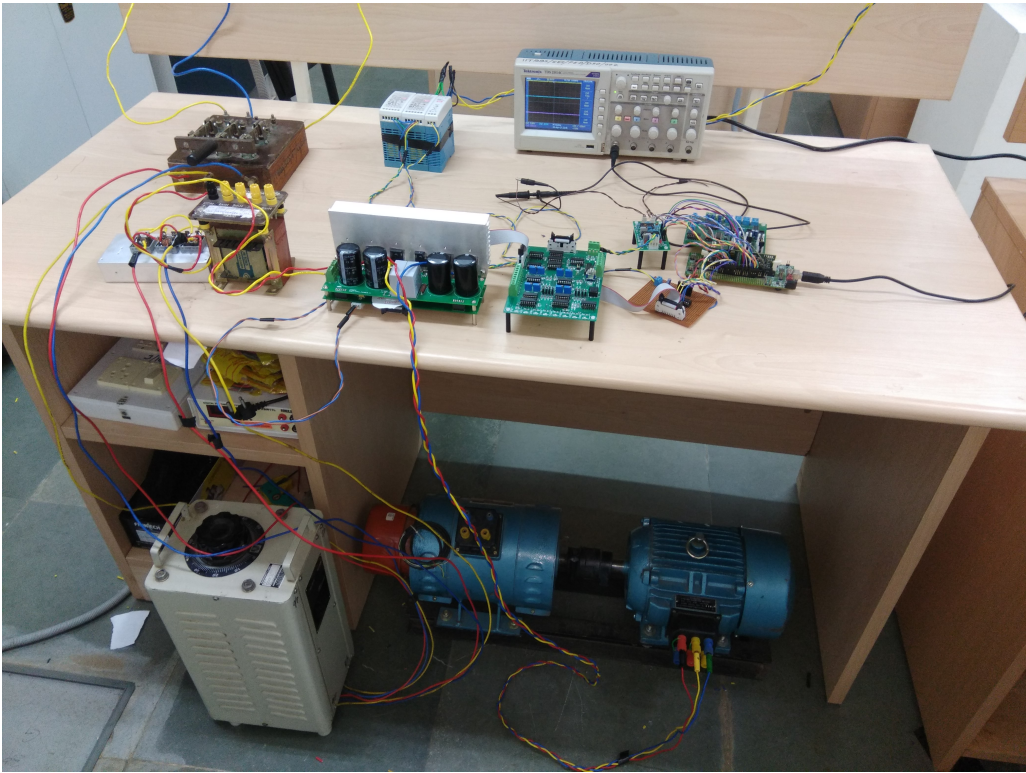


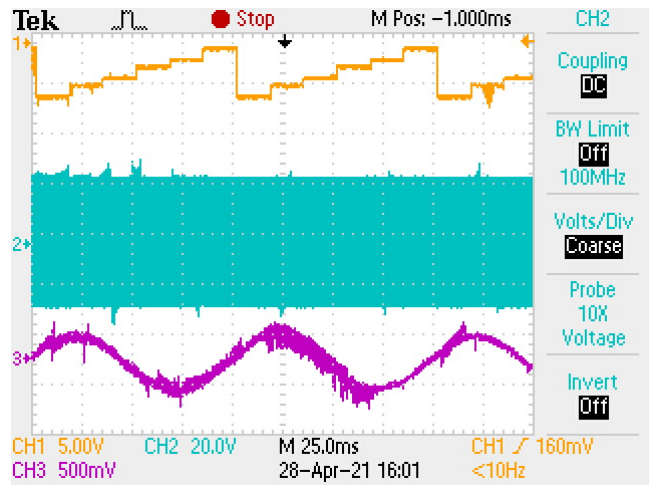
Figure 6.1: Project Setup

Sequence	10Hz		20Hz		30Hz		40Hz		50Hz	
	V	THD	V	THD	V	THD	V	THD	V	THD
0127	64.38	422.71	116	268.88	173.8	163.71	235.5	107.78	294.4	66.87
012	62.39	544.81	117.2	277.02	179.5	169.61	238.6	109.41	295.8	69.16
721	52.66	639.21	122.2	264.57	178.9	169.71	239.8	108.41	296.7	66.23
7212	56.55	608.71	114.2	283.4	173.1	167.11	226	117..65	279.2	78.43
0121	37.05	589.04	77.32	266.44	112.7	171.19	146.3	113.87	182.9	73.07

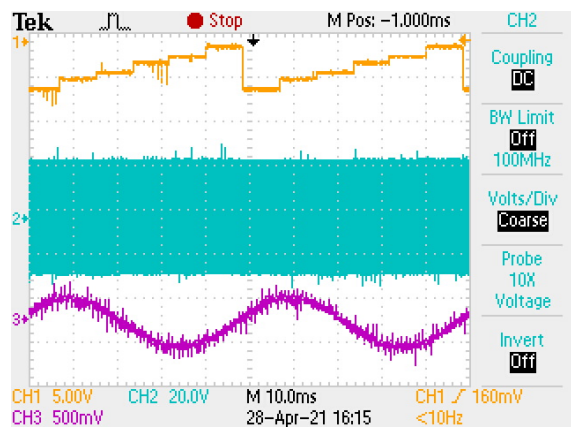
Table 6.1: Fundamental voltage and its THD values for different sequences at different frequencies

and operating sector for 0121 sequences in Over-modulation region at different voltage references. The figure 6.17 and figure 6.19 shows the FFT analysis of the inverter phase voltage and current for 0121 sequences in Over-modulation region at different reference voltages. This sequence operated in under modulation is excellent, but in over-modulation is not good. It is mainly due to the false switching during sector change. This problem should be rectified to get good results. The figure 6.20 shows the voltage between inverter phase to dc bus neutral, phase current and operating sector for 7212 sequences at different frequencies in under modulation region. The figure 6.21 and figure 6.22 are showing the FFT analysis of the inverter phase voltage and current for 7212 sequences at different frequencies. Here also some problem is happening with switching.

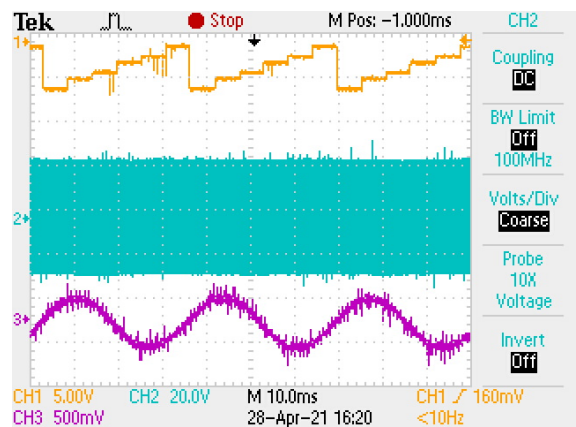
The table 6.1 shows the fundamental values of voltage and their THD values for different sequences in under modulation region at different frequencies. From this table, we can say that at low frequencies the THD value is very high because the less value



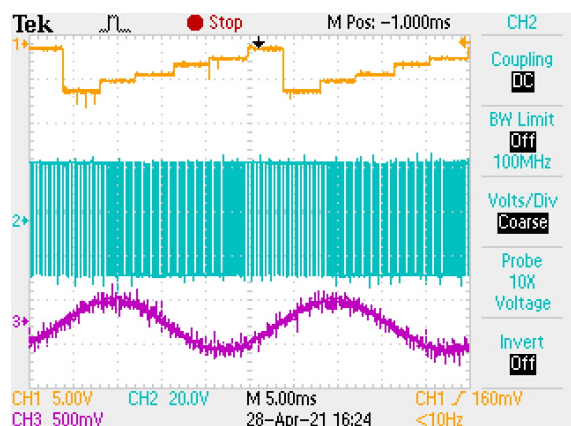
(a) 10Hz



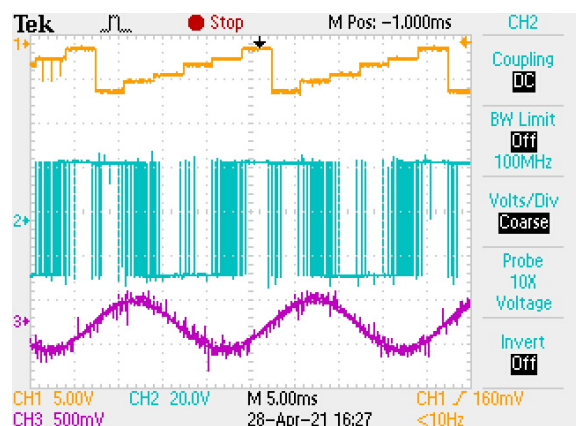
(b) 20Hz



(c) 30Hz

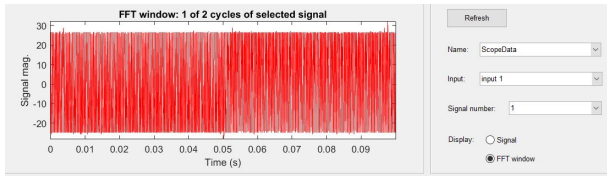


(d) 40Hz

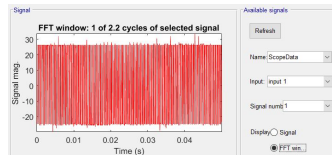


(e) 50Hz

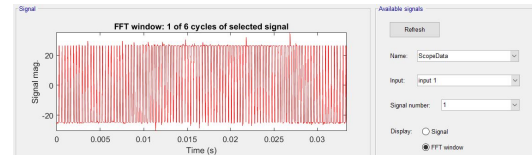
Figure 6.2: The voltage between inverter phase to dc bus neutral, phase current and operating sector for 0127 sequences at different frequencies



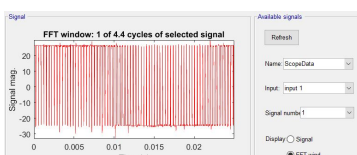
(a) 10Hz



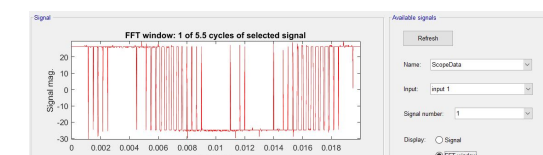
(b) 20Hz



(c) 30Hz

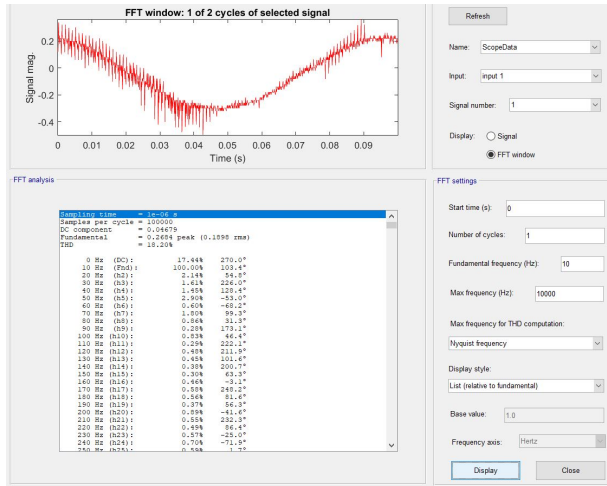


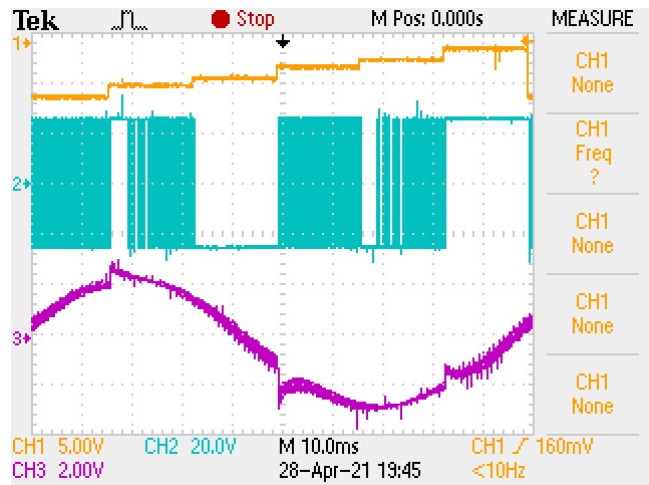
(d) 40Hz



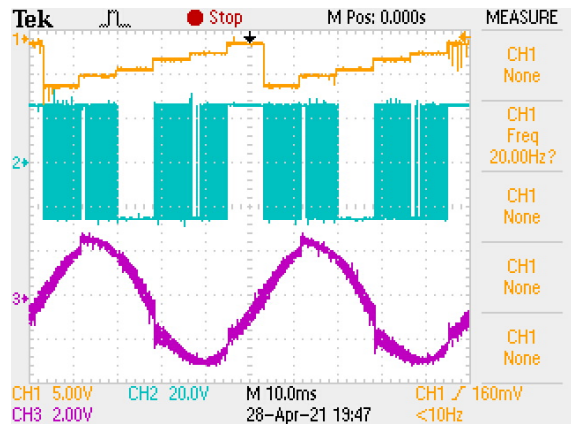
(e) 50Hz

Figure 6.3: FFT analysis of the voltage between inverter phase to dc bus neutral for 0127 sequences at different frequencies

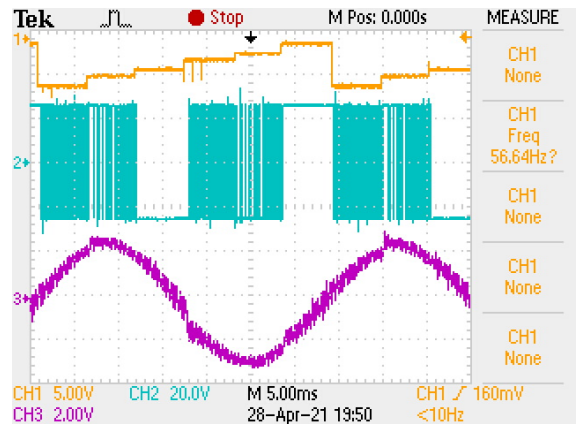




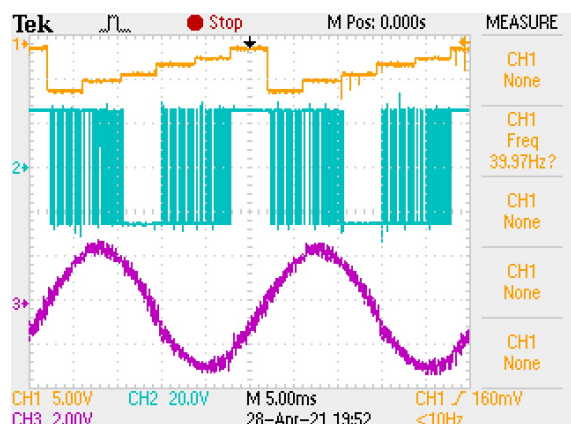
(a) 10Hz



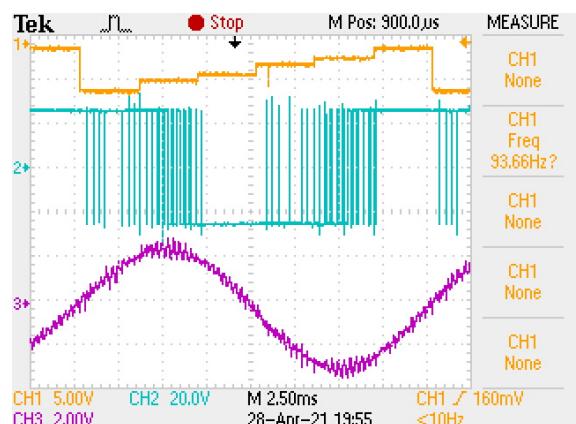
(b) 20Hz



(c) 30Hz

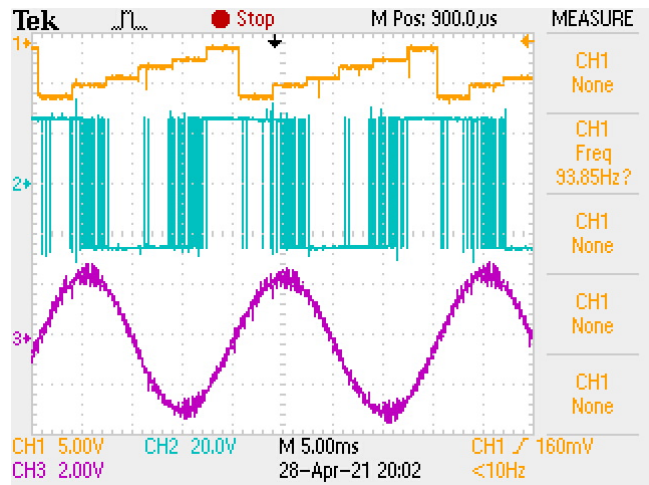


(d) 40Hz

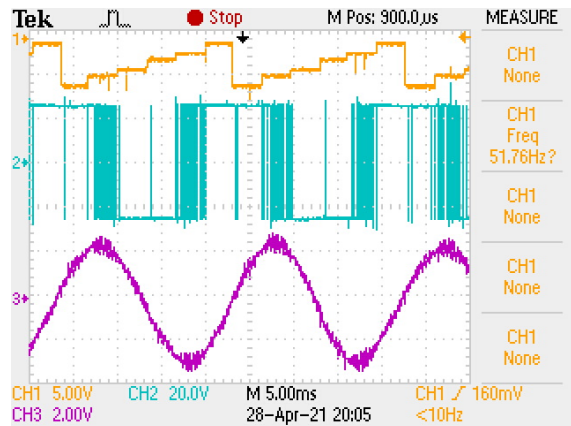


(e) 50Hz

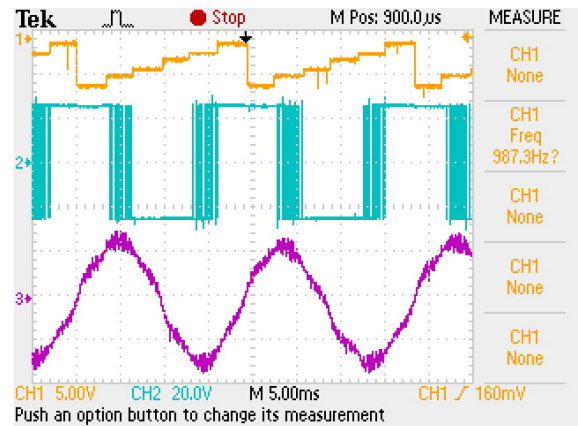
Figure 6.5: The voltage between inverter phase to dc bus neutral, phase current and operating sector for 012 sequences at different frequencies



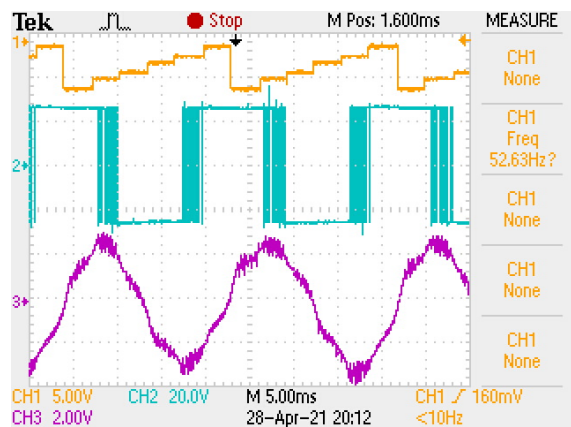
(a) 290V



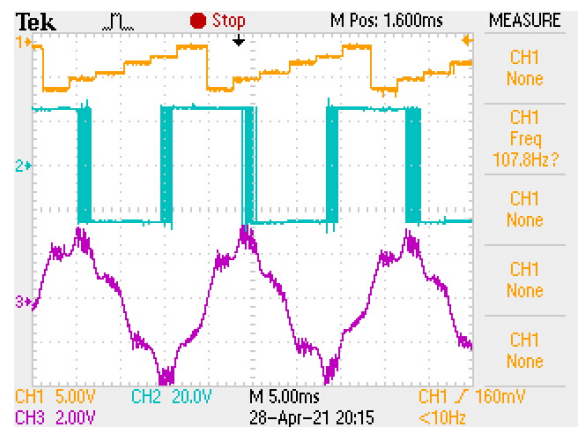
(b) 295V



(c) 302V



(d) 305V

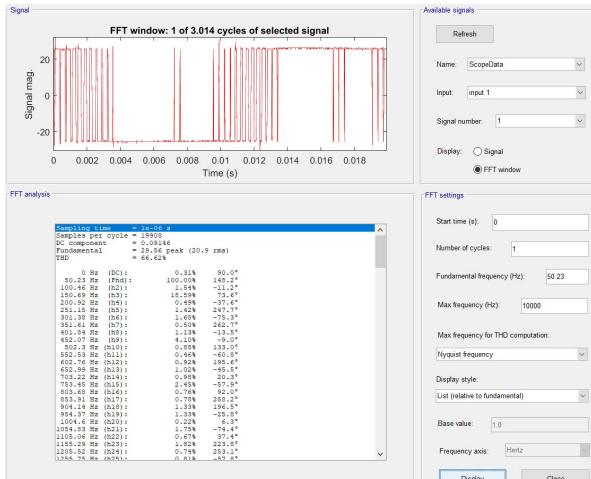


(e) 310V

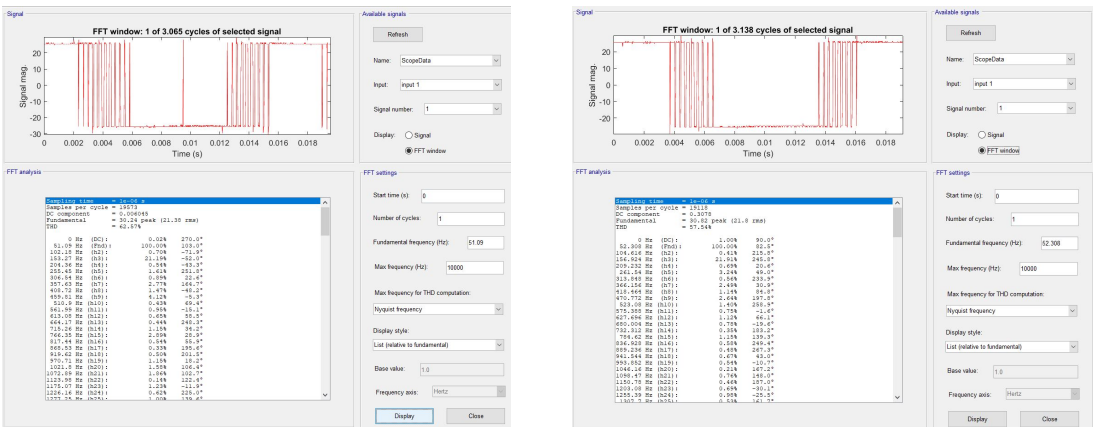
Figure 6.6: The voltage between inverter phase to dc bus neutral, phase current and operating sector for 012 sequences in Over-modulation region at different voltage references



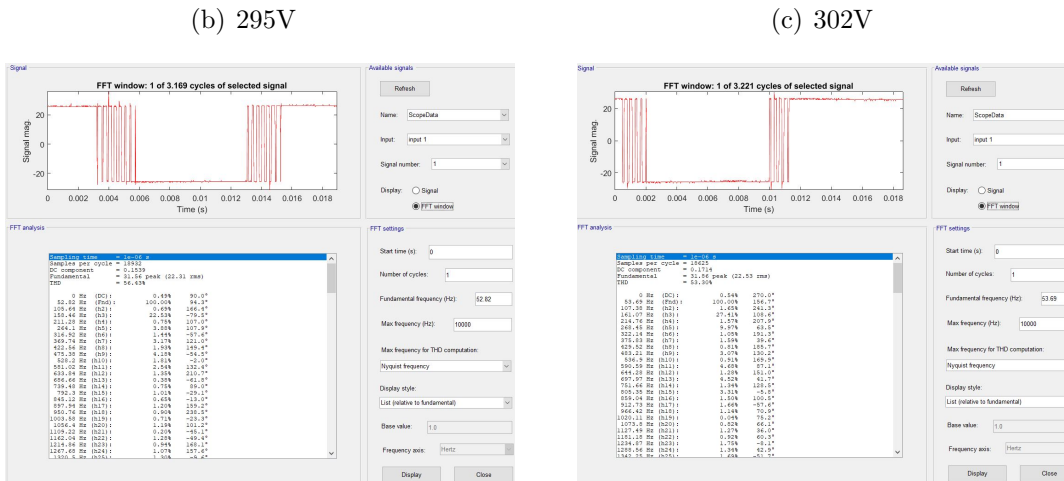
Figure 6.7: FFT analysis of the voltage between inverter phase to dc bus neutral for 012 sequences at different frequencies



(a) 290V



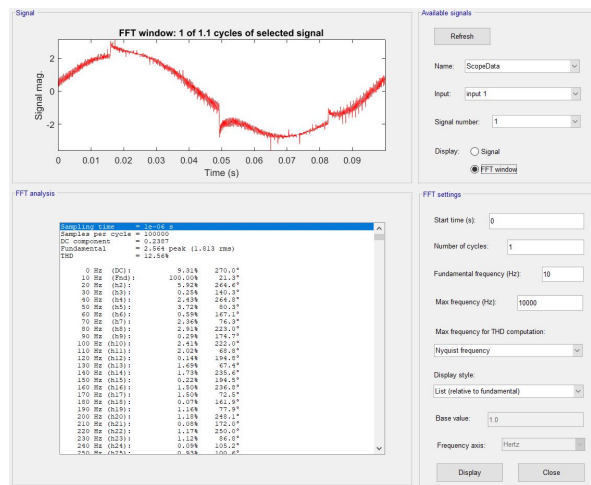
(c) 302V



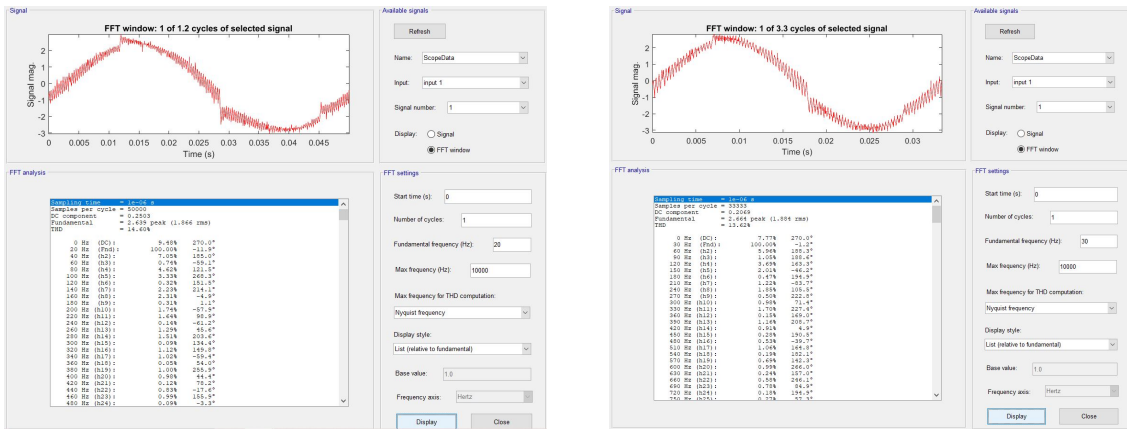
(d) 305V

(e) 310V

Figure 6.8: FFT analysis of the voltage between inverter phase to dc bus neutral for 012 sequences in Over-modulation region at different reference voltages

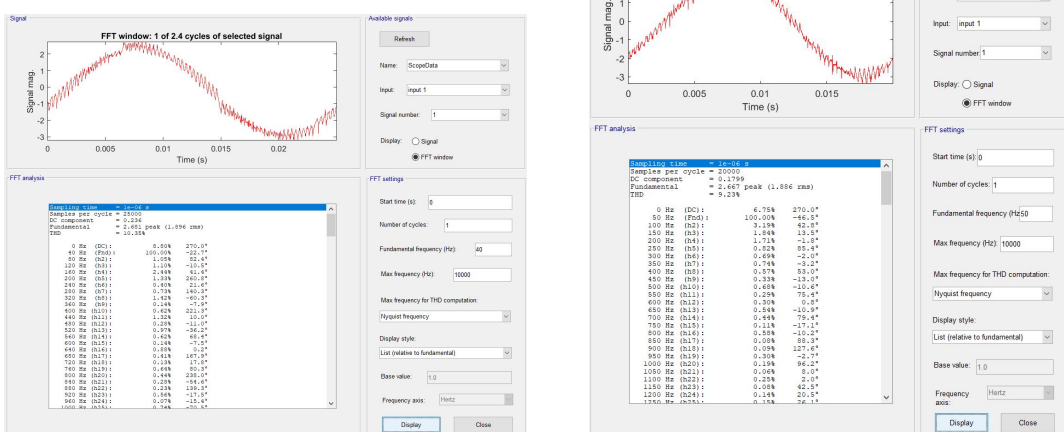


(a) 10Hz



(b) 20Hz

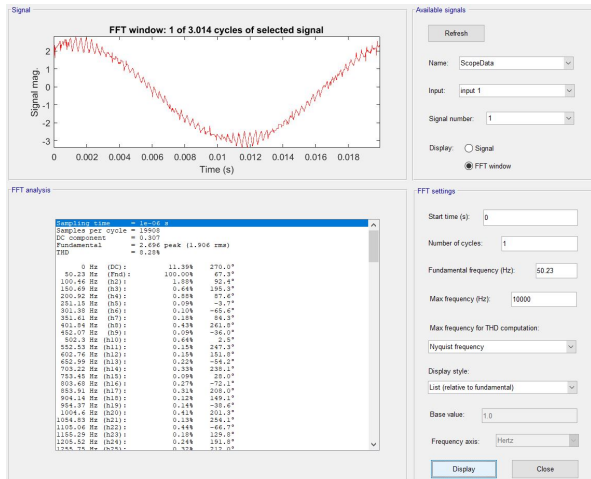
(c) 30Hz



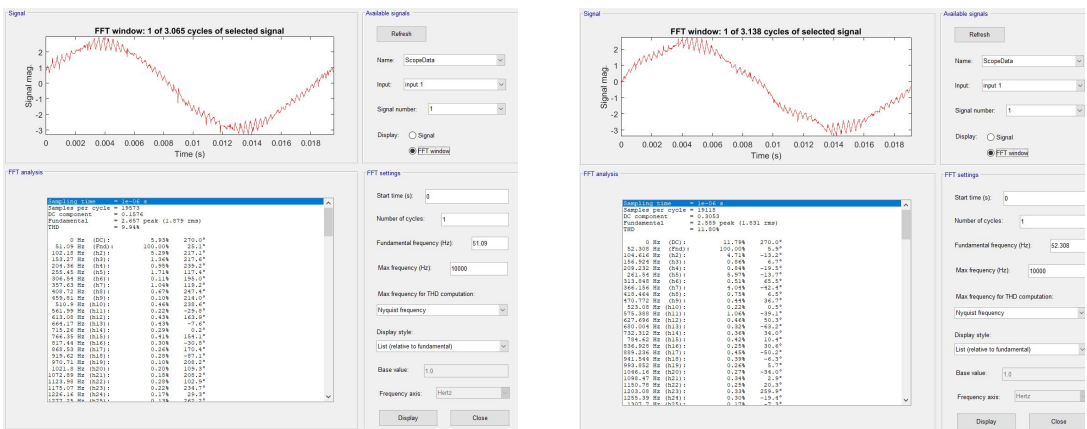
(d) 40Hz

(e) 50Hz

Figure 6.9: FFT analysis of the inverter phase current for 012 sequences at different frequencies

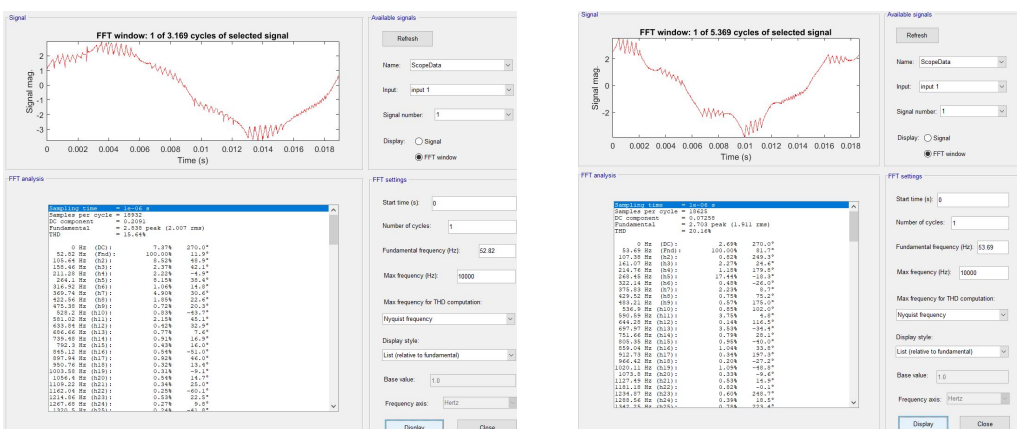


(a) 290V



(b) 295V

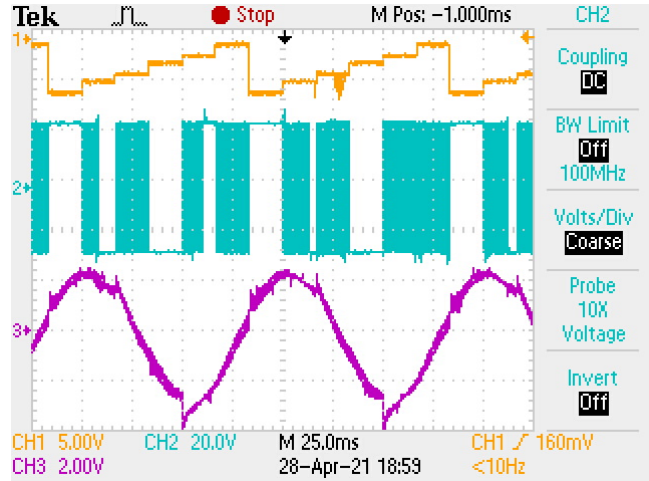
(c) 302V



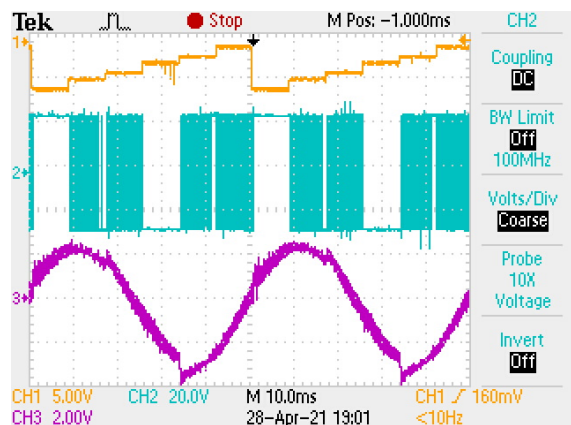
(d) 305V

(e) 310V

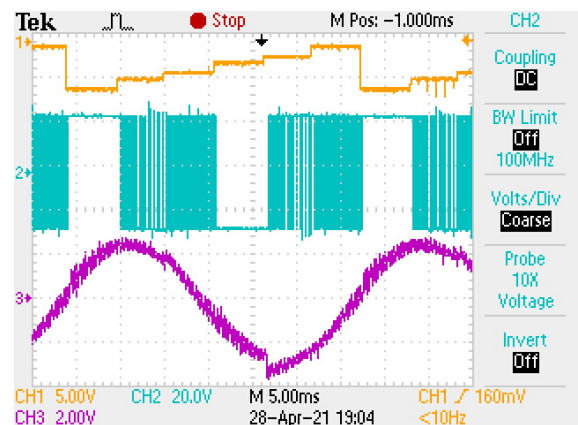
Figure 6.10: FFT analysis of the inverter phase current for 012 sequences in Over-modulation region at different reference voltages



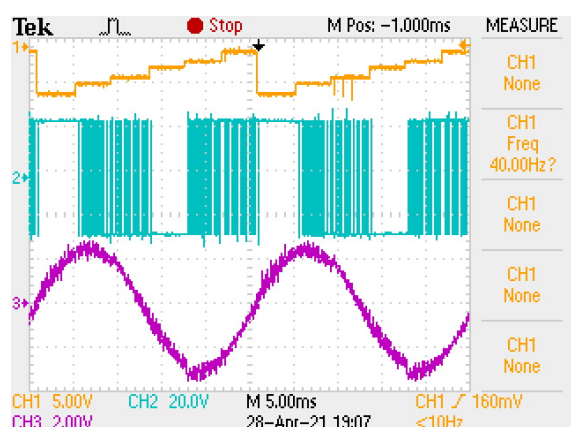
(a) 10Hz



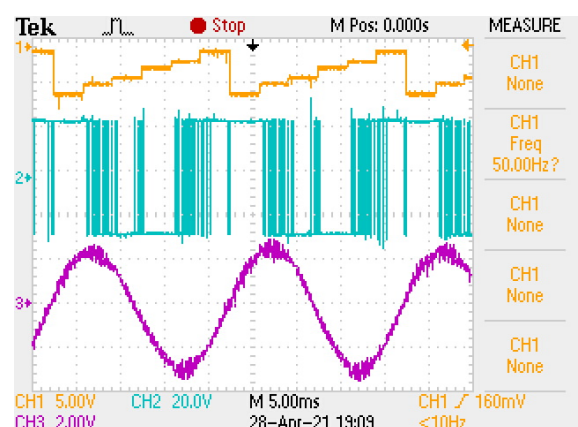
(b) 20Hz



(c) 30Hz

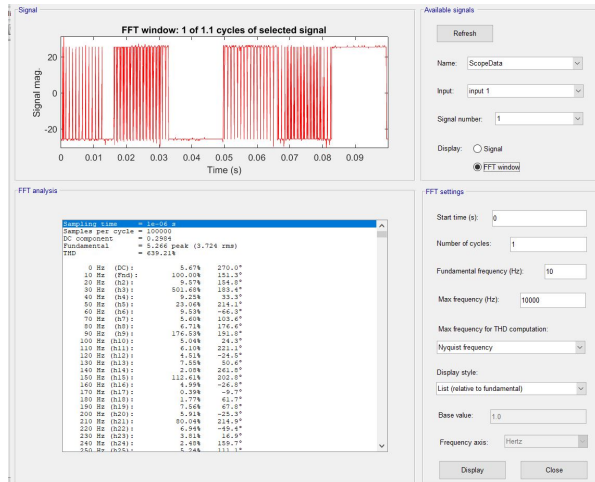


(d) 40Hz

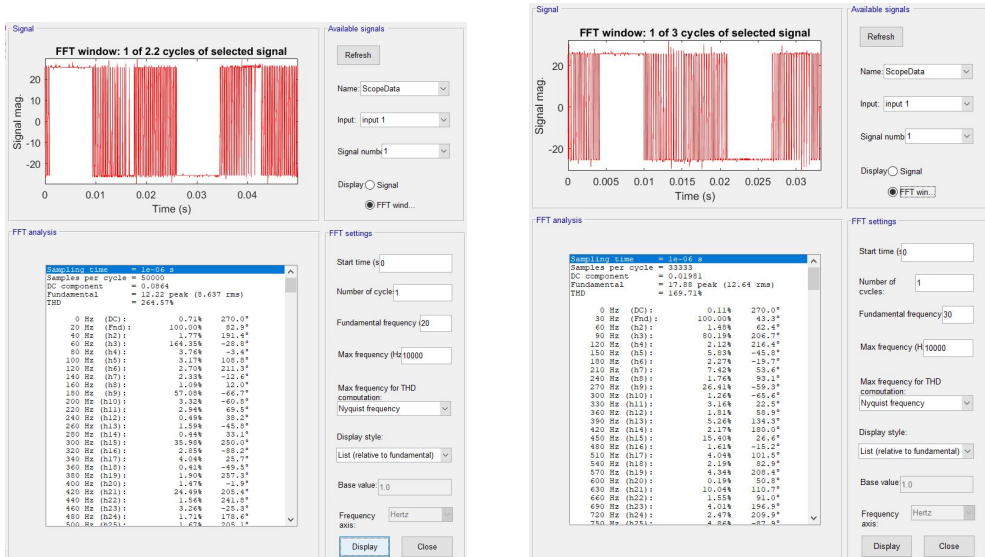


(e) 50Hz

Figure 6.11: The voltage between inverter phase to dc bus neutral, phase current and operating sector for 721 sequences at different frequencies

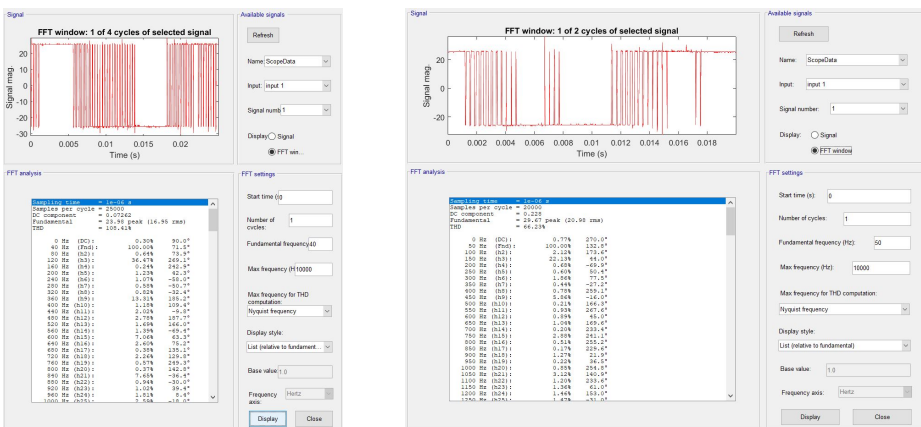


(a) 10Hz



(b) 20Hz

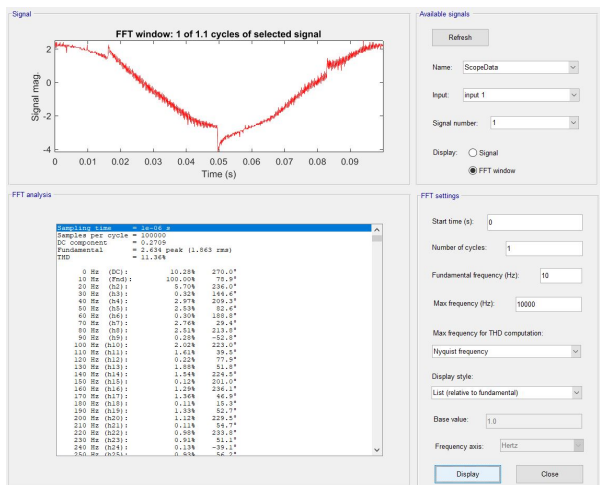
(c) 30Hz



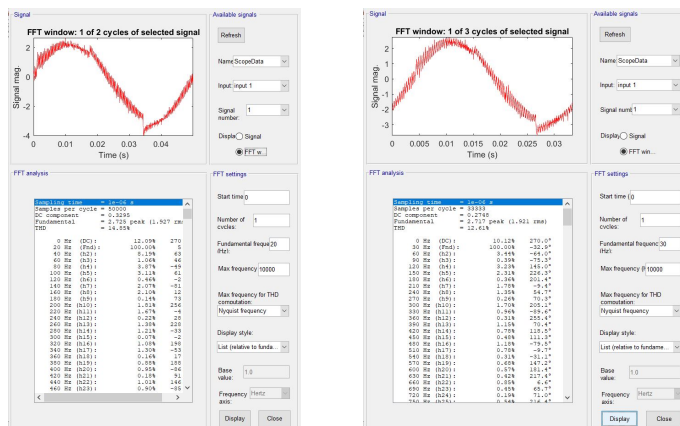
(d) 40Hz

(e) 50Hz

Figure 6.12: FFT analysis of the voltage between inverter phase to dc bus neutral for 721 sequences at different frequencies

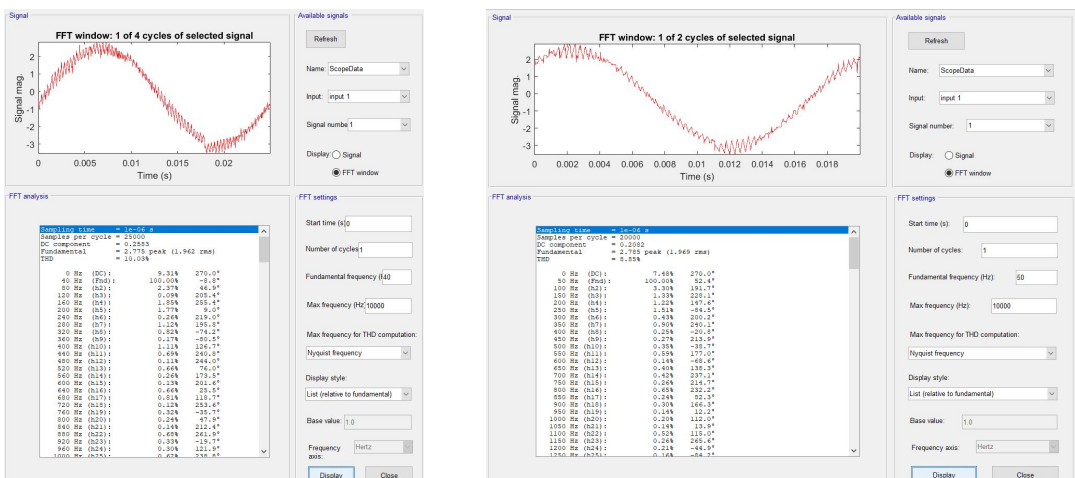


(a) 10Hz



(b) 20Hz

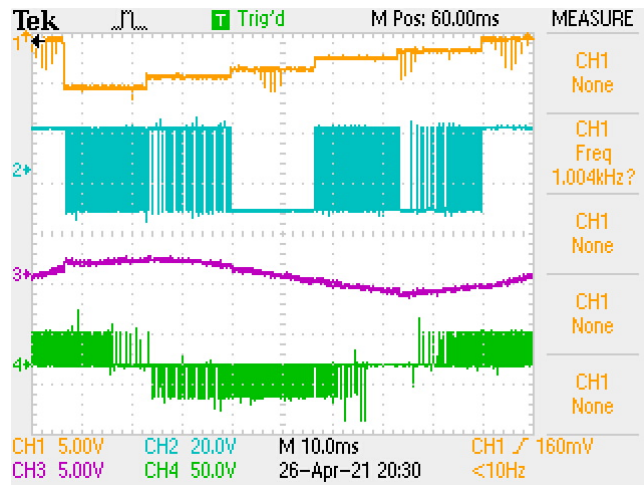
(c) 30Hz



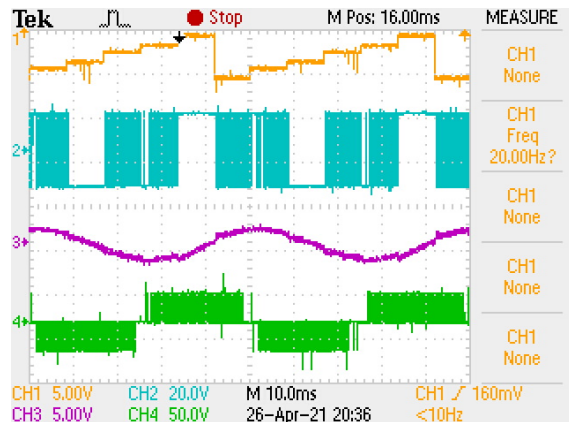
(d) 40Hz

(e) 50Hz

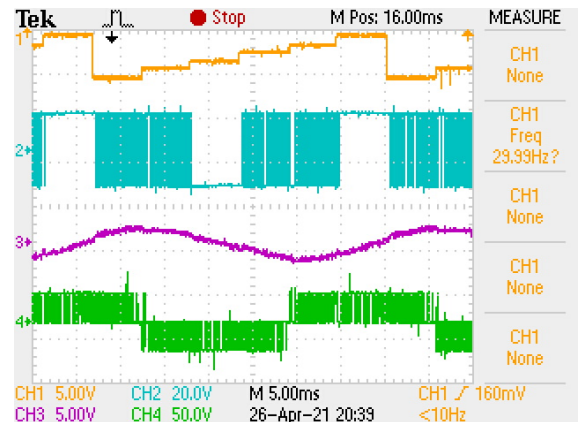
Figure 6.13: FFT analysis of the inverter phase current for 721 sequences at different frequencies



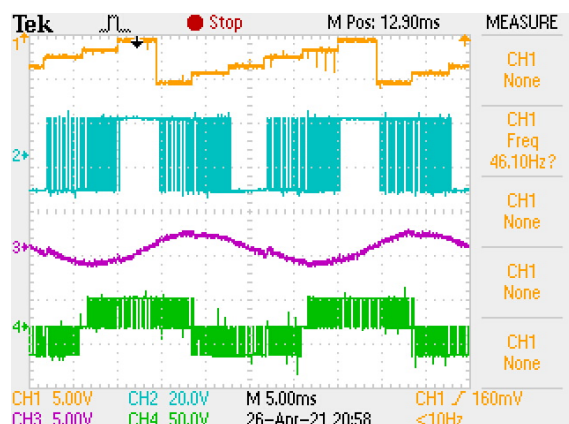
(a) 10Hz



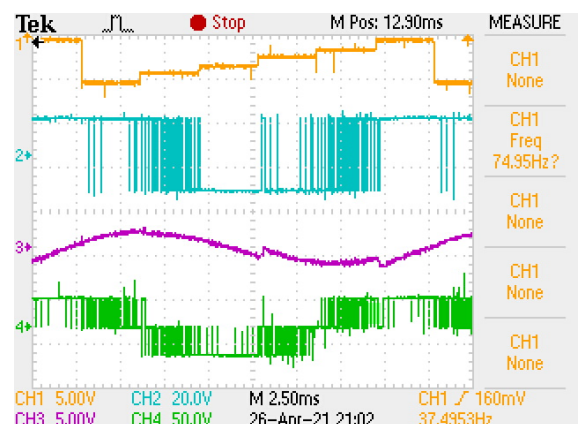
(b) 20Hz



(c) 30Hz



(d) 40Hz



(e) 50Hz

Figure 6.14: The voltage between inverter phase to dc bus neutral, phase current and operating sector for 0121 sequences at different frequencies

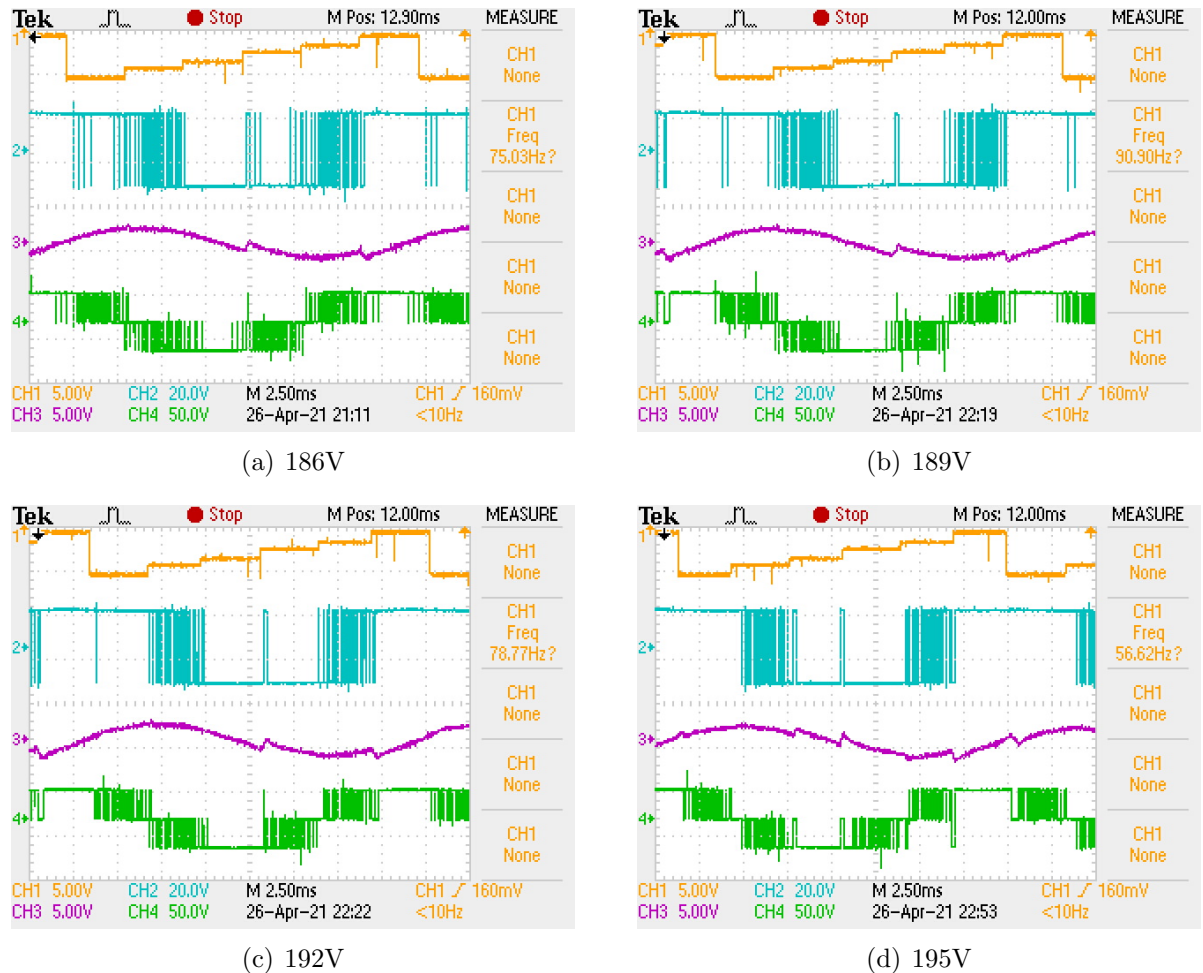


Figure 6.15: The voltage between inverter phase to dc bus neutral, phase current and operating sector for 0121 sequences in Over-modulation region at different voltage references

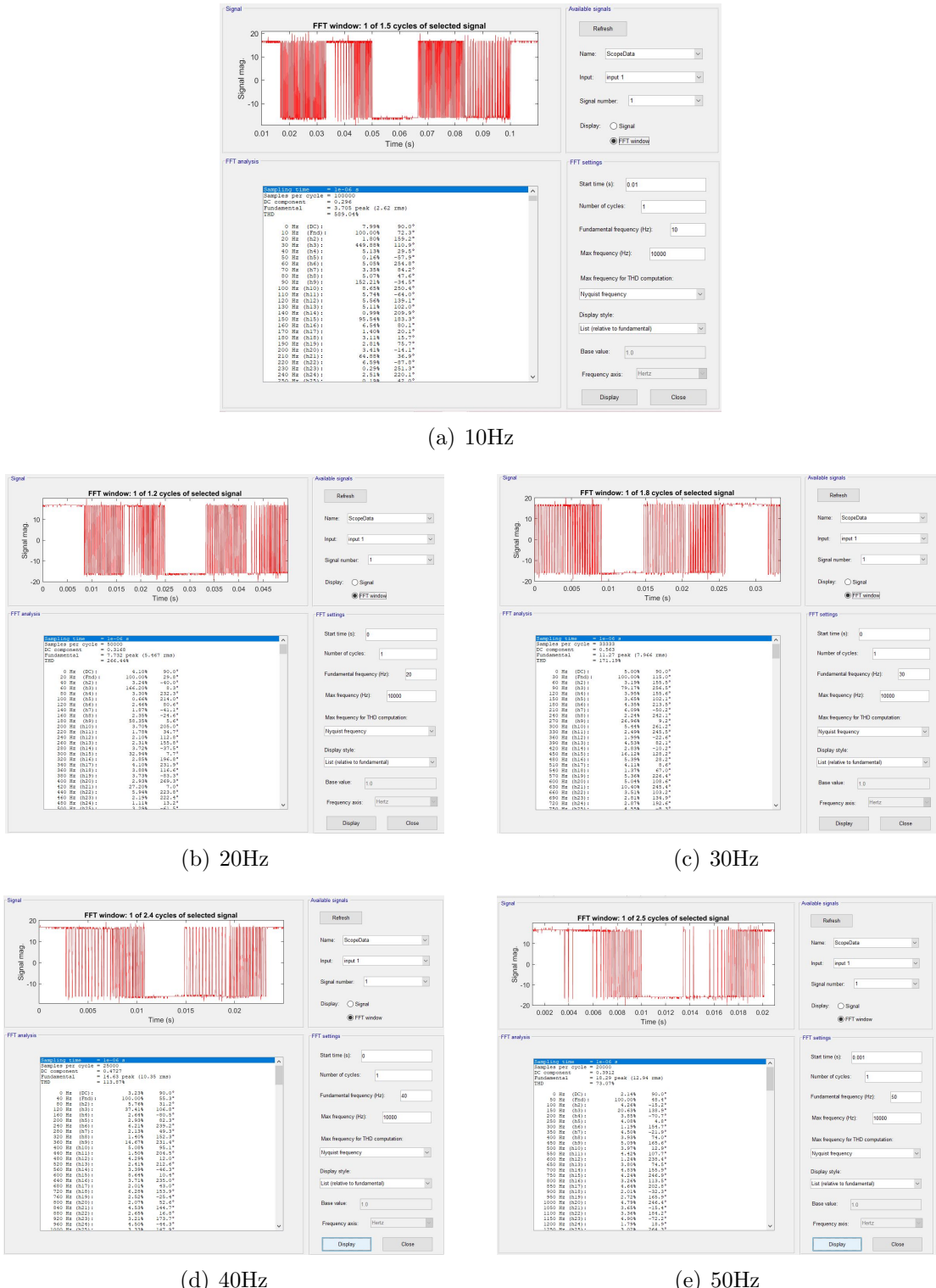


Figure 6.16: FFT analysis of the voltage between inverter phase to dc bus neutral for 0121 sequences at different frequencies

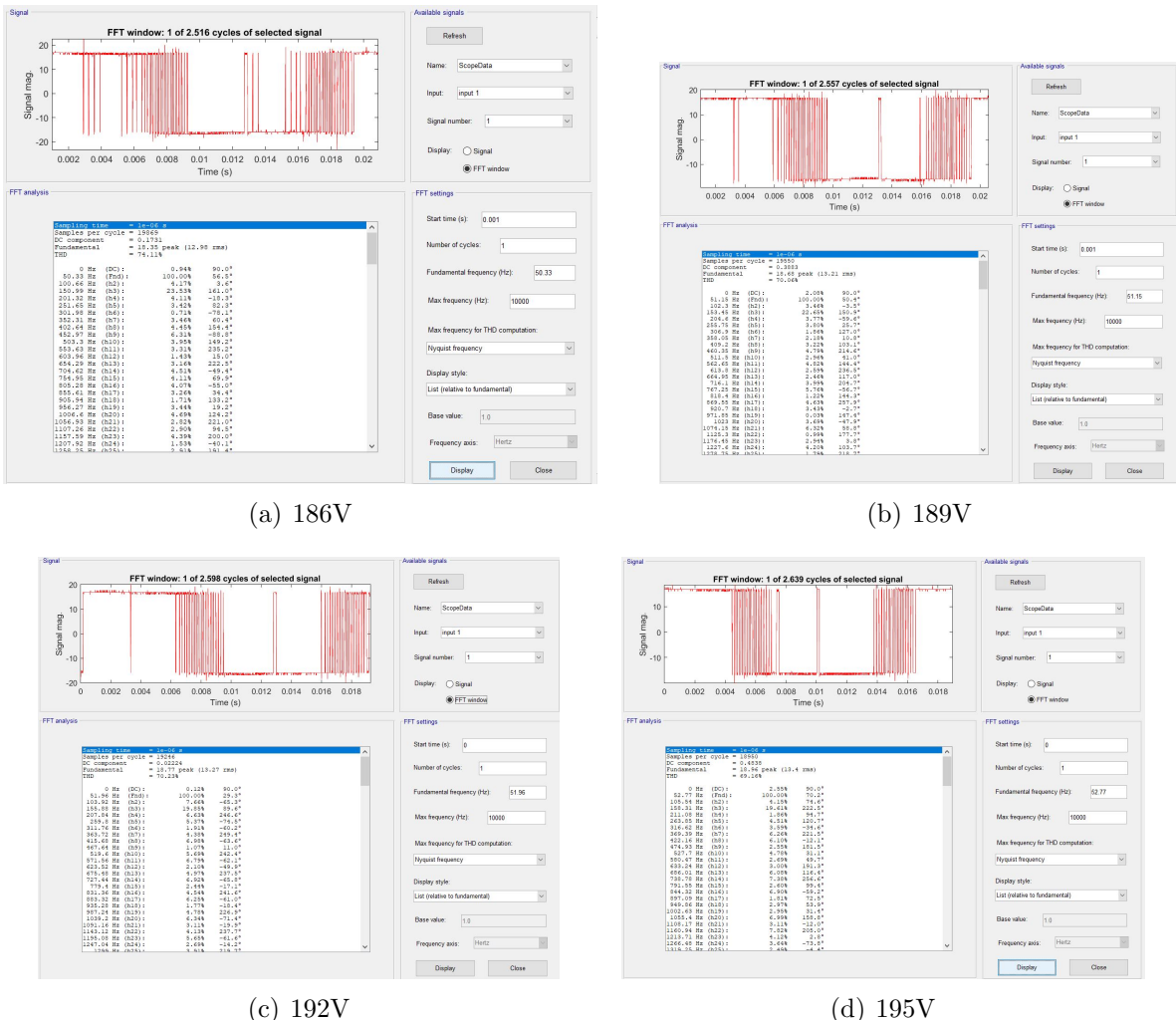


Figure 6.17: FFT analysis of the voltage between inverter phase to dc bus neutral for 0121 sequences in Over-modulation region at different reference voltages

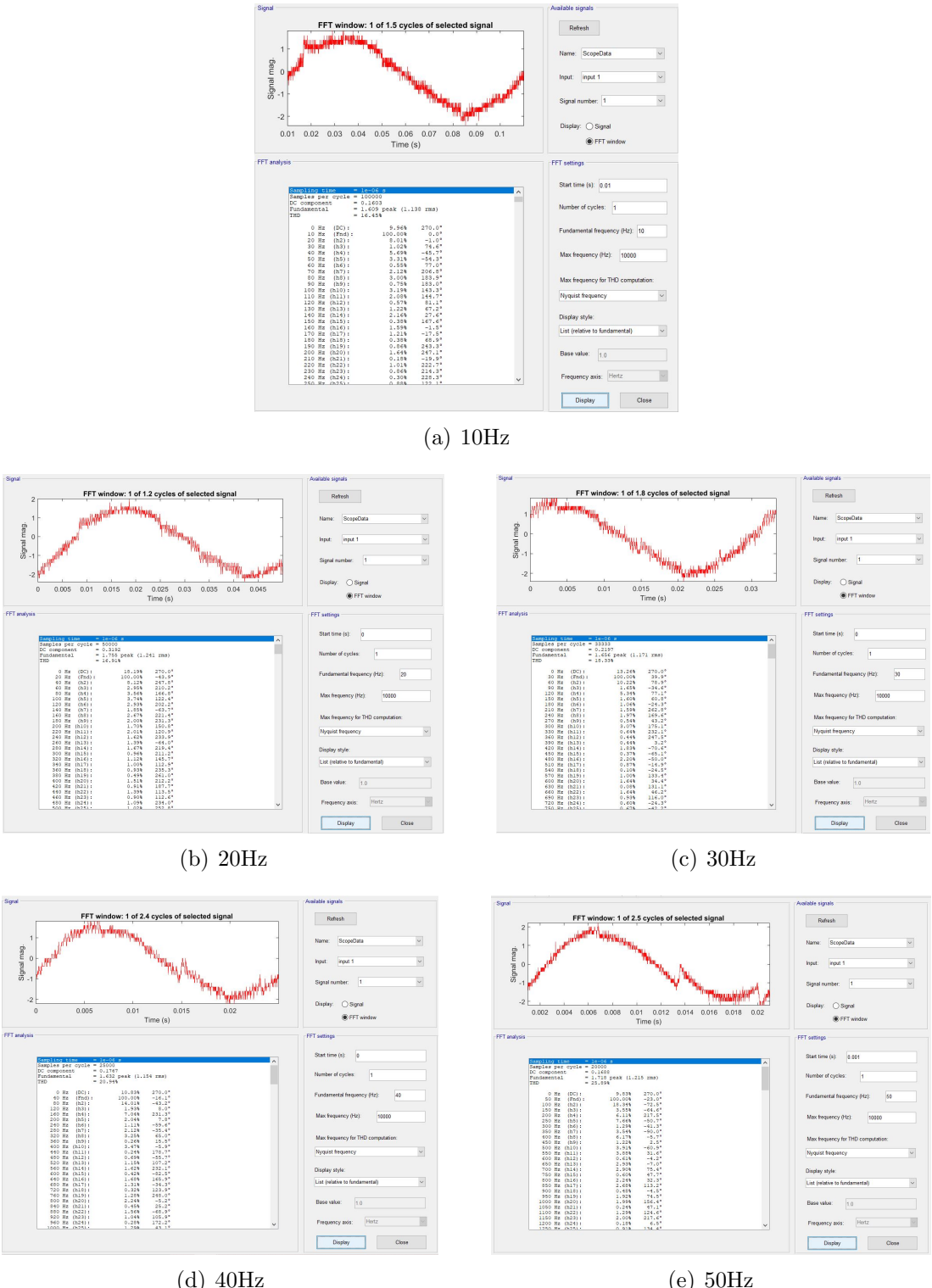


Figure 6.18: FFT analysis of the inverter phase current for 0121 sequences at different frequencies

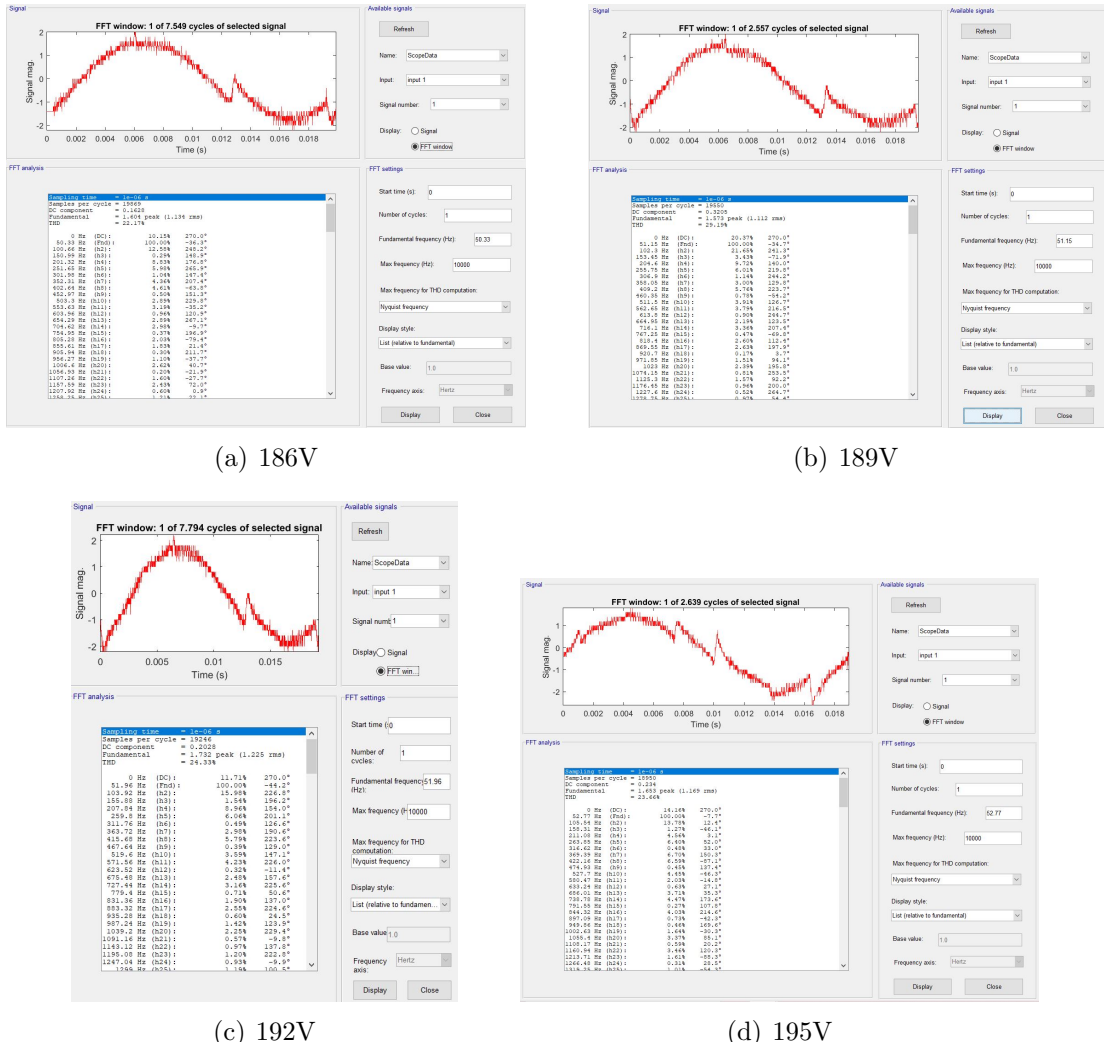
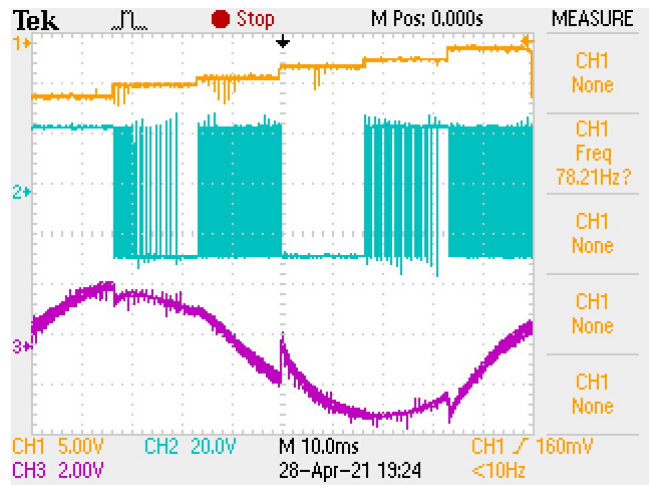
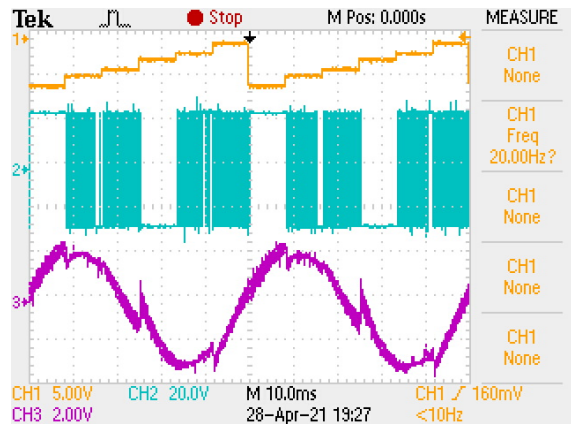


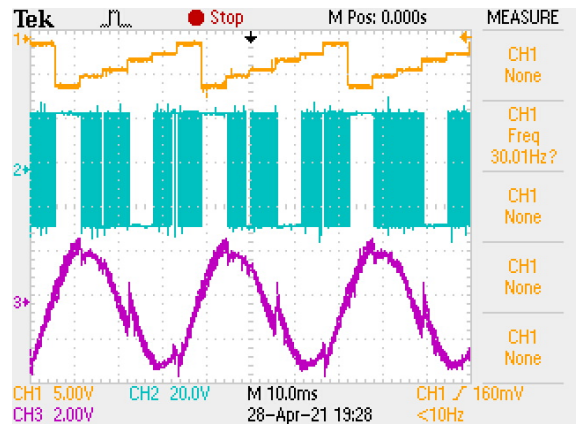
Figure 6.19: FFT analysis of the inverter phase current for 0121 sequences in Over-modulation region at different reference voltages



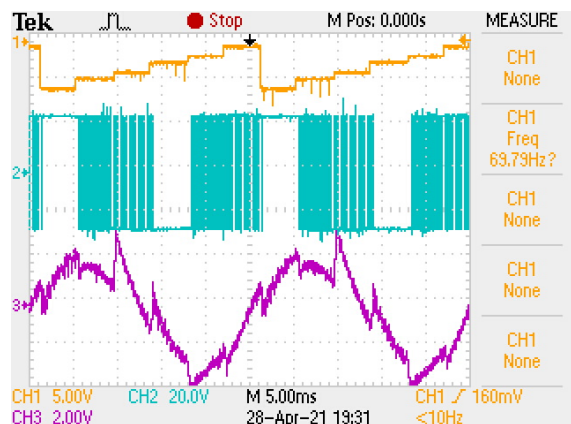
(a) 10Hz



(b) 20Hz



(c) 30Hz



(d) 40Hz

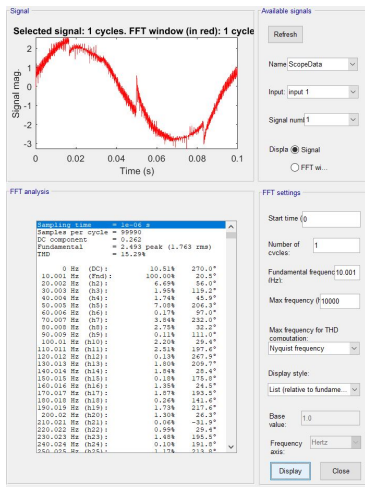


(e) 50Hz

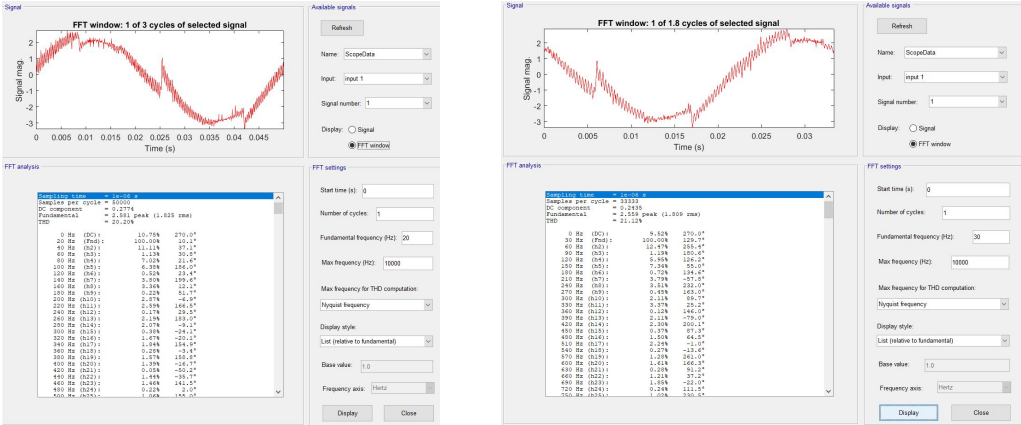
Figure 6.20: The voltage between inverter phase to dc bus neutral, phase current and operating sector for 7212 sequences at different frequencies



Figure 6.21: FFT analysis of the voltage between inverter phase to dc bus neutral for 7212 sequences at different frequencies

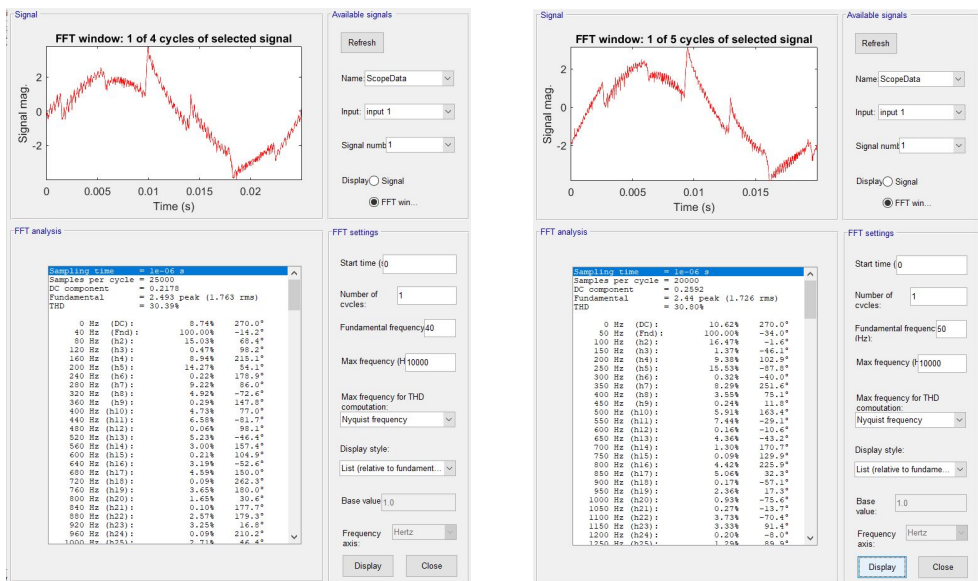


(a) 10Hz



(b) 20Hz

(c) 30Hz



(d) 40Hz

(e) 50Hz

Figure 6.22: FFT analysis of the inverter phase current for 7212 sequences at different frequencies

Sequence	10Hz		20Hz		30Hz		40Hz		50Hz	
	I	THD								
0127	2.684	18.2	2.733	16.16	2.793	15.06	2.799	15.52	2.878	12.67
012	2.564	12.56	2.639	14.6	2.664	13.62	2.681	10.35	2.667	9.23
721	2.634	11.36	2.725	14.35	2.717	12.61	2.775	10.03	2.785	8.85
7212	2.493	15.29	2.581	20.2	2.559	21.12	2.493	30.39	2.44	30.8
0121	1.609	16.45	1.755	16.91	1.656	18.33	1.632	20.94	1.718	25.89

Table 6.2: Fundamental current and its THD values for different sequences at different frequencies

of fundamental voltage. As the frequency increases the the fundamental voltage value is also increases. Due to that, we get better THD components than the low frequency components. We can also say that the fundamental voltage values for all sequences except 0121 sequence, is more or less equal. This is because, to maintain the v/f ratio constant. The fundamental voltages have little bit variations due to the fluctuations in DC bus voltage. From remaining sequences, the 0121 sequence has the less values of fundamental voltages. This is because of using 320V as DC bus voltage. Where as in remaining sequence we use the DC bus voltage as 500V.

The table 6.2 shows the fundamental values of current and their THD values. Here are also we can observe that, the THD values at low frequencies more than the higher frequency components. 7212 sequence has more THD value, due to the distortions at sector change. This is because of some false pulses are generated during the sector change. Similarly, the 0121 sequence also has the same issue.

V _{Ref}	Voltage	THD	Current	THD
290	295.6	66.62	2.696	8.28
295	302.4	62.57	2.657	9.94
302	308	57.54	2.589	11.8
305	315.6	56.43	2.838	15.64
310	318.6	53.3	2.703	20.16

Table 6.3: Fundamental voltage, current and Their THD values for 12 sequence in over-modulation at different reference voltages

The table 6.3 shows the fundamental values of voltage and current and their THD values for 12 sequence in over-modulation region at different reference voltages. From under modulation to over-modulation the THD values of voltage is decreasing gradually. Due to, increasing in fundamental voltage value. But, where as the value of current THD, first decreases up to boundary of under modulation region and starts increasing in the over-modulation region.

The table 6.4 shows the fundamental values of voltage and current and their THD values of 121 sequence in over-modulation at different reference voltages. Similar to 12 sequence, here also increase in reference voltage cause to reduction in voltage THD value.

V_{Ref}	Voltage	THD	Current	THD
186	183.5	74.11	1.604	22.17
189	189.8	70.06	1.573	29.19
192	187.7	70.23	1.732	24.33
195	189.6	69.16	1.653	23.66

Table 6.4: Fundamental voltage, current and Their THD values for 121 sequence in over-modulation at different reference voltages

But, here the current THD is very high compared to 12 sequence. This is because of, false switching pulse. Actually, here also current THD is increases like 12 sequence only.

Chapter 7

Conclusion and Future Work

The output of voltage source inverter can be controlled by using space vector PWM technique. In that, different switching sequences are presented. The V/F controlling implemented for different sequence of operations. Those switching sequences are simulated by using MATLAB Simulink and different types of parameters are compared for these sequences. The concept of flux ripple is also analysed. The switching losses with rise of temperature considered by using PLECS and some of results are also shown. The 012 sequence and 0121 sequences are extended to over modulation region. Those over-modulation region results and their FFT analysis are also included. All the sequences are implemented by using DSP board for hardware implementation. In over-modulation, 121 sequence is used instead of 12 sequence. With using 121 sequence the flux ripple is decreased. All of these things are implemented in simulation and same things are verified experimentally also. But, in 121 sequence at over-modulation region unwanted pulses are appearing at sector change in hardware. Due to that, The current waveform getting disturbed and having a huge amount of harmonics.

In future, we can do following things

- This unwanted pulses in over-modulation region at zone-2 get nullified to get better voltage and current waveforms.
- We can integrate this improved space vector PWM technique to Renewable energy resources also.

Appendix-A

The simulation parameters used are listed in table 7.1

Parameter	Value
No. of stator poles	4
Stator Resistance, R_s	1.5313
Rotor Resistance, R_r	1.5313
Modulation Index, M	0.5
Stator and rotor inductances, L_s and L_r	0.2194
Stator Leakage Inductance, L_{ls}	0.0094;
Rotor Leakage Inductance, L_{lr}	0.0094;
Inertia Constant, J	0.25
Switching Time Period, T_s	1/3000
DC Bus voltage, V_{dc}	500
Frequency, f	50

Table 7.1: Simulation parameters

Appendix-B

The steps for DSP coding with including over-modulation and six step mode with v/f control for 012 sequence is given below

Step-1: Define the all input as well as out put variables

Step-2: Provide the reference voltage and by using v/f control the reference frequency value should be generated

Step-3: From reference voltage and frequency values the reference three phase voltages are generated

Step-4: The reference three phase voltages are converted into two phase voltages

Step-5: From two phase voltages, the magnitude and phase of reference vector is calculated and from magnitude the modulation index value is calculated

Step-6: According to phase angle value, the operating sector is selected

Step-7: Inside of each sector, according to the modulation index value the operating zone is selected

Step-8: If modulation index is less than or equal to 1, it operates in under modulation region

Step-9: In under modulation calculate different timing values for different operating vectors.

Step-10: If modulation index is greater than 1 and less than or equal to 1.05, it operates in over-modulation zone-1

Step-11: In over-modulation zone-1, according to the modulation index value the θ is selected

Step-12: If ($M_a \sin \alpha$ greater than $M_a \sin \theta$) and ($M_a \sin(60-\alpha)$ greater than $M_a \sin \theta$), then generate only time for active vectors and time for zero vector becomes 0. Otherwise, it generates three timings like under modulation region

Step-13: If modulation index is greater than 1.05 and less than or equal to 1.1, it operates in over-modulation zone-2

Step-14: In over-modulation zone-2, according to the modulation index value the α_h is selected

Step-15: If ($M_a \sin \alpha$ less than $M_a \sin \alpha_h$), then the timing for second active vector becomes T and remaining timings are zero. Otherwise go to next step

Step-16: If ($M_a \sin(60-\alpha)$ less than $M_a \sin \alpha_h$), then the timing for first active vector becomes T and remaining timings are zero. Otherwise calculate timings for both active vectors like zone-1

Step-17: If modulation index is greater than 1.1, then it operates in six-step mode and timings are generated like that only

Bibliography

- [1] Keliang Zhou and Danwei Wang, Member, "Relationship Between Space-Vector Modulation and Three-Phase Carrier-Based PWM: A Comprehensive Analysis", *IEEE Trans. Industrial Electron*, vol. 49, no. 1, February 2002.
- [2] G. Narayanan, Member, IEEE, Di Zhao, Harish K. Krishnamurthy, Rajapandian Ayyanar, Senior Member, IEEE, and V. T. Ranganathan, Senior Member, "Space Vector Based Hybrid PWM Techniques for Reduced Current Ripple", *IEEE Trans. Industrial Electron*, vol. 55, no. 4, April 2008.
- [3] Kaushik Basu, J. S. Siva Prasad, and G. Narayanan, Member, IEEE, "Minimization of Torque Ripple in PWM AC Drives", *IEEE Trans. Industrial Electron*, vol. 56, no. 2, Feb 2009.
- [4] Tushar Bhavsar and G. Narayanan, Member, IEEE, "Harmonic Analysis of Advanced Bus-Clamping PWM Techniques", em *IEEE Trans. Power Electron*, vol. 24, no. 10, Oct 2009.
- [5] G. Narayanan and V.T.Ranganathanb, "Overmodulation algorithm for space vector modulated inverters and its application to low switching frequency PWM techniques", *IEE Proc.-Electr. Power Appl.*, Vol. 148, No. 6, November 2001.
- [6] G. Narayanan, Member, IEEE, and V. T. Ranganathan, Senior Member, IEEE, "Analytical Evaluation of Harmonic Distortion in PWM AC Drives Using the Notion of Stator Flux Ripple", *IEEE Trans. Power Electron*, vol. 20, no. 2, March 2005.
- [7] G. Narayanan, Member, IEEE, Harish K. Krishnamurthy, Di Zhao, and Rajapandian Ayyanar, Member, IEEE, "Advanced Bus-Clamping PWM Techniques Based on Space Vector Approach", *IEEE Trans. Power Electron*, vol. 21, no. 4, July 2006.
- [8] J. Holtz, "Pulsewidth modulation—A survey", *IEEE Trans Ind. Electron.*, vol. 39, no. 5, pp. 410–420, Dec. 1992.
- [9] D. G. Holmes and T. A. Lipo, "Pulse Width Modulation for Power Converters: Principle and Practice". New York: Wiley, 2003.
- [10] G. Narayanan and V. T. Ranganathan, "Analytical evaluation of harmonic distortion in PWM AC drives using the notion of stator flux ripple," *IEEE Trans. Power Electron.*, vol. 20, no. 2, pp. 466–474, Mar. 2005.
- [11] V. G. Agelidis, A. Balouktsis, I. Balouktsis, and C. Cossar, "Multiple sets of solutions for harmonic elimination PWM bipolar waveforms: Analysis and experimental verification," *IEEE Trans. Power Electron.*, vol. 21, no. 2, pp. 415–421, Mar. 2006.

- [12] S. R. Bowes and D. Holliday, "Optimal regular sampled PWM inverter control techniques," *IEEE Trans. Ind. Electron.*, vol. 54, no. 3, pp. 1547–1559, Jun. 2007.
- [13] A.M. Hava, R. J. Kerkman, and T. A. Lipo, "Simple analytical and graphical methods for carrier-based PWM-VSI drives," *IEEE Trans. Power Electron.*, vol. 14, no. 1, pp. 49–61, Jan. 1999.
- [14] D. Casadei, G. Serra, A. Tani, and L. Zarri, "Theoretical and experimental analysis for the rms current ripple minimization in induction motor drives controlled by SVM technique," *IEEE Trans. Ind. Electron.*, vol. 51, no. 5, pp. 1056–1065, Oct. 2004.
- [15] A. Cataliotti, F. Genduso, A. Raciti, and G. R. Gullazzo, "Generalized PWM-VSI control algorithm based on a universal duty-cycle expression: Theoretical analysis, simulation results, and experimental validations," *IEEE Trans. Ind. Electron.*, vol. 54, no. 3, pp. 1569–1580, Jun. 2007.
- [16] KAURA, V.: "A new method to linearise any triangle-comparison based PWM by reshaping the modulation command", *IEEE Trans. Ind. Appl.*, 1997, 33, (5), pp. 1254-1259.
- [17] HANDLEY, P.G., and BOYS, J.T.: "Practical real-time PWM modulators - an assessment", *IEEE Proc. B, Elecectr. Power Appl.*, 1992, 139, (2), pp. 9102.
- [18] C. M. Wu, W. H. Lau, and H. Chung, "Analytical technique for calculating the output harmonics of an H-bridge inverter with dead time," *IEEE Trans. Circuits Syst. I*, vol. 46, no. 5, pp. 617–627, May 1999.
- [19] "Algorithms of space vector PWM IN overmodulation area" by Z. Peroutka, T. Glasberger University of West Bohemia / Department of Electromechanics and Power Electronics, Plze, Czech Republic.